OPTIMIZATION OF BIO-BASED GLASS - POLYFURFURYL ALCOHOL PREPREG FOR COMPOSITE MATERIAL APPLICATIONS

A submission in partial fulfilment of the requirements of the University of Derby for the award of the degree of Doctor of Philosophy

In the College of Science and Engineering

January 2023

Daniel Chika Odiyi

Supervisors:

Dr Tahir Sharif

Dr Rizwan Choudhry

Table of Contents

List of Figures

List of Tables

List Abbreviations

PFA	Polyfurfuryl Alcohol
FA	Furfuryl Alcohol
DSC	Dynamic Scanning Calorimetry
DMA	Dynamic Mechanical Analyzer
TMA	Thermo- Mechanical Analyzer
FR	Friedman
OFW	Ozawa Flynn Wall
NFRP	Natural Fibre Reinforced Polymer
FRBP	Fibre Reinforced Biopolymer
PLA	Poly Lactic Acid
FST	Fire Smoke Toxicity
VARTM	Vacuum-Assisted Resin Transfer Moulding
LVDT	Linear Variable Differential Transformer
OVC	Oven Cured
CM	Compression Moulding

Author Declaration

I Daniel Odiyi hereby the author of this PhD thesis declare that no portion of this work referred to in this dissertation has been submitted in support of an application for another degree or qualification of this or any other university or other institution of learning.

Abstract

Global sustainability and emissions concerns in the manufacture and application of fibre composites have recently fuelled research and development of bio-based alternatives to mitigate these challenges. One such material that has been developed and recently explored for composites applications is bio-based polyfurfuryl alcohol resin. It has demonstrated impressive mechanical and thermal properties in fibre applications. However, this comes with a major disadvantage of the long processing time, which for its manufacture is synonymous with manufacturing processes such as oven or autoclave curing, which limits its application for high volume production. To this end, this project aims to optimize the curing cycle of the glass / PFA prepreg for rapid manufacturing. Model-free and model-based kinetic studies were performed to understand the curing mechanism that occurs during the curing reaction. The Friedman and Ozawa-Flynn wall models were used to investigate the conversion-dependent activation energy. Both methods found that the average activation energy for the curing process was 88.9 ± 4.9 kJ/mol and further revealed a curing mechanism with a multi-step curing reaction consisting of parallel and competing reactions taking place simultaneously during the reaction. This was found to be relatively consistent with that obtained by the Kamal-Sourour fitted model. The excellent correlation between the Friedman model and the experimental data made it suitable for predicting the evolution of the reaction time under isothermal conditions, leading to an optimization of the total process cycle time from the manufacturer's recommended cycle of 113 minutes to 30 minutes when held isothermally at 160℃. Thus, suggestively making it suitable for rapid manufacturing processes such as the compression moulding process.

Mechanical and thermal characterization was performed on Glass/PFA laminate manufactured by a hot press using the optimized cycle from the kinetic study at two different pressure (5 and 10bars) and this was benchmarked against laminates manufactured by the vacuum bagging - oven curing method using the manufacturer’s recommended cycle. The experimental results reveal that the cured glass/PFA laminate manufactured using the optimized cycle at 5 bar pressure was found to exhibit the best result showing an increase in the glass transition temperature (Tg) from 175℃ to 201℃. The impact of the optimized cure parameters on the mechanical properties of the glass/PFA composite was significant. It resulted in a notable 10.25% improvement in tensile strength, a substantial 13.04% increase in flexural strength, and a commendable 10.34% enhancement in apparent shear strength compared to the reference

oven-cured glass/PFA sample. This successful study has effectively established the ideal cure parameters for the glass/PFA prepreg, enabling rapid and efficient composite fabrication.

Acknowledgement

I give all thanks to God Almighty for the opportunity, strength, and for making this work complete.

First, I would like to thank my supervisors Dr Tahir Sharif and Dr Rizwan Choudhry for their insightful knowledge, invaluable patience, guidance, and support throughout this project. Their unflinching moral support and encouragement pulled me through an exceedingly difficult period of my life. I am forever grateful, and words cannot express my deep gratitude. This work would not have been made possible without you.

I would like to appreciate my wonderful research colleagues and team members Dr Marzena Pawlik, Jawwad Ahmed and Temitope Omisore for their support and all your contributions in every measure towards the completion of the work.

I also like to acknowledge my line manager Richard Bostock and my colleagues in the technical team for their understanding and every support they provided.

Special thanks to my friends Edmund Nwagbaraocha and Oludayo Fatunke for all their support in all measures. I appreciate you.

Finally, a deep sense of gratitude goes to my Family. Auntie! thank you for your relentless love, prayers, and unending support. To all my brothers and my lovely sister Gloria Odiyi, I cannot thank you all enough. You all are the best!! I could not have done this without you all. Thank you and God bless you all.

Chapter 1 Introduction

1.1 Research Background

Fibre-reinforced polymer composites are commonly employed as alternatives to conventional materials for a wide range of products and applications due to their remarkable mechanical properties and lightweight. Aerospace, rail, automotive, and sporting goods industries are increasingly attracted to this class of materials due to their excellent specific stiffness, strength, ease of manufacture, non-corrosion, resistance to chemical attack, and performance tailoring capacity. As these materials gain traction in their existing industries and establish themselves in relatively new fields, such as biomedical and civil structures, the use of fibre-reinforced polymer composites continues to rise at a rapid rate. Fundamentally, the constituents of these materials (fibre and matrix) are sourced from fossil fuels, which have been discovered over time to be non-biodegradable and harmful to the environment. Consequently, this results in significant environmental and sustainability concerns. This has resulted in environmental regulation and customer demand in many nations, thereby increasing the pressure on manufacturers of materials and finished products to assess the ecological impact of their products throughout their entire life cycle, including recycling and final disposal (Malathi and Kumar, 2018). With sustainability at the forefront of recent global product and manufacturing discussions, innovation has led to the exploration and development of fossil-based composite material alternatives. Studies have focused their efforts on developing eco-friendly materials that could replace traditional composites (Das and Chaudhary, 2021). This has resulted in a growing interest in biobased fibre-reinforced polymer composites. Bio composites are composites that contain one or more phases of natural origin (Fowler, Hughes and Elias, 2006; Asyraf *et al.*, 2022). Primarily sourced from renewable resources, majorly plants, this class of materials also maintains carbon-dioxide neutrality (Mohanty, Misra and Drzal, 2002) providing a pathway for the reduction of greenhouse gas emissions, which is a global challenge. This group of materials includes Natural Fibre Reinforced Polymer (NFRP) composites, which use natural fibre reinforcements made from plants, animals, or geological processes and a synthetic matrix, Fibre Reinforced Biopolymer (FRBP) composites, which have a synthetic fibre reinforcement with a partially or fully bio-derived matrix (Fitzgerald *et al.*, 2021). The property comparability and ecological benefits provided by this class of material have contributed to its increased application in industries. In fact, according to Gurunathan, Mohanty, and Nayak in (Gurunathan, Mohanty and Nayak, 2015), it is anticipated that two-

thirds of the USD 1.5 trillion global industries will be reliant on renewable resources in the future. The roadmap to ensure the transition from fossil-based polymers to renewable polymers thus implies unlocking numerous gateways. (Guigo and Sbirrazzuoli, 2018). Key industrial drivers of the development of these types of material for applications include rail, sports goods, aerospace, biomedical and automotive. The automotive interior sector has been recognized as the second biggest application sector (Carus, 2015). Within these industries, a lot of research and development has been given to the synthesis of thermoset and thermoplastic biopolymer systems. This is so because, beyond the physical and mechanical properties they possess, they also offer the potential of intrinsic or enhanced special properties such as chemical inertness, thermal stability, and water absorption thus making them suitable for a range of applications. For instance, due to its low water absorption capabilities, biobased polyamide (PA6,10) is utilised in transmissions and connections in a cooler circuit, wheel speed sensors, fuel lines, and specific cables applications (Ogunsona, Misra and Mohanty, 2017; Prasanth *et al.*, 2021). The success of these biopolymer systems, particularly thermoplastics such as Poly Lactic Acid (PLA), Polyhydroxy-alkanoates, and poly (butylene succinate), has led to their commercialisation. (Lutton, Taylor and Sonebi, 2017). However, the same cannot be said for biobased thermosetting resins. Although this rapidly changing with the recent development of fully biobased epoxies and benzoxazines (Liu *et al.*, 2021), Humins (Sangregorio *et al.*, 2021) and polyfurfuryl alcohol resin (Singh *et al.*, 2022).

Polyfurfuryl alcohol resin, often known as Furan resin, (Moazzen *et al.*, 2018) is one such thermosetting matrix that is continually being researched. Drawing from its use in foundry applications (Belgacem and Gandini, 2003), researchers have explored its use in advanced composites driven by its remarkable inherent thermal, fire, smoke, and toxicity (FST) properties. In addition, its compliance with Registration, Evaluation, Authorization, and Restriction of Chemicals (REACH) regulation due to its low residual monomer level during manufacturing makes it a potential replacement for phenolic resin, which contains carcinogenic formaldehyde during synthesis (Asad, Mahmood and Shah, 2020).

Reinforced with a range of fibres including carbon, glass, aramid, flax, and basalt (for 100% Natural Fibre Reinforced Polymer), the polyfurfuryl alcohol resin-based composite is well suited for applications within industries such as the automotive, rail and aerospace where stringent fire safety standards are critical. Nevertheless, despite the endearing properties provided by this resin and its composite, these materials are not problem-free. They do have some drawbacks, such as void formation caused by water release during processing, prolonged

resin manufacturing times, viscosity challenges limiting the range of manufacturing processing, and the suitability of the processing window (cure cycle) for rapid manufacturing production. Additionally, these limitations come with expensive equipment (usage of autoclave and oven) and processing (energy and time) costs, all of which have a negative impact on its commercial application. For this reason, this research work attempt to address this challenge by optimizing the cure cycle of this material for rapid manufacturing.

Thus, this thesis reports the study of the optimization of the glass fibre-reinforced polyfurfuryl alcohol prepreg for rapid manufacturing. In this work, the advantage of analytical kinetic modelling is employed to determine and predict the processing window (cure cycle) suitable for rapid manufacturing processes like compression moulding.

1.2 Research Problem

As one of the few fully developed bio-based resins (Kumar, 2016), the PFA bio-resin has demonstrated comparable mechanical properties to some commonly used epoxy systems (Crossley, Schubel and Stevenson, 2014) in a wide range of applications, including fibre-reinforced application. Some of these applications include high-performance products ranging from large panels to small parts in the rail and automotive industry (Kumar and Anandjiwala, 2013). As with most fibre-reinforced composites, achieving the desired mechanical properties of the PFA in the fibre-reinforced application is highly dependent on the manufacturing process.

Studies (Kumar and Anandjiwala, 2013; Domínguez and Madsen, 2015a; Kandola, Ebdon and Chowdhury, 2015; Talent and Wang, 2015; Kumar, 2016; Marefat Seyedlar, Imani and Mirabedini, 2018; Ipakchi *et al.*, 2020) involving the manufacture and processing of PFA resin and its fibre reinforced composites shows that crosslinking of the resin is usually slow or gradual, with the temperature typically being from 20°C to 180°C over 1 to 96 hours (Rivero, Villanueva and Manfredi, 2014; Kandola, Ebdon and Chowdhury, 2015; Talent and Wang, 2015; Sharib, Kumar and Kumar, 2018; Ma *et al.*, 2020). This is believed to be due to mitigating the problem of inherent water content in the resin which evolves as vapour, bubbles, or volatiles during the condensation reaction of the curing process (Rivero, Villanueva and Manfredi, 2014; Domínguez and Madsen, 2015a; Talent and Wang, 2015; Foruzanmehr *et al.*, 2016). This effectively leads to the development of long cure cycles by prepreg manufacturers, explaining the popularity of using processing methods such as ovens or autoclaves during the curing of the PFA resin. The long curing cycle continues to be a problem as it limits the rapid

manufacture which is essential for mass production for high volume production. This inadvertently limits the application potential of fibre-reinforced PFA-based composites. Therefore, optimising processing parameters for rapid manufacturing techniques such as compression moulding (hot press) is crucial in the commercializing of the manufacture of biobased PFA composites for applications.

1.3 Aims

This research aims to provide insight into the curing mechanism of biobased glass-reinforced PFA - based prepreg to develop an optimised curing cycle for rapid manufacturing of biobased Glass/PFA composites with comparable properties.

1.4 Objectives

The key objectives of this research work are outlined as follows:

I. To review and achieve an in-depth understanding of the synthesis, properties, manufacturing, and challenges of the biobased PFA resin.
II. To employ cure kinetics in studies to understand the reaction mechanism of bio-based Glass/PFA prepreg.
III. To develop an optimized temperature-time cure parameter based on cure kinetic studies of the bio-based PFA prepreg suitable for rapid manufacturing (Compression moulding)
IV. To achieve a developed complete optimized cure cycle (Temperature -time -pressure) and perform comparative thermal and mechanical properties analysis based on manufacturing methods between the optimized cycle manufactured laminate and conventionally manufactured laminate.

For this reason, commercially available glass fibre-reinforced PFA prepreg obtained from a UK-based company was then selected. The manufacturer's cure data sheet states that the material was intended for autoclave and oven curing processes with a total cure time of 113 minutes, including ramp-up time. This cure period, however, limits its application in high-volume industrial manufacturing where time-saving is crucial and quicker cure cycles are required.

1.5 Significance of Research

The relevance of this work has practical suitability in application areas such as the rail and automotive industries, where rapid manufacturing of fire-retardant components and parts, such as interiors of cars and trains is required in large volumes.

1.6 Thesis Structure

This research presented in the thesis is divided into seven chapters.

Chapter one provides a broad introduction and background on the research work. It describes the main research challenge, defines the aims and objectives of the effort, and outlines its structure.

Chapter two presents an extensive literature review on PFA resin. This section reviews prior research on its synthesis, chemistry, and kinetic studies. It examines in greater detail how the resin is manufactured and processed, highlighting some of the most significant processing issues encountered throughout its production. This chapter also includes a discussion of the reported mechanical, thermal, and physical properties of several fibre-reinforced composites created using different techniques. This section finishes with a summary of research areas for future consideration as it relates to the fibre-reinforced PFA composite.

Chapter three outlines and explores the research's materials and methodology. This section begins with an overview of the methodology used to conduct the experiments. Detailed explanations of the materials and processes used to manufacture the Glass/PFA composite panels utilised in the research are provided. Also described were the techniques and equipment used to characterise the mechanical and thermal parameters of the Glass/PFA composite panel.

Chapter four provides a framework for the cure kinetic model and analysis employed to optimize the cure cycle of Glass/PFA prepreg. The chapter begins with an introduction to understanding the curing process in polymeric resins. It proceeds to define relevant kinetic equations necessary to describe the relationship between numerical simulation of material structure, performance, and process in terms of relevant kinetic data analysis from experimental data equations necessary for the application cure kinetic models It proceeds to discuss in detail the two methods of cure kinetic analysis employed, their relevant equation and the difference between them. Models for predictions for isothermal curing were presented and discussed.

Chapter five presents in detail the results of the glass/PFA prepreg cure kinetic modelling studies. Discussions on the evaluation of the results in terms of the investigated curing mechanism and the subsequent optimization of the curing cycle of the prepreg based on the completed kinetic analysis. Simulation of experimental cure and characterisation analysis were also reported.

Chapter six presents, analyses, and discusses the experimental results of the mechanical and thermal characterization of the glass/PFA laminates from the two manufacturing perspectives, based on the cure cycle optimization of the prepreg derived from the cure kinetics study in comparison to the Manufacturer's recommended cure

Chapter seven concludes the report with a summary of the findings from the research work. It also outlines some of the limitations of the work and proffers recommendations for future work.

Chapter 2 Literature review

2.1 Introduction

Over the years, the impressive properties of fibre-reinforced polymer have led to increased industries adopting it for various applications. In general, carbon or glass fibre-reinforced thermosets such as epoxies, phenolics, and polyesters are used in the majority of applications. A study by Michael and Carbon Composites e.V group (Michael and Carbon Composites e.V., 2019) reported the global production volume for Carbon Fibre Reinforced Plastic (CFRP) in 2019 at 128.5kt. In the same year, the production volume of Glass Fibre Reinforced Plastic (GFRP) in Europe alone was estimated at 1,141kt (Witten and Mathes, 2019) Furthermore, the report by Michael and Carbon Composites E.V. group, forecasted a global output of 197 kt of Carbon Fibre Reinforced Plastic (CFRP) alone in 2023. This inadvertently implies that large amounts of non-degradable petroleum-based polymers are continually manufactured globally, most of which are discarded as industrial waste products after being used in the atmosphere. (Larrañaga and Lizundia, 2019). Owing to these environmental concerns and sustainability problems, this century has seen remarkable developments in green materials in the field of polymer science through the development of bio-composites (Gurunathan, Mohanty and Nayak, 2015) as an alternative to mitigate this challenge. Over the last decade, the growth in the production and application of bio-composites in different industries has experienced a tremendous increase. Bio-based composites are finding increasing use for various applications within industries such as automotive, rail, sports goods, and aviation amongst others. This renewed interest stems from the need to find environmentally friendly and sustainable alternatives to the prevailing petroleum-based composite products. According to a report by the Nova Institute, an estimated 3.8 million tons of bio-based structural polymers were produced worldwide in 2019 (Chinthapalli *et al.*, 2020). In Europe alone, bio-based industries increased by 23% from 600 million euros in 2008 to around 750 million euros in 2017 (Porc *et al.*, 2020). Sustainability, industrial ecology, eco-efficiency, and green chemistry are the fundamental and ongoing drivers of this sector, spearheading the production of the next generation of materials, goods, and processes. Recently, research, technological advancement and modifications of naturally existing polymers, as well as the synthesis of novel new polymers from renewable monomers, have rapidly expanded (Ahmad, Luyt and Djoković, 2013). One such area which has experienced rapid growth is the bio-resin sector. For example, the global demand for furfuryl, which is a feedstock of many of these types of resins, was

estimated at (USD) USD 641.8 million in 2016 and is expected to reach USD 1,200.4 million in 2022, growing at a CAGR (Compound Annual Growth Rate) of 11.0 per cent between 2017 and 2022 (Ipakchi *et al.*, 2020). The continuous development and commercialization of bio-based resins are becoming increasingly important and have enabled the expansion of bio-composite applications in various industries.

PFA resin, also known as furan resin, is one such biobased resin (Tumolva *et al.*, 2011; Domínguez and Madsen, 2015b; Moazzen *et al.*, 2018; Resch-fauster *et al.*, 2018). The PFA resin, considered one of the fully bio-based resins, is a dark brown organic polymer obtained by the acid-catalysed polymerization of furfuryl alcohol derived from renewable agricultural waste(Zarbin, Bertholdo and Oliveira, 2002; Guigo *et al.*, 2009; Ahmad, Luyt and Djoković, 2013; Domínguez and Madsen, 2014; Kumar, 2016; Marefat Seyedlar, Imani and Mirabedini, 2017; Ipakchi *et al.*, 2020). The resulting highly crosslinked network forms a solid that is brittle but possesses comparable mechanical properties as well as remarkable thermal and chemical resistance to acids, alkalis, and solvents. (Marefat Seyedlar, Imani and Mirabedini, 2020). From an environmental point of view, the PFA resin has a remarkably lower CO2 emission compared to petroleum-based resins (Tumolva *et al.*, 2011; Bachmann, Hidalgo and Bricout, 2017; Ramon, Sguazzo and Moreira, 2018), since it is derived from furfuryl alcohol which has a global warming potential (in terms of kg-CO_2-eq) of 1.3, compared to the unsaturated polyester resin at 7.5 and epoxy at 6.5 (Mofidi, Abila and Ng, 2020). Traditionally, PFA resin has been used in a variety of applications, including but not limited to binders for moulding sand in foundries (Bobrowski and Grabowska, 2012; Rivero, Villanueva and Manfredi, 2013; Holtzer, Dańko and Kmita, 2016; Chate *et al.*, 2018; Holtzer *et al.*, 2020), chemical resistance and mechanical property enhancer in polymer concrete (Muthukumar and Mohan, 2005; Kumar, 2016; Katiyar and Shobhit, 2017), adhesives for wood composite panels (Ugryumov, Varankina and Katsadze, 2019; Varodi, Beldean and Timar, 2019; Pizzi, Papadopoulos and Policardi, 2020), coatings (Rivero *et al.*, 2014; Mokhothu and John, 2017; Marefat Seyedlar, Imani and Mirabedini, 2021), a precursor to different carbonaceous products (Gandini and Belgacem, 1997; Suárez-García *et al.*, 2002; Zarbin, Bertholdo and Oliveira, 2002; Burket *et al.*, 2006; Ruiz and Pandolfo, 2011; Pin, Misra and Mohanty, 2017; Vargas-Hernández, Sulbarán-Rangel and Vázquez-Torres, 2020; Zaharopoulou, Yannopoulos and Ioannides, 2020), and corrosion-resistant materials (Gandini and Belgacem, 1997; Principe *et al.*, 2000; Fink, 2013). More recently, its commendable mechanical and thermal properties have resulted in its use in fibre polymer composite applications. The advantages of its outstanding thermal

stability and fire smoke toxicity (FST) characteristic (Hans Hoydonckx *et al.*, 2015; Modica *et al.*, 2015; Zolghadr *et al.*, 2019) as well as its environmental friendliness, have enabled it to be used in some specialized applications in industries such as railways and aerospace as a viable alternative to traditional resin. These developments in the potential of the polyfurfuryl alcohol resin system in fibre-reinforced applications have prompted UK companies such as SHD, BITREZ, and Net Composite to show interest in further advancing and commercializing the development of its prepreg for applications in industries. In recent years, research efforts aimed at a fundamental understanding of the polyfurfuryl alcohol resin have been made.

A review of the literature on the PFA resin reveals that tremendous work has been done on its preparation, chemistry, kinetics, and characterization, particularly for non-composite applications. Several authors (Gandini and Belgacem, 1997; John and Sabu, 2012; Fink, 2013; Eseyin and Steele, 2015; Luckeneder *et al.*, 2016; Jia and Fiedler, 2018) have reported on its precursor (furfural alcohol) and highlighted the furan derived processes and its capabilities for a wide range of applications. However, a comprehensive review aimed at cataloguing their mechanical, thermal, and degradation behaviour in fibre-reinforced applications is still lacking. Therefore, this chapter aims to provide an overview of the PFA resin, with a focus on its applications in fibre-reinforced composites.

2.2 Polyfurfuryl Alcohol Resin

Similar to conventional thermoset resins (epoxy, phenolic, polyester), polyfurfuryl alcohol resin is a thermally cross-linked polymer synthesized from Furfuryl alcohol (Wang and Yao, 2006). It is considered bio-based because its main monomers come from renewable resources such as agricultural waste, e.g., rice hull, sugarcane bagasse, and corn cob. The early history of the development of polyfurfuryl alcohol resin can be traced back to 1923, after the start of the industrial production of furfural a year earlier (Fink, 2013). Before that, however, Scottish chemist John Stenhouse had discovered resin's ability to be produced from furfural in 1840 (Fink, 2013). According to Iroegbu et al. (2020), Johann Wolfgang Dbereiner discovered furfural in 1832, and further studies by Limpricht et al. (1870) confirmed furfuryl alcohol as the main precursor, as stated in the same report. Despite these historical events, initial commercialization began in the early 1920s with work to commercialize furfural from corncobs initiated by LaForge and Mains of the Bureau of Chemistry (Peters, 1936) (Sarika *et al.*, 2020). Between 1920 and 1953, Peter and Dunlop at the Hull Research Facility of the Quaker Oats Company significantly advanced the commercialization of furfuryl derivatives, which includes

the polyfurfuryl alcohol resin (Eseyin and Steele, 2015; Iroegbu *et al.*, 2020). In 1970, it successively found its use in the aerospace industry (Belgacem and Alessandro, 2003). Subsequently, it was further researched and developed for various other applications and recently introduced into fibre-reinforced applications.

2.2.1 Synthesis of Polyfurfuryl Alcohol Resin

Various methods for synthesizing polyfurfuryl alcohol resin have been published in numerous studies. The pathway to the polyfurfuryl alcohol resin manufacturing process starts with the extraction of furfural by acid-catalysed hydrolysis from pentosan-rich hemicellulose obtained from viable agricultural waste (Win, 2005; Corma Canos, Iborra and Velty, 2007; Machado *et al.*, 2016; Zheng *et al.*, 2019; AL-Rekabe, Saleh and Hanoosh, 2020; Sarika *et al.*, 2020). Conventionally, the extracted furfuryl is converted to furfuryl alcohol via a catalytic hydrogenation reduction process (Gandini and Belgacem, 1997; Kim *et al.*, 1998; Iroegbu and Hlangothi, 2018; Nanni *et al.*, 2019; Marefat Seyedlar, Imani and Mirabedini, 2021). Then, the furfural alcohol (FA) is converted by acid catalysis to obtain polyfufuryl alcohol resin. The entire process is illustrated in Figure 2-1.

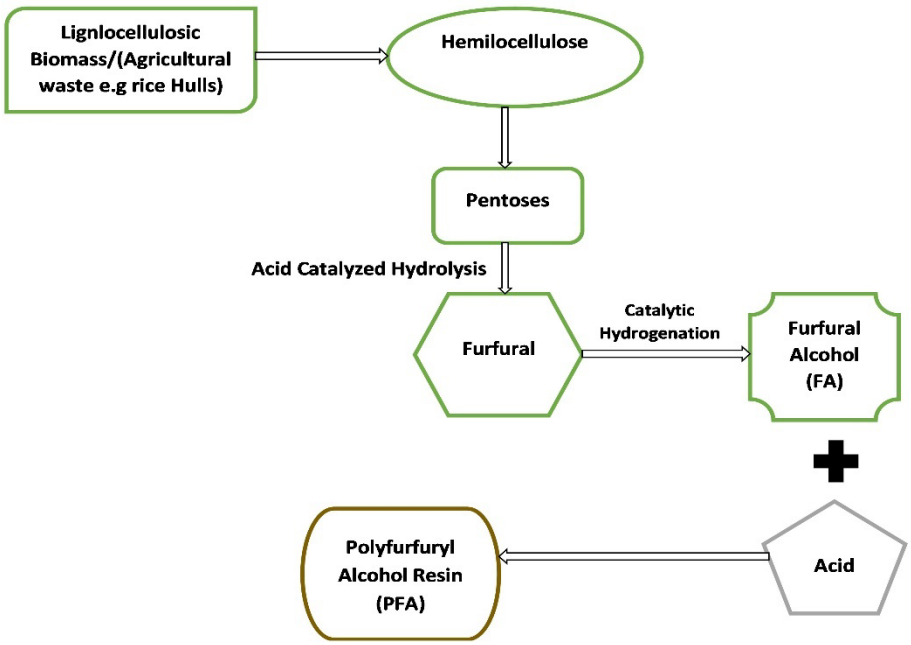

Figure 2-1 Schematic of polyfurfuryl alcohol resin manufacturing process

Furfural alcohol (FA) can be catalyzed by several types of acids. Studies show that either a strong or weak acid type can be used as a catalyst for the process. Some commonly used acid catalysts used for polymerization include mineral acids such as sulfuric acid (Oishi *et al.*,

2017), nitric acid (Origo *et al.*, 2016), organic acids (maleic anhydride, oxalic acid, p-toluenesulfonic acid monohydrate (PTSA)) (Kumar and Anandjiwala, 2012; Bosq *et al.*, 2015; Mohajeri *et al.*, 2017), and acid zeolites (zeolite Y) (Mariscal *et al.*, 2016). Greener and more sustainable catalysts such as Algerian-modified clay (maghnite-H^+ or mag-H^+) have also been found effective for polymerization as well as a potential replacement for hazardous acidic catalysts (Kherroub, Belbachir and Lamouri, 2015a). Fundamentally, the synthesis process involves mixing the furfural alcohol (FA) with the acid catalyst in a properly weighted ratio at controlled temperature and time This is done systematically to prevent explosions during the polymerization reaction while maintaining sufficient viscosity and low moisture content in the final product. Researchers have employed various techniques to achieve this. An early understanding of the process by Purnal in his patent (Purnal L. McWhorter, 1949) described the synthesis process to involve steps. The first step is the addition of acid to buffer-free hot furfuryl alcohol in an amount to initiate and continue the reaction to establish a boiling point of the reacting mixture. This is followed by continuing the reaction while boiling the furfuryl alcohol-water mixture until the condensation reaction has progressed to the desired point. Next is the removal of the acid from the system and lastly the product's distillation to obtain an anhydrous initial resin. The process of this invention offered a solution to alleviate the explosive exothermic difficulties encountered during the polymerization reaction process during synthesis. This technique was an inspiration for numerous subsequent works. As suggested in recent literature, in most cases, the acid is dissolved in a given volume of deionized water and gradually mixed with an aqueous solution of furfuryl alcohol (FA) in a given weight ratio with vigorous stirring. The mixture is heated to the FA-water azeotrope temperature for some time. Thereafter, the reaction mixture is cooled, and the pH is neutralized by the addition of an alkali such as sodium hydroxide (NaOH). The resulting emulsion mixture is broken by a saturated salt solution such as sodium chloride (NaCl) and then separated to remove the aqueous phase and water. It is worth noting that the choice of processing time and temperature depends on the type of acid used. Beyond the synthesis of the polyfurfuryl alcohol resin for reinforced composites, studies have shown its advancement for advanced applications such as resin modification (Mashouf Roudsari, Misra and Mohanty, 2017; Moazzen *et al.*, 2018; Hanifpour *et al.*, 2019; Sharma and Chopra, 2019; Zolghadr *et al.*, 2019), a precursor for various materials including polymeric carbon beads used as adsorbent for volatile organic compounds (Pophali *et al.*, 2019), carbon membranes for separation and purification applications (Zaharopoulou, Yannopoulos and Ioannides, 2020), nanocomposites for sodium-

ion battery cathode material (Hu *et al.*, 2020). The polyfurfuryl alcohol resin has also been synthesized as powders, flakes, films, and nanospheres (Pophali *et al.*, 2019).

2.2.2 Structure and Chemistry of Polyfurfuryl Alcohol Resin

A tremendous amount of research has been done using various analytical techniques to understand the polymerization chemistry involved in the synthesis and curing of polyfurfuryl alcohol resin. The molecular structural arrangement of the polyfurfuryl alcohol resin contributes significantly to physical properties such as viscosity, bonding (interaction) and thus to its processing (resinification, prepreg and curing) and thermomechanical properties, especially in fibre-reinforced applications. Despite initial assumptions that the exact structure is difficult to determine due to the rapid three-dimensional crosslinking during polymerization (Tondi *et al.*, 2015), many studies have been conducted to elucidate the molecular chemistry of the crosslinking mechanism. Tondi et al. (2019) detailed a review of various scientific studies suggesting that the molecular structure arrangement be linear, ring-opening, α, β-unsaturated γ-lactons, Methylene bridge, conjugated or Diels-Alder. Kherroub et al. (2015b) posited that the crosslinking mechanisms involve a series of acid-catalysed condensation steps which produce linear oligomers that can contain both types of molecular bridged structural arrangements namely methylene and dimethylene moieties. Overall, the consensus remains that the chemistry of its thermoset nature shows that the crosslinking process is a product of polymerization, which consists primarily of two steps. The first consists of linear oligomer formation through polycondensation and the other composition of a structural network of ring-opening and Diels arrangements leading to high branching density (Fink, 2013; Foruzanmehr *et al.*, 2016; Falco, Nathanael Guigo, *et al.*, 2018; Sommerauer *et al.*, 2019). This was corroborated by Joshua et al. (2018) who found that the Diels-Alder crosslinking and branching were prevalent in the polymerization of PFA. He attributed a significant influence on the viscosity of the resin to the chain-branching mechanism. These reactions explain the high crosslink density of PFA (Marefat Seyedlar, Imani and Mirabedini, 2017). The polymerization reaction can be complex, so variables such as acid catalyst type, concentration, temperature and solvent type have a significant impact on the overall process (Jia and Fiedler, 2018). At room temperature, the rate of polymerization can vary from hours to weeks, depending on the acid catalyst (Origo *et al.*, 2016). Wang et al. (2018) and Origo et al. (2016) postulated that a strong mineral acid generally results in a very rapid cure, while a complete cure is difficult when using weak acids. Therefore, the polymerization kinetics can be varied considerably for specific applications (He *et al.*, 2012).

2.3 Cure Kinetics of Polyfurfuryl Alcohol Resins in Fibre-reinforced Application

Efficient processing of the bio-based polyfurfuryl alcohol resin for various applications or investigations requires knowledge of its processing conditions (curing temperatures, time, pressure). Therefore, the essence of understanding its cure behaviour cannot be overstated. Researchers have employed various techniques to understand the cure behaviour and evaluate the kinetics of polyfurfuryl alcohol resin from different perspectives. For example, Domínguez and Madsen (Domínguez and Madsen, 2014) documented research into the resin's rheological and chemorhelogical behaviour. Their study found the flow activation energy of the PFA resin increases with a corresponding increase in the amount of catalyst. However, despite a documented curing activation energy of 96 kJ mol−1, they found no catalytic dependence on the curing activation energy. The complete curing and polymerization complexity of the resin was studied using chemorheological and isoconversional analysis by Guigo et al. (2007),. Vargas, Scheubner and Guthausen (2018) studied the polymerization of the resin through the influence of nanoparticles on the curing reaction kinetics. Further studies on the kinetics of the resin were carried out by Lopez De Vergara et al.(2014) using a chemical characterization method to understand the mechanism responsible for the main reactions of the resins during curing., Similarly, Sadler et al. (2018) detailed the resin polymerization reactions and kinetics of the study from a molecular structure viewpoint. Regarding the manufacturing process, Seyedlar, Imani and Mirabedin (Marefat Seyedlar, Imani and Mirabedini, 2016) and Behzadfar, Imani and Farahmandghavi (Behzadfar, Imani and Farahmandghavi, 2019) investigated its reaction kinetics to determine the resin’s pot and shelf life respectively. Additional works by Domínguez, Grivel, and Madsen (2012), Seyedlar, Imani, and Mirabedin (2017), and Rivero et al. (2011) attempted to characterize the polyfurfuryl alcohol resin through kinetic studies by the varying catalyst type, quantity and filler effects. The outcome of these various studies has provided industrial manufacturers with the fundamentals of a window for selecting parameters suitable for using the selected manufacturing process cycle in various applications, including fibre-reinforced composites. Despite the successes, it is worth noting that all previous research studies were performed using synthesized neat resin alone leaving the kinetic studies of fibre-reinforced polyfurfuryl alcohol-based prepreg still to be researched.

2.4 Polyfurfuryl Alcohol Resin Processing and Fibre Reinforced PFA Composites Manufacture

With the resin processing condition window determined via various kinetic methods, the processing and manufacturing of fibre-reinforced polyfurfuryl alcohol-based composites with different manufacturing processes are made possible. Conventional manufacturing techniques such as hand layup, autoclave processing, resin transfer moulding (RTM), microwave processing and compression moulding are some of the commonly used techniques in the manufacture of fibre-reinforced PFA composites. Several types of fibre have been reportedly used as reinforcements in the manufacture of polyfurfuryl alcohol-based composites. For example, conventional fibre like glass fibre was used in the manufacture of PFA-based composite for comparative property studies with fibre-reinforced phenolic composites by authors (S. Giannis *et al.*, 2008; Hans Hoydonckx *et al.*, 2015; Ipakchi *et al.*, 2020). Natural fibres such as abaca, flax, basalt, rayon and jute have also been reported as reinforcement for PFA-based composites for various investigative and comparative research studies (Arnold *et al.*, 2009; Kumar and Anandjiwala, 2013; López De Vergara *et al.*, 2014; Talent and Wang, 2015). Processing polyfurfuryl alcohol resin, like other thermosetting matrices for composites, requires a careful application of processing conditions to monitor the viscosity formation in the final composite, which is highly dependent on temperature and polymer structure. Fibre wettability, bubble formation and growth, and composite consolidation are all affected by the continuous transition of resin from a low-viscosity liquid monomer at the start to a solid polymer at the end of the phase (Carotenuto and Nicolais, 1998).

2.4.1 Resin and Laminate Curing

With appropriate curing parameters and process, the PFA resin, like other matrices, can be cured in neat or fibre-reinforced form. However, unlike other resins which are relatively easy to cure, PFA resin cannot be said to be the same. This type of resin requires careful application of processing conditions because volatiles and water (moist) evolve during the curing process These emissions are by-products of (i) solvent water from the resin; (ii) solvent water from the catalyst; and (iii) condensation water from curing of the resin (Domínguez and Madsen, 2015a). In fact, according to Foruzanmehr et al. (2016) and Deka et al. (2014), one mole of water in vapour evolves for every mole of crosslinked resin formed during curing due to the exothermic reaction. This phenomenon allows for the occurrence of potential problems such as warping, voids, and delamination Figure 2-2 (A) and (B), which result in reduced mechanical properties

of the final cures resin or composite when processed incorrectly. To mitigate this challenge, a slow and multi-stage curing cycle is typically employed during processing. This is done to potentially limit the water formed during the condensation reaction during curing (Rivero, Villanueva and Manfredi, 2014).

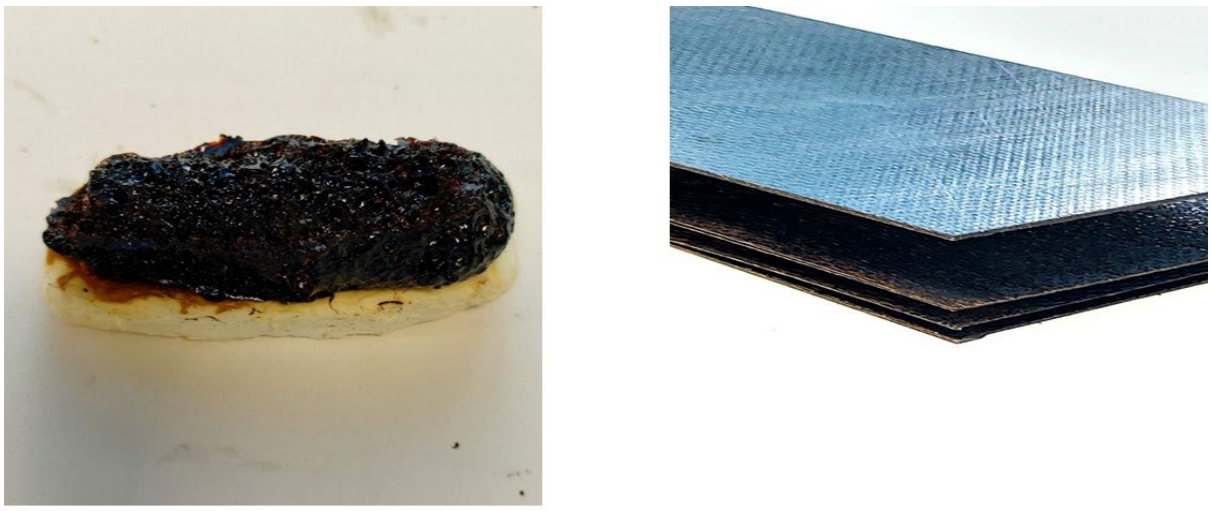

(A) (B)

Figure 2-2 (A) Bubble defects of an improperly cured PFA resin (B): Delamination of an improperly cured PFA Prepreg

A combination of multistep curing and modification in manufacturing methods have also been reported to help mitigate this challenge. For example, Dominguez et al. (2015a) effectively employed the combination of two steps curing cycle and the double-vacuum-bag technique to study the volumetric composition and mechanical properties of the glass fibre/PFA composites with an emphasis on porosity content. They concluded that with higher water removal efficiency during manufacture, lower porosity and brittle stress-strain behaviour of the furan matrix would develop. Other water reduction techniques include intermittently opening and closing moulds in manufacture using compression moulding processes by Džalto et al. (2014) and Resch-fauster et al (2018) in their respective studies. Improving the processability of the PFA-based composite through the use of hydrophilic reinforcements such as hemp, and flax was another technique also considered (Resch-Fauster *et al.*, 2018). Overall, a review of major studies reveals the cure processing temperature could range from 20°C to 180°C over a cure duration range of between 1 hour – 96 hours regardless of the manufacturing method employed (Rivero, Villanueva and Manfredi, 2014; Kandola, Ebdon and Chowdhury, 2015; Talent and Wang, 2015; Sharib, Kumar and Kumar, 2018; Ma *et al.*, 2020).

2.5 Review of Properties of Polyfurfuryl Alcohol Reinforced Composite

2.5.1 Mechanical Properties

The mechanical properties of PFA resin and its reinforced composites depend on the configuration of several factors. Some of these factors include curing conditions and parameters, manufacturing method, fibre type, fibre orientation, form type (Fabric or fibre), and matrix modification amongst others. As a result, several studies have been conducted to evaluate the strength and other properties of this resin and composites as a function of some of these factors. The mechanical properties of the PFA resin and its reinforced composite are well reported. In comparison to other neat resins, Crossley et al. (2014) found the neat PFA resin to have a max tensile strength of 39.4Mpa and a tensile modulus of 3.0 GPa. They discovered that the cured PFA resin had comparable tensile properties to the phenolic resin but was 60% less than the neat, cured polyester resin. In the study of renewable resource green blends from polyfurfuryl alcohol resin and lignin, Deka et al. (2014) reported the flexural strength and modulus of the pristine resin to be 23 MPa and 1.9 GPa, respectively, while recording 15 Jm^{-2} as the impact strength found using the IZOD test. The study found the effect of blending improved the properties of flexural strength, storage modulus, and glass transition significantly. Similarly, the impact strengths, flexural strengths and moduli of a cured blend of furfuryl alcohol/epoxy/methyl-tetrahydro-phthalic anhydride blends with different ratios was found superior to the neat cured PFA resin in the studies by Wang et al. (2017, 2018). Both studies documented 38.05 MPa, 2.2GPa and 2.50 kJ/m^2 as the respective value for the flexural strengths, flexural modulus, and impact energy of the neat resin. The incorporation of 0.5% polylactic acid (PLA) fabric into the PFA resin was also found to increase the tensile strength of the neat PFA resin from 11.2 ± 1.1 MPa to 33.2 ±3.5 MPa (Sharib, Kumar and Kumar, 2018). Similarly, for the same percentage weight of polylactic acid (PLA) fabric PLA in the PFA resin, the flexural modulus increased from 1.96 GPa to 3.37 GPa.

Furthermore, the addition of fibre reinforcement has proved to improve the mechanical properties of the PFA-based composite. Several studies have been conducted to investigate some of the different mechanical behaviour of these PFA-based composites as a function of different manufacturing configurations. Table 1 summarizes the findings of some studies on the mechanical properties of some of the common fibre-reinforced PFA-based composites.

Table 2-1 Mechanical properties of fibre-reinforced polyfurfuryl alcohol composites from literature.

PFA Composite	Form (Fabric or Fibre)	Manufacturing method	Cure Cycle	Fibre Content	Tensile strength (MPa)	Tensile Modulus (GPa)	Flexural Modulus (GPa)	Flexural strength (MPa)	Impact strength (kJ/m^2)	Reference
Flax /PFA	Fabric	Vacuum-assisted resin transfer moulding (VARTM)	60°C at 4h (1°C/min ramp) 95°C for 4h (Post Cure)	31.5 (%vol)	41	5.6	~ 7	~ 80	~ 80	(Crossley, Schubel and Stevenson, 2014)
Glass/PFA	Fabric	Vacuum-assisted resin transfer moulding (VARTM)	60°C at 4h (1°C/min ramp) 95°C for 4h (Post Cure)	44.6 (%vol)	850	36.5	~ 30	~ 850	~ 350	(Crossley, Schubel and Stevenson, 2014)
Basalt /PFA	Fabric	Hand lay-up/Compression moulding	80°C for 8h & incremental to 220°C	71 (% wt)	-	-	5.45 ± 0.90	94.15 ± 8.50	70.51 ± 6.31	(Wang *et al.*, 2017)
Glass/PFA	Chopped Strand Mat fabric	Vacuum Bag	Room temperature at 140°C, 50°C for 45mins and 80°C for 45mins,80°C for ~18hrs (Post cure)	68 (% wt)	93 ± 8	7.2 ± 1.0	-	-	-	(S. Giannis *et al.*, 2008)
Flax /PFA	Prepreg	Vacuum Bag	150°C for 15mins	60 (% wt)	64 ± 9.5	8.5 ± 0.8	-	-	-	(S. Giannis *et al.*, 2008)

Flax & Polyester / PFA	Woven Prepreg	Compression moulding	150°C for 7mins	52 – 58 (% wt)	38 - 58	9-May	-	-	28-Sep	(Džalto, Medina and Mitschang, 2014)
Kenaf/PFA	Fibre	Hand lay-up/Compression moulding	50-55°C for 30mins 60°C for 4h 80°C for 4h 100C for 1h (Post cure)	20 (%wt)	~ 41	~ 1.36	~ 4.6	~ 75	60	(Deka, Misra and Mohanty, 2013)
Flax/PFA	2X2 Twill prepreg	Vacuum moulding	150°C for 20mins (5°C/min ramp)	-	34.9±1.84	6±0.47	-	-	-	(Crossley *et al.*, 2012)
Flax/PFA	UD Flax, roller infused	Vacuum moulding	150°C for 20mins (5°C/min ramp)	-	59 ± 4.3	10±0.8	-	-	-	(Crossley *et al.*, 2012)
Flax/PFA	UD Flax Prepreg	Compression moulding	140°C for 20mins (5°C/min ramp)	-	211 ± 24	25.6±1.9	-	-	-	(Crossley *et al.*, 2012)
Flax/PFA	2X2 Twill prepreg	Compression moulding	140°C for 20mins (5°C/min ramp)	-	69 ± 3	10.4 ±0.4	-	-	-	(Crossley *et al.*, 2012)
Glass/PFA	Woven Fabric	Hand lay-up	80°C for 24h 100C for 24h (Post cure)	58 (%wt)	150	1.6	12.75 ± 0.18	201.99 ± 1.52	-	(Ipakchi *et al.*, 2020)
Glass/PFA	Chopped Strand Mat fabric	Vacuum moulding	20°C for 150mins 50°C for 45mins	44 (%wt)	103	7.7	4.7	110	-	(Arnold *et al.*, 2009)

			80°C for45 mins							
Hemp/PFA	Non-woven mat	Vacuum moulding	150°C for 15mins	23 (%wt)	-	-	~ 2.9	-	-	(Arnold *et al.*, 2009)
Flax/PFA	Flax UD stitched fabric	-	-	41 (%vol)	-	-	9.6	99.4	-	(Arnold *et al.*, 2009)
Carbon/PFA	Carbon fibre twill	-	-	39 (%vol)	-	-	26.2	364.7	-	(Arnold *et al.*, 2009)
Glass/PFA	Glass plain weave fabric	-	-	47 (%vol)	-	-	9	104.6	-	(Arnold *et al.*, 2009)
Jute/PFA	Mat	Compression moulding	150 °C for 90 min	50 (%wt)	11.0 ± 1.3	371 ± 15	-	-	-	(Sangregorio *et al.*, 2021)
Flax/PFA	Woven fabric	Compression moulding	170 °C for 2 h	40 (%wt)	15.53	-	2.4	23.2	24.9	(Kumar and Anandjiwala, 2013)
Rayon/PFA	UD Rayon (HTR)	Compression moulding	40°C for 12 h 60°C for 12h 80°C for 6 hours. 110°C for 1h (Post Cure)	64 (%wt)	121	5.58	5.91	87.4	-	(Talent and Wang, 2015)

Looking at the data in Table 2-1, the variation in the established mechanical properties regardless of fibre/PFA configuration gives a clear indication that the mechanical properties are significantly affected by several factors such as those mentioned previously. This concept was corroborated by Fam et al. (2014) who found out that parameters such as type of resin, type and dosage of catalyst, and curing time have little effect on Young's modulus but a significant effect on tensile strength. A comparative study of the mechanical properties of the PFA-based composites with conventional resin-based by Crossley et al. (2012) reveals that the mechanical performance of the glass/PFA was shown to be equal to that of the glass-reinforced epoxy, polyester, and phenolic composites with only a minor performance loss observed in the flexural strength in comparison to glass/phenolic. Ipakchi et al. (2020) reported 45% and 33% higher flexural and tensile strengths than that of a glass/ phenolic composite. S. Giannis et al. (2008) also found its tensile strength to outperform both glass/polyester and Flax/PFA composites. Natural fibre reinforcement composites in general, such as flax/PFA, have lower mechanical properties than glass/PFA or carbon/PFA, according to Table 2-1.

2.5.2 Thermal Properties

Numerous studies have established the thermal stability of the polyfurfuryl alcohol resin and its composites. Its excellent thermal and fire properties have been attributed to its extensive charring (Monti *et al.*, 2015). The aromatization that the resin achieves through thermal dehydration of the Diels– Alder adduct structures explains its thermal resistance, stability and response to fire (Monti *et al.*, 2015). According to Rivero et al. (2013), the degradation behaviour of the PFA resin is similar to that of a typical phenolic resin. Overall degradation occurs at temperatures ranging from 350°C to 600°C, which they attribute to the occurrence of molecular chain scission/fragmentation. At temperatures above 600°C, they observed the development of carbonaceous residue or char. Monti et al. (2015) observed through thermogravimetry that the thermal decomposition mechanism of the resin's chemical bonding structure leads to the disintegration of the crosslinked structure, generating volatile combustible chemical moieties, while simultaneously undergoing rearrangement to form a stable char structure.

Guigo et al. (2009) in a comparative study with a PFA Silica hybrid discovered that the degradation of the resin involved several steps beginning with the chain scission at over 200°C. This allows for the weakening of the chemical bonds leading to the second and third decomposition steps that occur at about 320°C. The thermal decomposition temperature which

corresponds to the 10% weight loss was around 340°C. In a related study of the thermo-oxidative degradation of the polyfurfuryl alcohol /plasticized lignin blend (Guigo *et al.*, 2010), it was found that the neat PFA exhibited better thermal stability compared to the blend. It was found that the thermal stability of the PFA decreases with increasing lignin content. Menager et al (2019) in agreement with other authors Bosq et al. (2015) and Falco et al. (2018), confirmed a multi-step degradation process of the PFA resin with a corresponding degradation temperature of 10% weight loss is about 378 °C. Recently, a characterization study by Ma et al. (2020) also found that the thermal stability of PFA resin is improved with increasing modified hollow glass microsphere (HGM) content (0% to 20%). The mass residual rate was also reported to increase from 53% to 64.4%. For fibre-reinforced PFA-based composites, their degradation behaviour has been compared to some conventional-based composites. The degradation behaviour of the glass/PFA composite was reported to be comparable with that of a glass/phenolic composite in a study by Ipakchi et al. (2020). Their study revealed char yields of up to 77-85% for PFA samples measured at 800°C. For natural fibres such as kenaf bio fibre, the degradation pattern has been reported to show a four-stage degradation pattern. The green composite (kenaf/PFA) showed the same decomposition onset temperature as the neat PFA resin, however, the maximum decomposition rate decreased from 468°C to 458°C with increasing fibre content and a 45 per cent retention of char residue. The decrease was attributed to an increase in the thermally unstable non-cellulosic structure of the fibre composite (Deka, Misra and Mohanty, 2013). Similarly, Talent and Wang (2015), reported a 7% mass loss at 200°C in a study that addressed the thermal degradation of unidirectional Cordenka rayon/PFA composite. At a temperature of 275°C, the composite showed rapid mass loss attributed to the degradation of the cellulosic structures of the unidirectional cordenka rayon (CR) fibres. The degradation effect worsened as the per cent fibre weight in the composite increased.

2.5.3 Water Absorption

It is known that water absorption affects the physical, mechanical and thermal properties of fibre-reinforced composites (Assarar *et al.*, 2011; Apolinario *et al.*, 2016). For composite applications where exposure to the atmosphere or wet conditions is required, evaluation of this property is very important. The PFA resin is known to be inherently hydrophobic (Vargas, Scheubner and Guthausen, 2018; Vargas-Hernández, Sulbarán-Rangel and Vázquez-Torres, 2020) and therefore, it can be expected to result in increased water resistance of its composite. Menager et al. (2019) noted this in their work on green composite with cork residues, where they discovered that the hydrophobicity of PFA composites increases with a corresponding

increase in PFA content. The resin was also found to improve the moisture resistance of the treated flax fibre in a study by Jia and Fiedler (2018). The study found that treated flax fibre absorbed only 1.389% of the water of its original weight over 10 days. In a related study on green composites, Deka et al. (2013) reported that the water uptake of the pure PFA resin at saturation is 1.12%. In a comparative study between Glass/Phenolic and Glass/PFA composite by Foruzanmehr et al. (2016) the sorption rate of the Glass/PFA composite was 3.35 times higher than the Glass/Phenolic composite. At saturation, moisture absorption was found to be higher in Glass/PFA composite than in glass/phenol. This they attributed to the high porosity level of the Glass/PFA. The effect of which was evident in their interlaminar shear property which showed a 13.1% increase in favour of Glass/Phenolic composite after 90 days. Relatedly, Sangregorio et al. (2021) reported no increase in mass of Jute/PFA over eight hours in their work whilst a 25% increase in mass was observed for Jute/Humins composite after half an hour attributing this to the low porosity level in the PFA based composite in comparison to the Humins based composite.

Beyond investigating the water absorption behaviour of glass/PFA, flax/PFA and glass/polyester composite, Giannis et al. (2008) went further to assess the behaviour of these composites on exposure to different fluids including motor oil, Hydraulic oil, Diesel oil, Antifreeze, windscreen wash and pesticide and distilled water. Both cases of the PFA-based composite were reported to absorb a significant amount of fluids, with the flax/PFA absorbing the most. They observe the effect of the fluid exposure to be more detrimental on the flax/PFA composites than on others.

2.5.4 Fire, Smoke and Toxicity Properties

In recent years, fire, smoke, and toxicity (FST) properties are increasingly important factors in the choice of fibre-reinforced polymer composites for industrial applications. For example, within the rail industries, these properties are stringent fire, smoke, and toxicity FST requirements such as the R1HL3 classification are used to evaluate fibre-reinforced composite parts to be used indoor applications in railway vehicles (Elejoste *et al.*, 2022). Polyfurfuryl alcohol resin and its fibre-reinforced composite exhibit remarkable fire behaviour. This is due to the high aromatic content, which accounts for the transition to a carbonaceous barrier that serves as a thermal shield when the resin surface is exposed to fire. This is evident from the work of Crossley et al. (2014) which compared the flammability of glass and flax-reinforced polyfurfuryl alcohol composites with epoxy, phenolic, and polyester-reinforced glass and flax

composites, respectively Using the UL94HB and UL94VB flammability test methods, they observed that both glass and flax-reinforced polyfurfuryl alcohol composites passed the UL94HB test with minimum smoke and no flame, attaining a standard rating of C. However, with the vertical burn test (UL94VB), the flax-reinforced polyfurfuryl alcohol composite failed the test. They noted that the flax-reinforced polyfurfuryl alcohol composite failed the vertical burn test (UL94VB) while the glass-reinforced polyfurfuryl alcohol composite was found to pass the same test without drips or smoke, earning a V-0 rating.

Similarly, other authors have documented the fire, smoke and toxicity (FST) performance of the polyfurfuryl alcohol resin and its reinforced composite in comparison to related composite materials. Table 2-2 below details some of the results documented in literature.

Table 2-2 Fire and smoke properties of polyfurfuryl alcohol resin and its fibre-reinforced composites from literature

Material Form	Test Method	Dimensions (mm)	Time to Ignition (TTI) (s)	Total heat released (THR) (MJ/m^2)	Peak of heat release rate (PHRR) (kW/m^2)	Total smoke released. (TSR) (m^2/m^2)	Maximum Average Rate of Heat Emission (MARHE) (KW/m^2)	Specific extinction area (m^2/kg)	Effective heat of combustion (EHC) (MJ/kg)	Reference
Neat PFA resin	Cone calorimetry	100 x 100	25	38.6	981	38.6		709	17.3	(Kandola and Krishnan, 2014)
Flax/PFA composite	Cone calorimetry	100 x 100	104 ± 2	45 ± 5	450 ± 50	315 ± 10			16	(Kumar and Anandjiwala, 2013)
Neat PFA resin	Cone calorimetry	5 (round)	25	39	981	290			17.3	(Kandola, Ebdon and Chowdhury, 2015)
Neat PFA resin	Cone calorimetry	100 × 100	50	75.4	393			36.8	19.8	(Rivero, Villanueva and Manfredi, 2014)
Neat PFA resin	Cone calorimetry	52	98	30.9	682	15.3	154			(Monti *et al.*, 2015)
Glass/PFA	Cone calorimetry		125	19.6	44,09		16.96			(Hans Hoydonckx *et al.*, 2015)

2.6 Applications Of Fibre Reinforced Polyfurfuryl Alcohol Composites

The application of fibre-reinforced Polyfurfuyl Alcohol composites applications in various applications has gained much attraction recently. Since then, several joint European Union projects to develop the PFA have yielded impressive results. For example, in the FIRE RESIST project, where the aim was to study the resin for fireproof composite applications, it was found that the developed glass fibre-reinforced PFA composite achieves an HL3 classification of the fire safety standard for rail applications. The glass/PFA laminates were also used in a sandwich construction of an innovative partition that met stringent fire test criteria well below the 60-minute limit (Hans Hoydonckx *et al.*, 2015). A related BIOCOMP project of the European Commission through the 6th Framework Program evaluated the applicability of the polyfurfuryl alcohol resin for composite fabrication. The outcome of the project led to comparable prototypes of automotive exterior panels, vehicle mounts and bathroom floor sandwich panels made of glass and natural composite (Flax/PFA) respectively (Eisenreich, 2008; S. Giannis *et al.*, 2008; Arnold *et al.*, 2009). Within the rail industry, a UK-based TRB Lightweight Structures Ltd. has developed and produced a railway carriage carbon-reinforced polymer (CFRP) sandwich panel door appropriate for subterranean rail applications utilising a carbon fibre/ PFA prepreg and recycled foam (Iroegbu and Hlangothi, 2019).

2.7 Summary and Critical Review

So far, the polyfurfuryl alcohol resin has been reviewed extensively, focusing on its fibre-reinforced composites. The bio-based resin is produced through the synthesis of furfuryl alcohol and a catalyst under controlled conditions. A review of existing studies on resin structure, chemistry and cure kinetics was also highlighted. The fabrication of the reinforced composite was also discussed, detailing the key challenges during the curing process as well as some mitigation techniques found in the literature. In addition, the mechanical and thermal properties of the resin and its common fibre-reinforced composites were reviewed. Its mechanical properties also proved to be comparable to conventional matrices and their composites as posited by literature. Regardless of the fibre/PFA configuration, it is evident from the review that the mechanical properties of the various composites are highly dependent on factors such as curing conditions and parameters, manufacturing process, fibre type, fibre orientation, shape type (fabric or fibre), and matrix modification, among others. The review

also noted the excellent thermal stability and fire response of PFA resin and its composites. Despite the thermal benefits and structural potentials of reinforced- PFA composites, it is clear from the literature that the major drawback of a lengthy manufacturing process cycle has often prevented the industrial scaling up of its use for applications. Therefore, there is a need for researchers to develop applicable techniques to aid the reduction in manufacturing process time without any detrimental effect on its mechanical or thermal properties. Diverse techniques have been successfully employed to achieve a similar goal with conventional resin and its composites. However, with the PFA resin and its composites, these same techniques are directly inapplicable due to their unique curing nature. As a result, it does require an adequate understanding of its curing mechanism to enable process optimization for rapid manufacturing. Despite researchers efforts to understand the cure kinetics of the polyfurfuryl alcohol resin as earlier discussed, these efforts have been limited to the resin alone leaving the understanding of the curing mechanism of the fibre-reinforced prepreg to be desired. Consequently, highlights the need for this research study.

Chapter 3 Material and Research Methodology

3.1 Introduction

Figure 3-1 illustrates the methodology used to conduct this research work. It begins with incorporating experimental thermal analysis of the biobased glass/PFA material from the Dynamic Scanning Calorimetry (DSC) and the Dynamic Mechanical Analyzer (DMA) into phenomenological cure kinetic models taken from the literature to understand the unique cure mechanism of the biobased Glass/PFA prepreg's, developed an optimized cure cycle (temperature-time), and make kinetic cure predictions. A comparison is then made between the optimal cure cycle derived from the kinetic studies and the curing cycle recommended by the manufacturer, leading to the second phase of the work, which involves the actual laminate fabrication. Laminates were then manufactured using two different manufacturing methods. First, by oven curing method using the manufacturer-recommended cure schedule and then by the application of compression moulding technique using a developed optimized curing cycle at two predetermined pressures. Panels manufactured using the compression moulding methods were then subjected to mechanical and thermal properties characterization to ascertain the pressure, temperature, and time combination with the best property. This would then be compared to the mechanical and thermal characterized properties of the oven-cured sample manufactured using the manufacturer's recommended cure cycle.

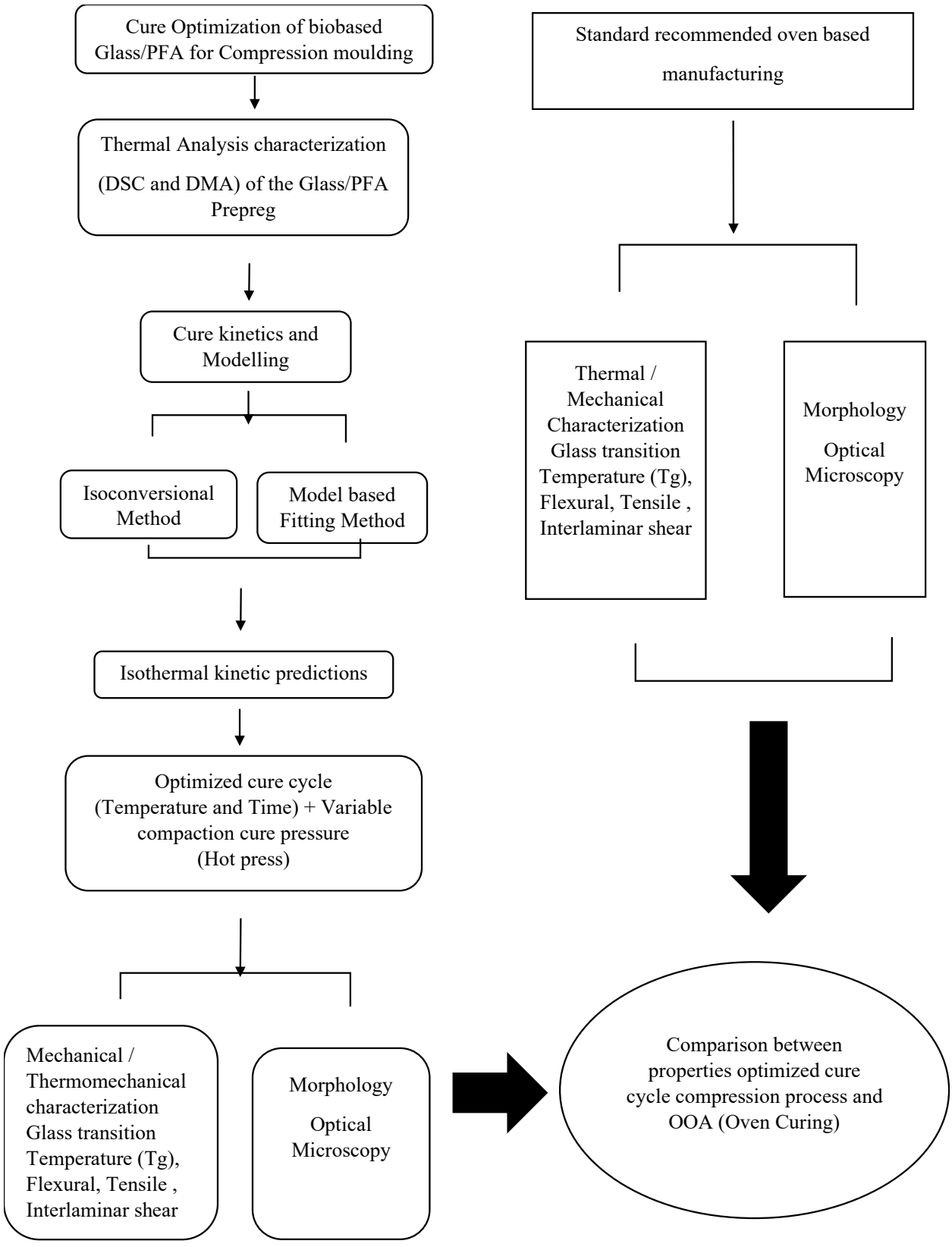

Figure 3-1 Illustration of research methodology

3.2 Material

This research work was conducted using a commercially available glass fibre pre-impregnated with polyfurfuryl alcohol resin manufactured by SHD Composites UK. Prepreg materials are generally resin-enriched reinforced fabric pre-cured with high molecular weight to limit the resin flow, which enhances storage and processing (Shah *et al.*, 2019). The prepreg consists of 7781 styled E-Glass fabric with eight harness satin weave structures and an area weight of 300 grams per square meter infused with a polyfurfuryl alcohol matrix. The composition and concentration of the resin system are not disclosed. The prepreg had a resin weight content of 38%. The prepreg manufacturer suggested a cure cycle (Figure 3-2) of a ramp-up from room temperature to 130°C at 2-3°C/min, followed by a 60-minute dwell at the same temperature. After curing, the laminate is allowed to cool down to room temperature before demoulding, as no specific cooling rate was specified. The cycle was recommended for both autoclaves and oven-curing processes.

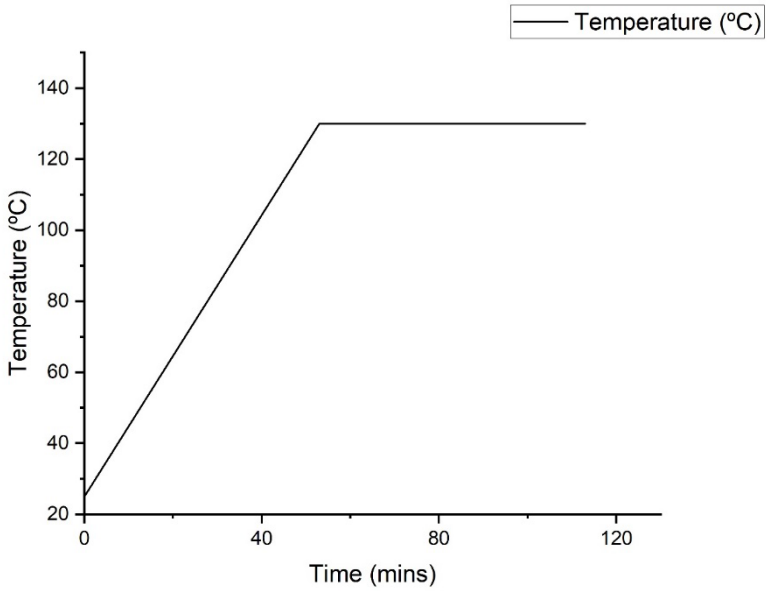

Figure 3-2 Prepreg Manufacturer's recommended cure cycle

3.3 Thermal Analysis Technique

The application of thermal analysis cuts across various processes in different fields. According to Guigo and Sbirrazzuoli (Guigo and Sbirrazzuoli, 2018), "Thermal Analysis is a set of techniques of "materials" characterization (in the wide sense of the term) based on the variation of a physical property with time (at constant temperature or, if this condition cannot

experimentally be fulfilled, it is at least measured) or with temperature". It is extensively used in polymer composite application areas and has been employed to characterize polymers ranging from basic applications such as enthalpy measurement, glass transition temperatures, melting temperatures, and heat of crystallizations to more advanced applications involving kinetic evaluations of thermally stimulated processes such as degradation, polymerization, and crystallization (Vyazovkin, 2019). Thermogravimetric Analysis (TGA), Differential Scanning Calorimetry (DSC), Evolved Gas Analysis (EGA), Differential Thermal Analysis (DTA), and Derivative Thermogravimetry (DTG), among others, are common experimental techniques used to perform thermal analysis. The definition of each technique depends on the kind of physical transformation being analysed.

For this, based on the requirement of research to investigate the curing process, parameters on the enthalpy, glass transition, dimensional stability and shrinkage are necessary for which of the investigated material, the Differential Scanning Calorimetry (DSC), Dynamic Mechanical Analyzer, (DMA) and Thermomechanical Analyzer (TMA) were employed for the investigative work.

3.3.1 Differential Scanning Calorimetry (DSC) Measurements

Differential Scanning Calorimetry (DSC) is a thermodynamical tool for direct assessment of the heat energy uptake, which occurs in a sample within a regulated increase or decrease in temperature (Gill, Moghadam and Ranjbar, 2010). In other words, Differential Scanning Calorimetry (DSC) makes it possible to quantitatively measure endothermic or exothermic enthalpy changes in a material. Typically, the temperature program for a DSC analysis is designed so that the sample pan temperature increases linearly with time. (Nagashree, 2015). The application of DSC analysis enables the measurement and evaluation of thermal transitions such as glass transition temperatures, melting, thermal curing and enthalpy of polymeric material as a function of temperature. Based on the mechanism of operation, DSC can be categorized into two common types: heat-flux DSC and power-compensated DSC (Hatakeyama and Hatakeyama, 2005; Gill, Moghadam and Ranjbar, 2010).

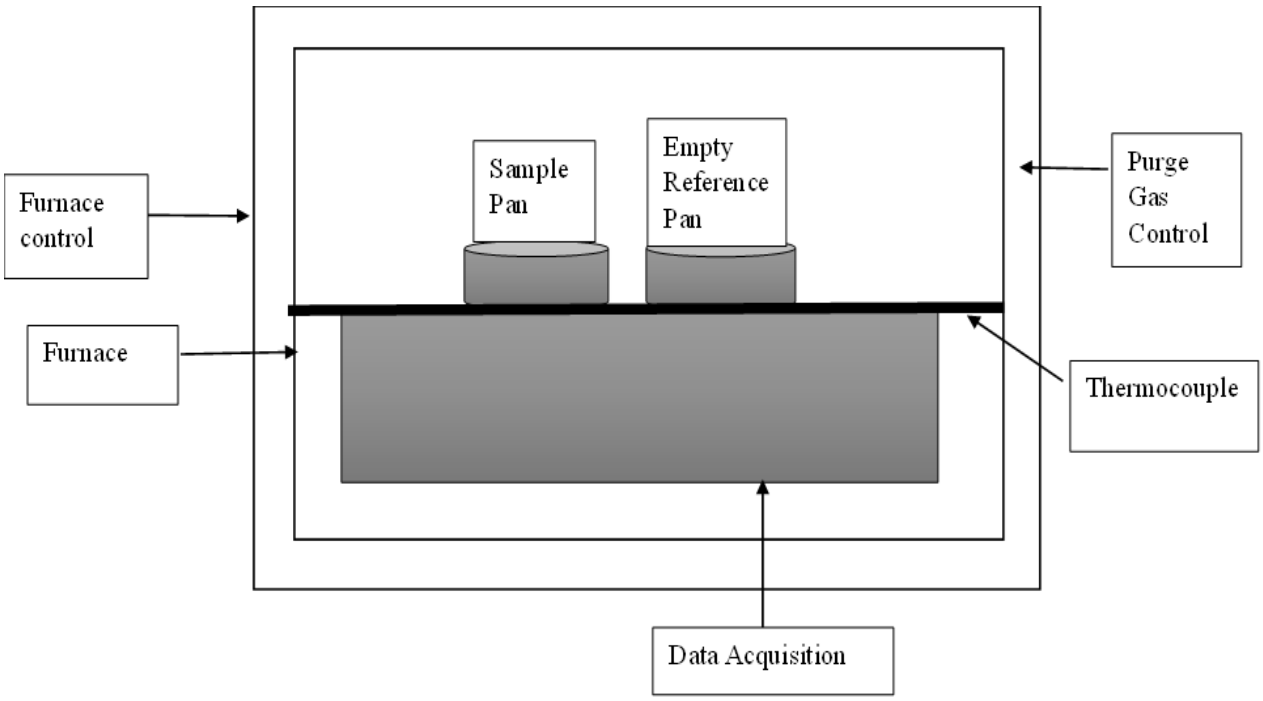

Figure 3-3 Block diagram of heat flux DSC principle.

The operating principle of the heat flux DSC which is commonly used is shown in the schematic block diagram in Figure 3-3, the operating principle of a DSC experiment involves heat flow from a furnace to a sample material which is measured relative to a heat flow to reference material. The reference and sample pans are identical except that the reference pan is empty. In other words, during a temperature change, DSC measures a heat quantity, which is radiated or absorbed excessively by the sample based on a temperature difference between the sample and the reference material. It is sensitive enough to detect the heat changes associated with melting, evaporation, glass transition, and chemical reactions (Stark, 2013). The total heat flow from the DSC is simply proportional to the temperature difference between the pans (Heinze and Echtermeyer, 2018) and maybe as expressed in equation *(3.1)*

$$\Delta \boldsymbol{T} \propto \frac{\boldsymbol{dQ}}{\boldsymbol{dt}} = \left(\frac{\boldsymbol{dQ}}{\boldsymbol{dt}}\right)_{\boldsymbol{sample}} - \left(\frac{\boldsymbol{dQ}}{\boldsymbol{dt}}\right)_{\boldsymbol{reference}} \qquad (3.1)$$

The heat flow measurement of the Glass /PFA Prepreg sample material was performed on a Perkin Elmer 4000 Differential Scanning Calorimetry (DSC) calibrated by an indium standard under a nitrogen atmosphere of 20 mL/min shown in Figures 3-4.

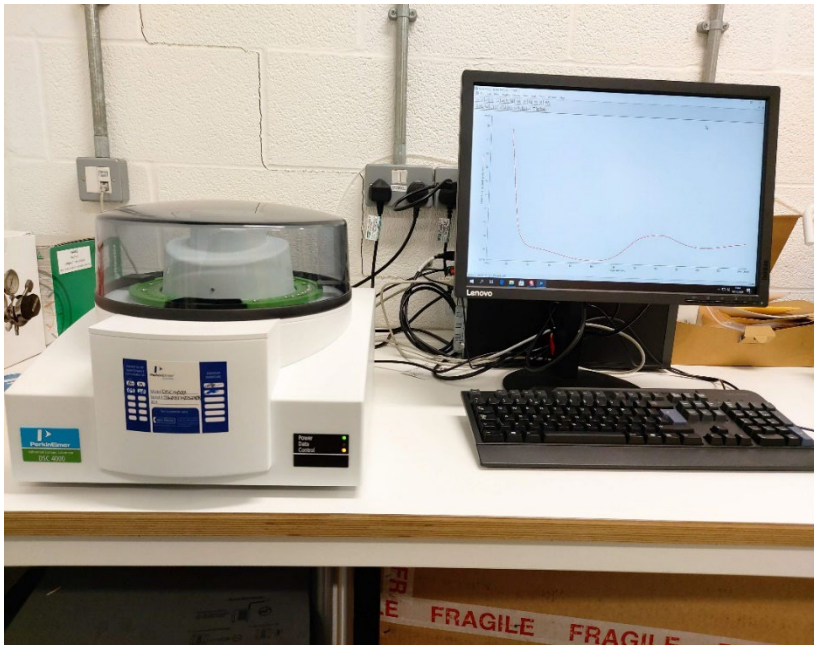

Figure 3-4. Perkin Elmer Dynamic Scanning Calorimetry (DSC) 4000

9-10 mg of the sample prepreg material was placed into a sealed crucible pan and heated under non-isothermal conditions according to the recommendations of the ICTAC Kinetics Committee (Vyazovkin *et al.*, 2014). A sealed crucible was used to avoid endothermic variations associated with the evaporation of vapour during the polycondensation of furfuryl alcohol monomer on heating (Guigo and Sbirrazzuoli, 2018).

Dynamic temperature runs were carried out at four different heating rates (5,10,15,20 °C/min) within a scanning temperature range of 25°C-250°C. The experiments were performed under a constant flow of nitrogen gas of 20 mL/min. At least two repetitions were carried out for each sample. For each test, the instrument was set to equilibrate at 25 °C before the heating cycle. Isothermal runs were also performed at 120°C and 160°C were performed to verify the reliability of the aftermath reaction kinetic prediction. Initial analysis were performed using Pyris software. For the integration of DSC peaks, a straight line was used as the baseline and the overall computational analysis was performed by using the NETZSCH kinetics (Neo Trial) software.

3.3.2 Dynamic Mechanical Analyzer Measurement (DMA)

Dynamic mechanical analysis (DMA) is a thermal characterization technique used to measure the mechanical properties of viscoelastic materials as a function of temperature or frequency. Dynamic mechanical analysis (DMA) works by applying stress or strain to a sample and analyses the material's response to obtain phase angle and deformation data (Menard and

Menard, 2015). This is performed sinusoidally. The sinusoidal wave is generated by a force motor transmitted to the sample through a driveshaft. The raw signals that are recorded by the machine are the force and the amplitude. These parameters are used to compute the stiffness and the modulus computed by multiplying the stiffness by a suitable geometry factor. A schematic representation of this is shown in Figure 3-5. In polymer-related applications, the study of molecular relaxation behaviour as well as the determination of inherent mechanism or flow properties as a function of time and temperature is possible by dynamic mechanical analysis (DMA).

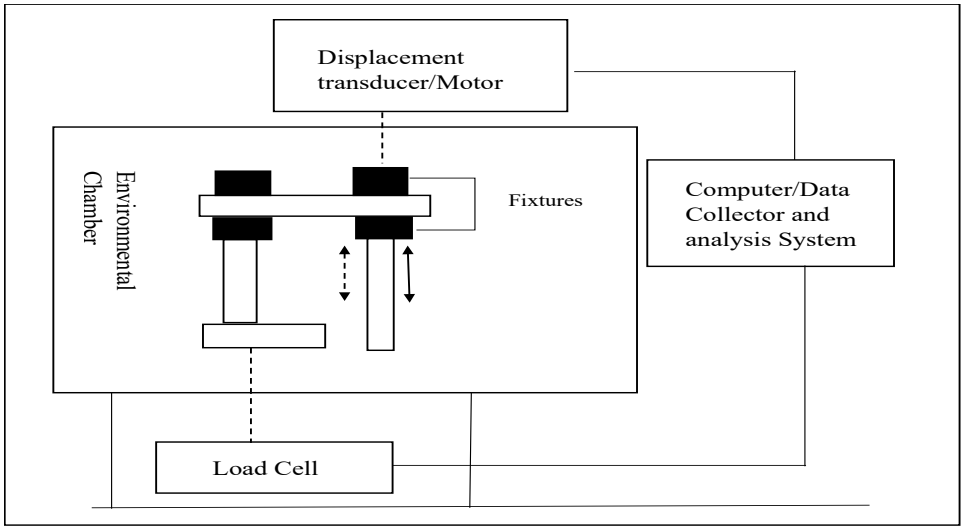

Figure 3-5 DMA principle in block diagram

In applications involving polymers, DMA allows for the study of molecular relaxation behaviour as well as the determination of inherent mechanism or flow parameters as a function of time and temperature. It reports modulus properties, such as storage modulus, (which is a measure of stress stored in the sample as mechanical energy), Loss modulus, (which is a measure of stress released as heat), and tan delta which is the damping measure. Determined plots of storage modulus, and loss modulus tan δ as a function of time/temperature are suggestive of thermal changes and viscoelastic behaviour of the material as it varies with the temperature.

For this research, the investigation of the thermo-mechanical behaviour of the Glass/PFA prepreg was studied using the Perkin Elmer DMA 8000 (Figure 3-6).

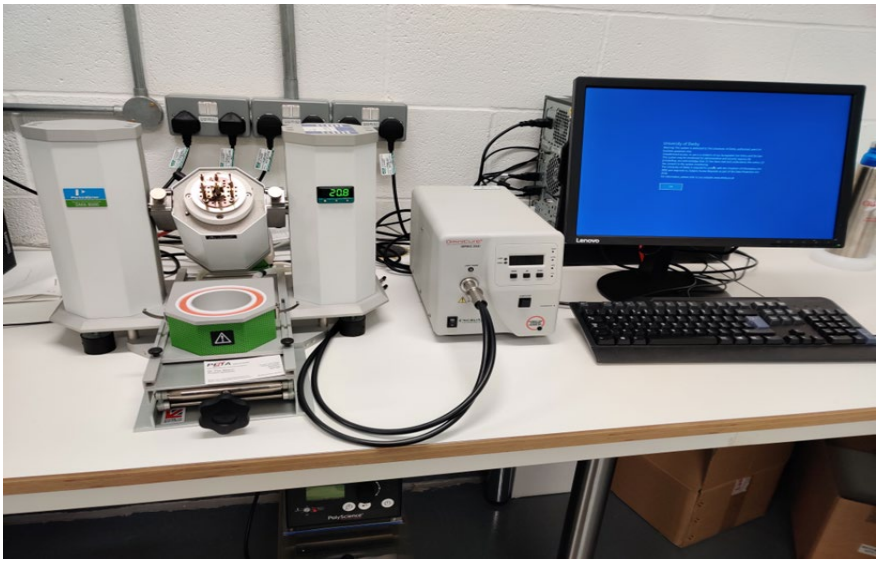

Figure 3-6. Perkin Elmer Dynamic Mechanical Analyzer (DMA) 8000

Two functions were provided by the Dynamic Mechanical Analyzer (DMA) analysis. First, for experimental cure simulation and viscoelastic characterization of cure cycles of the uncured biobased prepreg. Secondly, it was utilised to investigate the thermomechanical properties of composite panels manufactured afterwards.

In the initial instance, the viscoelastic behaviour during curing of the biobased Glass/PFA was investigated by curing on the Dynamic Mechanical Analyzer (DMA). To do so, uncured Glass/PFA prepreg samples of about 0.25mm thickness were cut into a 30mm x 7.5mm stainless steel material pocket as shown in Figure 3-7 and cured using the manufacturer-recommended cure cycle of 130°C for 1hr at a heating rate of 2°C/min.

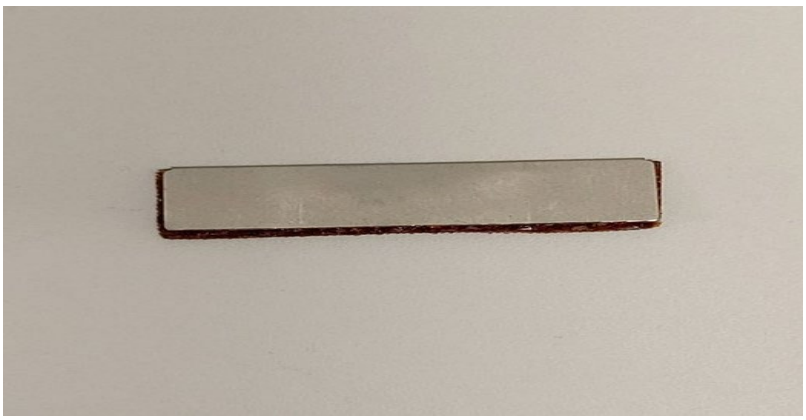

Figure 3-7 Sample of Uncured Glass/PFA prepreg in a stainless-steel DMA pocket.

Similarly, for comparison and validation of the optimized cure cycle prediction from the kinetic study, the procedure is repeated however at the optimized cure cycle as determined cure cycle

from the kinetic study, an optimized cure cycle of 160°C for 30 minutes from the kinetic model prediction was also employed to cure another sample. Both these cured samples were then analysed for dynamic behaviour using a dynamic heating run of 25°C to 300°C at 2°C /min.

The second phase involves its application in characterizing the thermo-mechanical properties of actual manufactured samples based on kinetic studies. In this case, rectangular strips size 30mm x 8mm (Figure 3-8) are cut from each manufactured panel using the varying cure cycles.

Figure 3-8 DMA coupon sizes cut from the manufactured sample.

These tests were run in the single cantilever mode at an oscillation amplitude of (20 μm) and frequency of 1Hz. For each test in both phases, the instrument was set to equilibrate at 25 °C before the heating cycle. In all experimental cases, both the storage modulus and glass transition temperature were measured. However, it is important to note that in the case of the uncured prepreg where the material pocket was used, the measured storage modulus is an estimated value due to the influencing effect of the stainless steel pocket. The glass transition temperature was recorded as the peak of the tan delta curve.

3.3.3 Thermomechanical Mechanical Analyzer (TMA) Measurement

The TMA measures the dimensional change of a material as a function of temperature or time. under a defined mechanical load. The technique involves the deformation of a material under a non-oscillatory load which is measured as a function of time or temperature while the substance is subjected to a controlled temperature program. The block diagram of the TMA shown in Figure 3-9 illustrates the working principle of the thermomechanical Mechanical Analyzer (TMA). A constant load from the measuring probe is applied to a sample placed on a support in the sample cylinder. The probe remains in contact with the sample and moves

upward or downward as a change in thickness of the sample changes with temperature. The displacement is then measured by the LVDT detector.

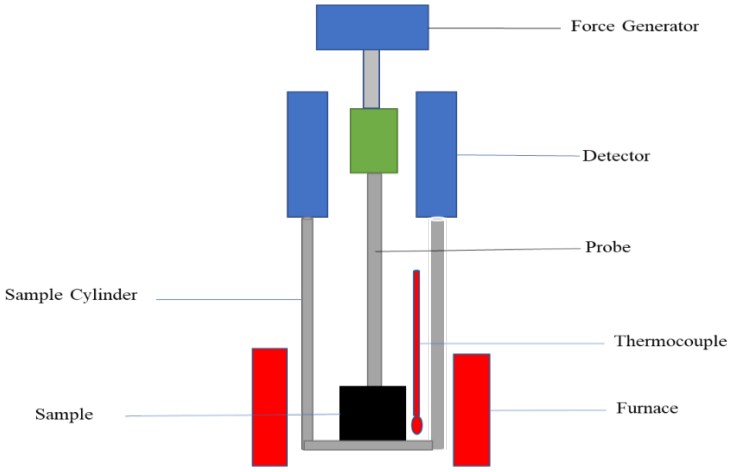

Figure 3-9 Schematic illustration of TMA working principle.

For this research work, the Perkin Elmer TMA 4000 in an expansion measurement mode setup was used in Figure 3-10. The specimen size is 8mm x 8mm x 2mm. These specimens were tested in non-isothermal mode between 25°C and 250°C at a heating rate of 5°C/minute with exercising an oscillatory force of 0.1N on the specimens. The test was performed using Nitrogen as the purge gas flowing at a rate of 50 mL/min.

Figure 3-10 Perkin Elmer Thermo-Mechanical Analyzer (TMA) 8000

3.4 Manufacturing of Composite Laminates.

The completion of the cure kinetic analysis study on the uncured glass/PFA prepreg enabled the establishment of an optimized manufacturing cure cycle. Thus, leading to the manufacturing of glass/PFA composite panels. Two methods were employed for the manufacturing of the panels are:

Vacuum bagging with oven curing as recommended by the material manufacturer.

Compression moulding technique (Hot Press) for simulation of rapid manufacturing

3.4.1 Prepreg Layup, Vacuum Bagging and Oven curing

Vacuum bagging is one of the most common methods used in composite manufacturing. The technique utilizes pressure created by an airtightly sealed vacuum in a bag to consolidate the layers of material (Fibre and resin). In its application for processing prepregs, the consolidation occurs in three stages namely compaction, air evacuation and resin flow (Hubert *et al.*, 2017) which are subject to positive changes in temperature. A schematic of the setup is shown in Figures 3-11.

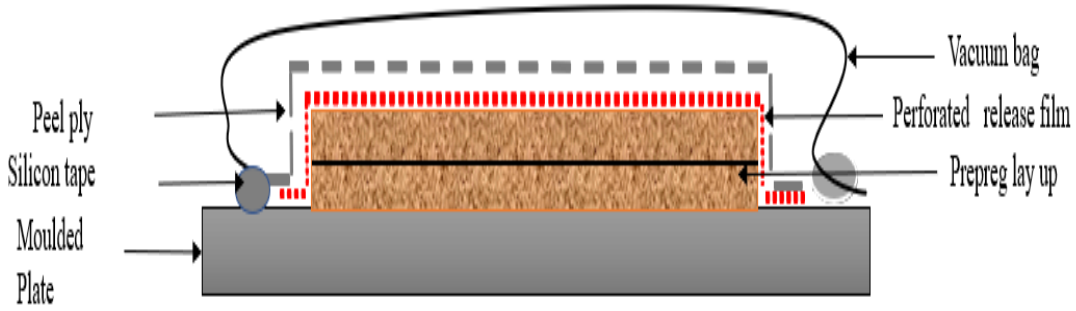

Figure 3-11 Schematic of the prepreg lay-up Vacuum bagging process

For this work, a machined flat-sized 350mm x 400mm aluminium was used as a mould. The surface of the plate was coated with a non-porous self-adhesive PTFE film (Figure 3-12) which acts as a barrier preventing the laminate from sticking to the mould surface.

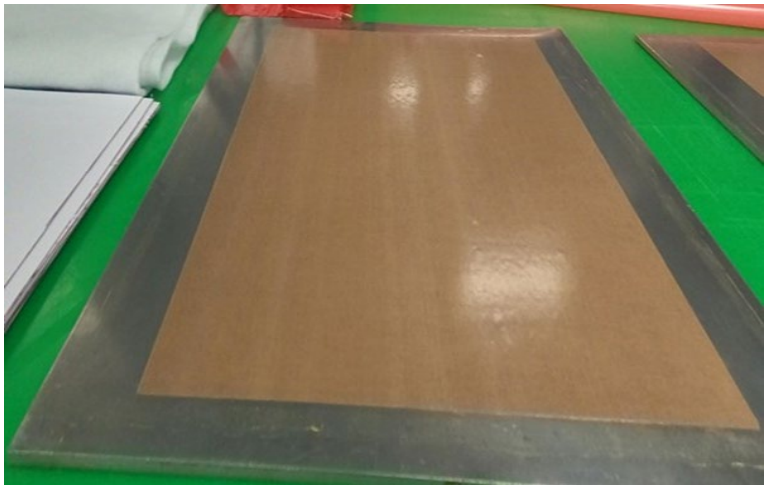

Figure 3-12 Flat mould (350mm x 400mm) coated with PTFE film sheet.

For the test panel, eight plies of 300mm x 300mm square size with an individual thickness of 0.25mm of the woven glass/PFA prepreg were cut from the prepreg material roll. Each of the plies was stacked on each other layer by layer with debulking performed on the first ply and repeated after four plies. An R120 P3 perforated release film was applied to the laminate (see Figure 3-9) to facilitate the release of volatiles and trapped air during the curing process.

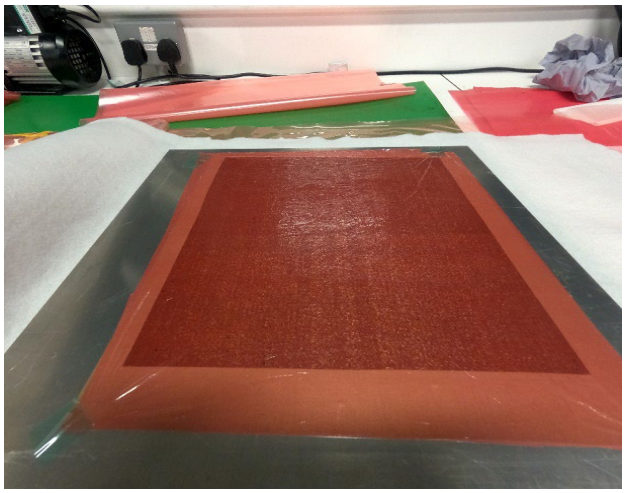

Figure 3-13 Layup process with Glass/PFA prepreg and perforated film.

Due to the peculiarity of the PFA resin, a layer of PP230 high spec 85gsm PA66 (Nylon 66) peel ply was placed on the release film as shown in Figure 3-14 to enhance the extraction of volatiles as well as aid the absorption of excessive resin from the laminate.

Figure 3-14 Layup setup covered with PA66 (Nylon 66) peel ply.

Following that, a caul plate is then placed on the top for added pressure and the entire set-up was then covered with a 140gsm non-woven polyester felt breather fabric and sealed in a vacuum bag film with the air drawn out via a vacuum pump resulting in a uniform consolidation pressure over the surface of the laminate as shown in Figure 3-15.

Figure 3-15 Vacuum bagged glass/PFA setup.

Next, it was placed in a curing oven as shown in Figure 3-16 (A) to cure using the manufacturer's recommended cure cycle discussed in section 3.2. Upon completion of the curing process, the manufactured panel is demoulded as shown in Figure 3-16 (B).

Figure 3-16 Vacuum bagged laminate in oven for curing (A) and demoulded oven-cured panel (B)

3.4.2 Compression Moulding (Hot Press)

The compression moulding process is one of the most common methods used for the rapid manufacturing of composite material. It is common in industrial applications where high-volume production is required. The technique employs the combination of simultaneous pressure and temperature over a period to cure laminates. A schematic of this process is shown in Figure 3-17.

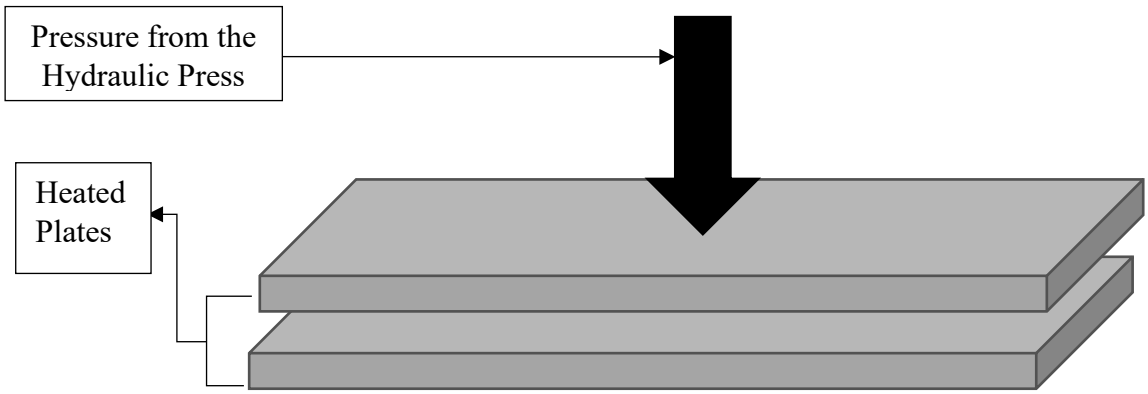

Figure 3-17 Schematic illustration of the compression moulding process

For this work, a self-manufactured laboratory scale size hot press made up of 30 tons hydraulic press, two 280 mm x 280 mm aluminium heating plates, four 800W heating cartridges and an electrical control system was used. A schematic flow chart of the designed and manufactured hot press operational system is shown in Figure 3-18.

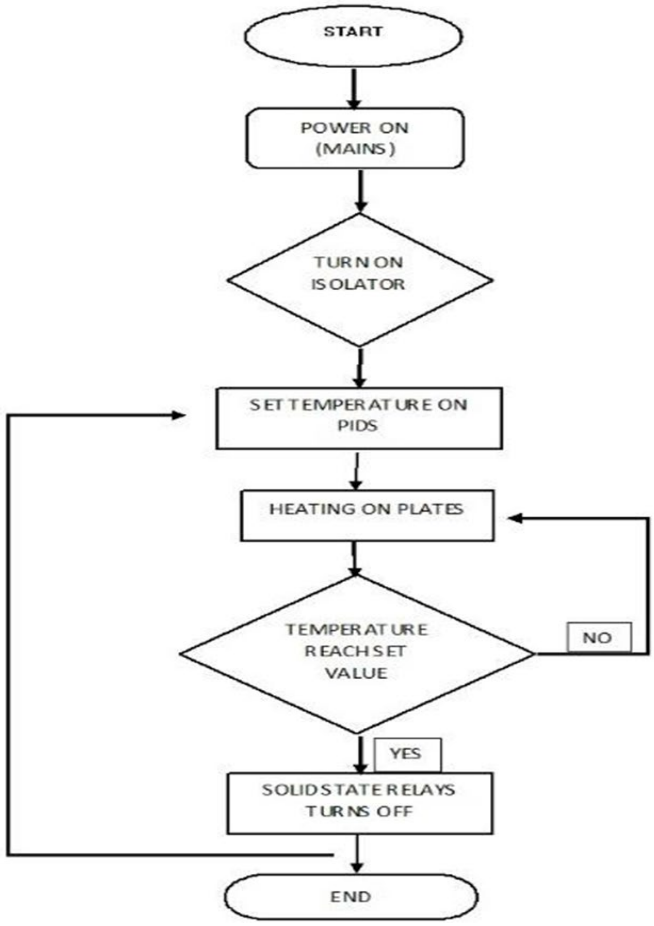

Figure 3-18 Schematic flow chart of the designed and manufactured hot press operational system.

The press was designed to achieve uniform heat and pressure for curing composite materials. The hydraulic press provides the necessary pressure through its arm lever and release knob, while the PID temperature controller regulates the cartridge heaters for consistent heating. The operation involves connecting the electrical panel, setting the desired curing temperature on the PID controller, and powering up the system. Current flows to the heaters, heating the plates to the set temperature. Thermocouples on each plate provide temperature feedback to their respective controller, which adjusts the heating until the desired temperature is reached. When the set temperature is reached, the solid-state relays temporarily shut off the voltage flow to prevent further heating. If a drop in temperature is sensed, the PID controller triggers the solid-state relay to allow current flow and maintain the desired temperature. This responsive process ensures uniform temperature between the plates, a key requirement for effective laminate manufacturing. The assembled setup is shown in Figure 3-19.

Figure 3-19 Lab-scale hot press

Manufacturing of the glass /PFA composite panels using the compression process involved first preparing the surface of the bottom plate by cleaning the surface with acetone and allowing it to dry. This is immediately followed by the application of a mould release agent to prevent the manufactured panel from bonding to the bottom mould plate. Plies of the pre-cut size glass/PFA prepreg (270mm x 270mm) is then laid up ply by ply (8plies in total) to achieve 2mm thickness on the bottom mould plate.

In the application of the compression moulding technique for manufacturing fibre-reinforced polymer composites, the processing parameters such as temperature, time, and pressure play a crucial role in defining the performance and characteristics of the composites (Medina, Schledjewski and Schlarb, 2009). These parameters have a significant impact on the quality of the laminate. With rapid manufacturing in mind, appropriate cure parameters (temperature and time) for the glass/PFA prepreg suitable for compression moulding were determined through optimization based on kinetic study results of the prepreg material. For compaction pressure, experiments were conducted at selected pressures of 5 and 10 bar to determine the optimal pressure for the optimized cycle obtained from the kinetic study. The choice of pressure levels was guided by the consideration that press moulding of natural fibre-reinforced polymers is typically performed at low pressure when the insulating properties of the composites are of great importance, while high pressures are used to emphasize the mechanical properties Medina, Schledjewski, & Schlarb, (2009).

The curing process of polyfurfuryl alcohol resin presents various challenges, as discussed in section 2.4.1, primarily due to the chemistry of polycondensation, which results in the release of moisture and volatiles. To validate this, an initial manufacturing test run was conducted, wherein a sample glass/PFA prepreg was manufactured using 5 bar pressure at the optimized cure cycle without venting during the curing process. The resulting cured laminate is depicted in Figure 3-20

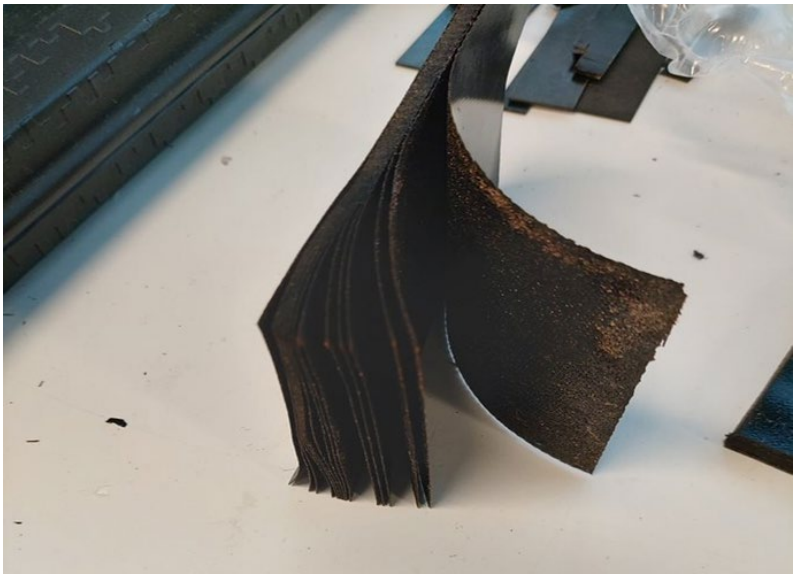

Figure 3-20 Glass/PFA sample manufactured via compression moulding without venting.

The observed delamination, as shown in Figure 3-20, can be attributed to the presence of trapped moisture and volatiles within the laminate, combined with unreleased stress during the curing process. Therefore, it is essential to address the expulsion of volatiles released during curing. To achieve this, a hot press cycle sequence was developed after a series of trials, which involves intermittently lifting the top mould during the curing process to allow venting. Figure 3-21 illustrates the press cycle sequence developed and implemented in the compression moulding manufacturing of laminates in this study.

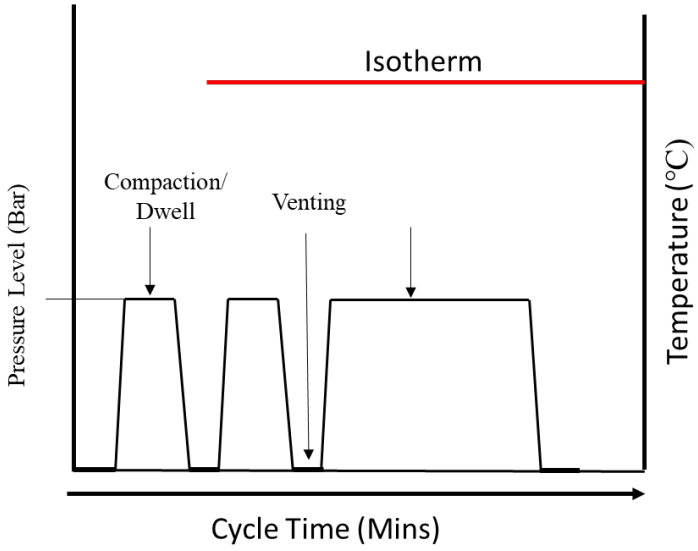

Figure 3-21 Developed press cycle sequence.

The manufacturing process for the Glass/PFA composite test panels involved several steps. First, the bottom plate was prepared by cleaning its surface with acetone and allowing it to dry. Then, a mould release agent was applied to prevent the panel from bonding to the bottom mould plate. Next, plies of pre-cut glass/PFA prepreg (270mm x 270mm) were layered one by one, totalling 8 plies to achieve a 2mm thickness on the bottom mould plate. The top mould, attached to the piston of the hydraulic press, was lowered to compact the prepreg. A pressure of 5 bar was applied by lowering the top plate, while both plates were simultaneously heated to 160°C, as determined from kinetic studies in Chapter 4. After 10 minutes of compression, the top platen was lifted for 60 seconds to vent, allowing volatiles and gases released during the polycondensation reaction to escape. The mould was then closed again for another 10 minutes of compaction, followed by another venting process. The mould remained closed until the end of the cycle (30 minutes) for proper curing. Once completed, the laminate was allowed to cool for stress relief before demoulding. The same process was repeated for manufacturing the sample at 10 bar pressure. Afterwards, the manufactured glass/PFA panels were demoulded, as depicted in Figure 3-20.

(A) (B)

Figure 3-22 Demoulded Hot-press manufactured Glass/PFA sample at (A) 5bar (B) 10bar.

3.5 Specimen Preparation

Following the manufacturing of the Glass/PFA panels using the oven curing and compression moulding method (as described in the previous section), five replicate specimens for each test (tensile, flexural, and interlaminar) were cut to appropriate dimensions using a Brilliant QCUT 240A cut-off machine (Figure 3-23)

Figure 3-23 Glass/PFA sample cut using Brilliant QCUT 240A machine.

The dimensions of the specimens were determined based on their respective standards, as shown in Figures 3-24, 3-25, and 3-26.

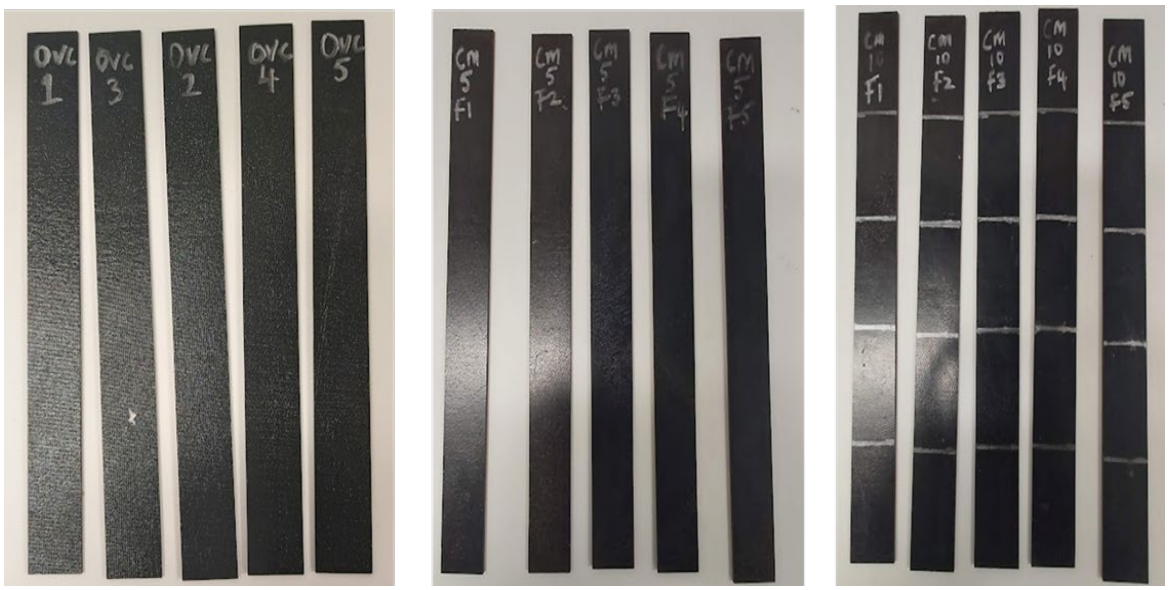

Figure 3-24 Tensile test specimens: (A) Oven cured, (B) CM5, (C) CM10.

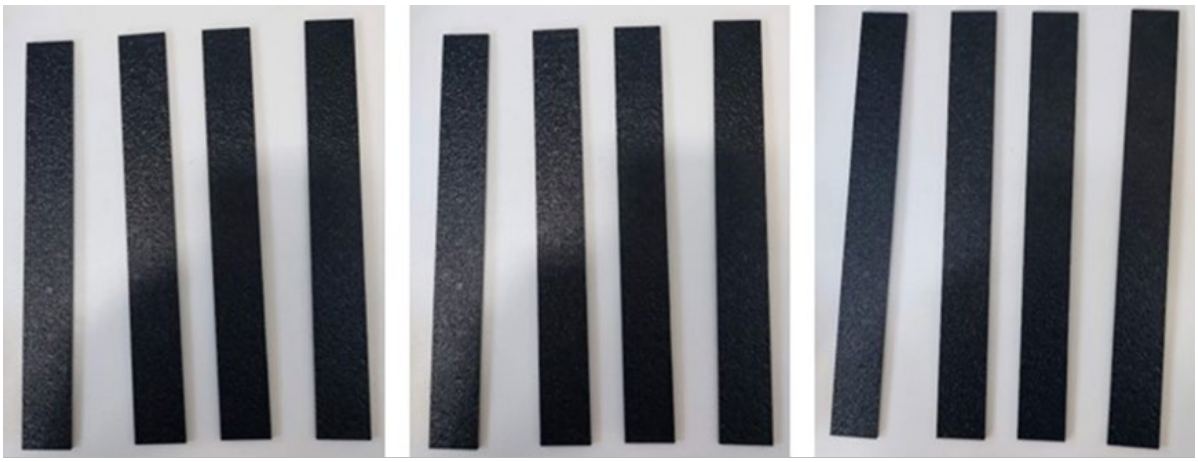

Figure 3-25 Flexural test specimens (A) Oven cured specimen (B) CM5 (C) CM10

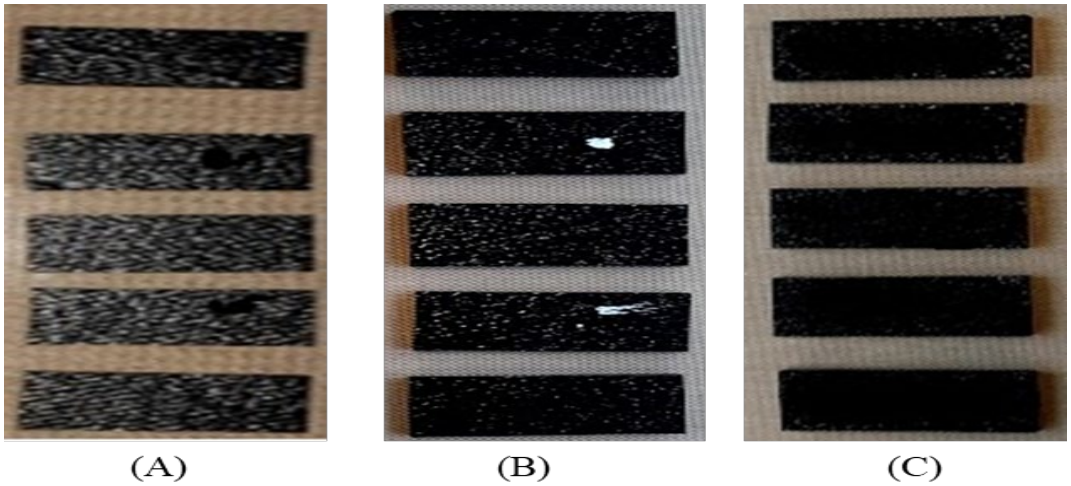

Figure 3-26 ILSS test specimens (A) Oven cured specimen (B) CM5 bar specimen (C) CM10 bar specimen.

3.6 Mechanical Characterization

Mechanical characterization of the composite panels manufactured using the techniques outlined in Section 3.4 is crucial for understanding the composite's behaviour as a function of the fabrication process and cure cycle. It is also critical for comparison required to adjudge the optimal process parameter for the optimized cure cycle. For this reason, three fundamental mechanical property tests were selected for this research work. They are (i) Tensile test (ii) Flexural (3point bend test) test (iii) Interlaminar Shear test (ILSS)

3.6.1 Tensile Test

When an axial load is applied to a fibre-reinforced composite material, the resulting stress is transferred from the matrix to the reinforcement. The determinant strength of the material is subject to the strength and modulus of the reinforcement. A tensile test is performed to determine the tensile strength and modulus of materials. It also provides information on the failure behaviour of the material under load.

Fundamentally, a test involves material being firmly held at both ends by the jaws of a piece of equipment which progressively pulls it along its length until failure. The recorded pulling force is plotted against the displacement of the material which is converted to a stress-strain plot. For the evaluation of the tensile properties of samples of each glass/PFA panel manufactured using techniques discussed in section 3.5, a test setup and procedure were carried out using a 50kN load cell Shimadzu Universal Tensile Machine according to ASTM 3039

standard. In conformance with the test standard, the specimens were held vertically in the machine grips. A 50mm extensometer mounted across the gauge length as seen in Figure 3-27 was used to measure the strain to obtain the modulus.

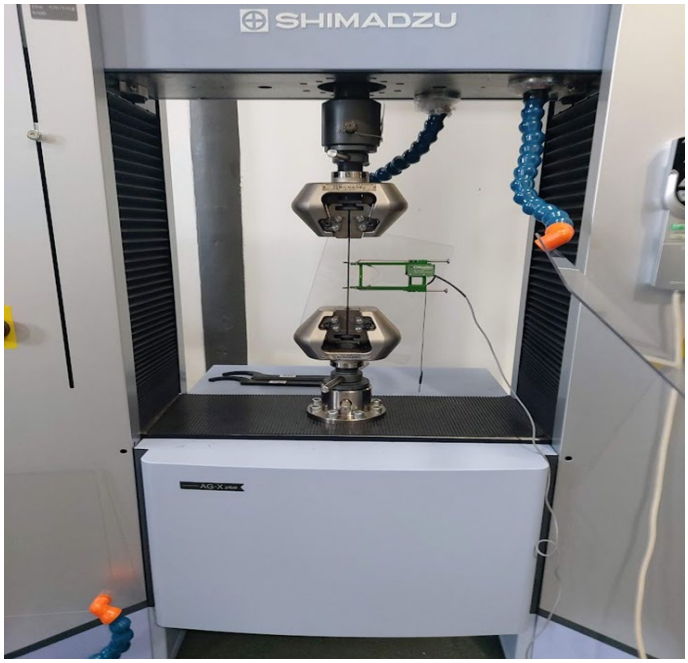

Figure 3-27 Tensile test setup with Shimadzu universal testing machine.

At a crosshead speed of 2 mm/min, uniaxial loads were applied through the specimen's two ends until the sample broke. Each manufactured laminate was subjected to five separate measurements and the average of these values was then reported. The failure mode at fracture was observed and recorded.

The tensile stress was evaluated using Equation (3.2)

$$\sigma = \frac{F}{A} \tag{3.2}$$

Where

σ = Tensile stress in (MPa)

F = Force at each data point (N)

A = Cross-sectional area of the specimen in (mm2)

The tensile strain was evaluated using the equation.

$$\varepsilon = \frac{\delta l}{l} \tag{3.3}$$

ε = Tensile strain

δl = Sample elongation

$l =$ Original length

3.6.2 Flexural Test

The flexural test determines the material's capacity to sustain bending force exerted perpendicular to its longitudinal axis. In a flexural test, rectangular bar specimens are subjected to three or four-point bending, causing tensile stress on the bottom of the specimen and compressive stresses at the load application point. The stresses are zero in the centre of the specimen beam and maximal at the top and bottom surfaces of the specimen. To evaluate the flexural properties of manufactured samples a 3-point bending was conducted for this study. According to ASTM standard D790, the test was conducted on a flexural rig equipped with a 50kN load cell on a Tinius Olsen Universal Testing Machine (see Figure 3-28). Five rectangular cross-sections of 100 mm x 13 mm x 2 mm were cut from each of the manufactured as shown in Figure 3-24

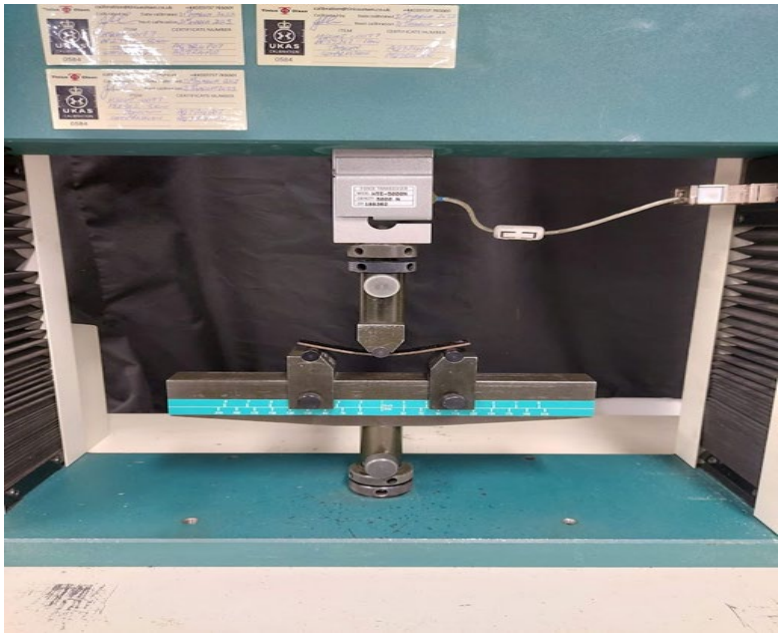

Figure 3-28 Flexural test setup with Tinius Olsen Universal Testing Machine

Following the standard, a span-to-depth ratio of 40:1 was used. The test was conducted at a crosshead speed of 2 mm/min while the load-deflection curve was recorded. An average of five measurements were obtained from each sample panel and the mean value was reported. Two key characteristics define a composite structure's flexural stiffness: (i) the elastic or Young's

modulus of the material that makes up the structure (i.e., the stress per unit strain) and (ii) the moment of inertia, which depends on the cross-section of the composites (Vignesh *et.al* 2021).

The flexural stress was calculated using equation (3.4)

$$\sigma_f = \frac{3FL}{2bh^2} \qquad (3.4)$$

Where

σ_f = *is the flexural stress at the break in (MPa)*

$F = is\ the\ Load\ at\ break\ in\ (N)$

L = *is the span length of the specimen in (mm)*

$b =$ *is the width of the specimen in mm*

$h = is\ the\ thickness\ of\ the\ specimen\ in\ mm$

The flexural strain was determined by the use of equation (3.5)

$$\varepsilon = \frac{6sh}{L^2} \qquad (3.5)$$

Where

$\varepsilon = is\ the\ thickness\ of\ the\ specimen\ in\ mm$

$s = is\ the\ deflection\ in\ mm$

$h = is\ the\ thickness\ in\ mm\ of\ the\ specimen$

$L = is\ the\ span\ length\ in\ mm$

The modulus was computed from the curve and the flexural strength and modulus can be calculated using standard relations.

3.6.3 Interlaminar Shear Strength Test

The interlaminar shear test also referred to as the short beam test is a matrix-dominated property test which is usually related to the shear behaviour of the matrix (Gagani *et al.*, 2019). The determination of the test is based on classical (Bernoulli–Euler) beam theory. Although the test has a limitation due to "inadequacies in classical beam theory in defining the stress state in the short-beam configuration"(ASTM International, 2003). The test is performed to measure the apparent values of interlaminar shear strength of fibre-reinforced composites. It is designed to

generate interlaminar shear indirectly through bending. The maximum interlaminar shear stress occurs at the mid-thickness of the beam between the centre and end supports for a rectangular cross-section loaded in three-point bending (Fan, Santare and Advani, 2008). This testing method was chosen primarily because of its simplicity as well as its demonstrated sensitivity to defects in the laminates. For this research work, the Interlaminar shear strength test was performed on the Tinius Olsen Universal Testing Machine with set-up as shown in Figure 3-29 and was used to measure the apparent ILSS of composite laminates. In the short beam shear test, the load increases linearly with deformation during deflection until the maximum load is reached. If the load decreases by 30 per cent or more soon after reaching the peak load, it is presumed that the specimen failed in laminar shear, and the maximum load is then utilised to calculate the apparent Interlaminar Shear Strength (ILSS).

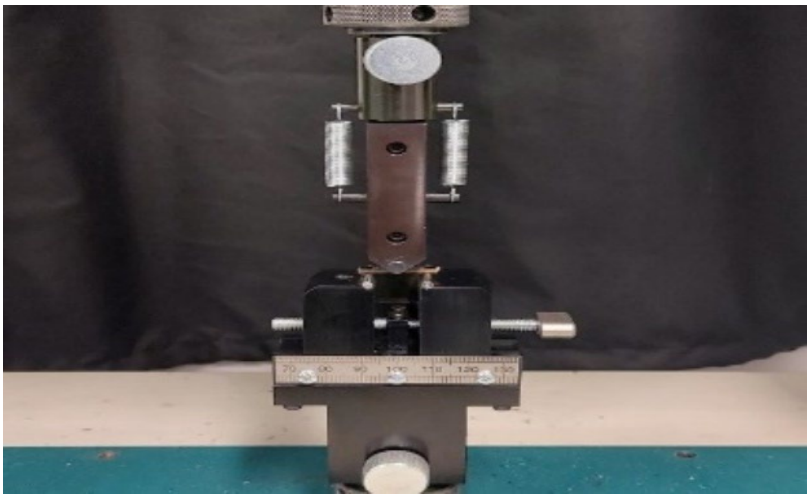

Figure 3-29 ILSS test setup with Tinius Olsen Universal Testing Machine

Following the ASTM D2344-06, the span is 13.2 mm to maintain the span/thickness ratio of 4 recommended for composites. Tests were conducted with a 1kN load cell at room temperature and 1 mm/min. ILSS parameter has been computed from the maximum load observed during the test according to the following Equation (3.6)

$$F^{sbs} = 0.75 \times \frac{P_m}{b \times h} \qquad (3.6)$$

Where

$F^{sbs} = is\ the\ short\ beam\ strenght\ (MPa)$

$P_m = is\ the\ maximum\ \ recorded\ during\ the\ test\ \ in\ (N)$

$b = is\ the\ measured\ \ specimen\ width\ (mm)$

$h = is\ the\ measured\ \ specimen\ thickness\ (mm)$

The mean values were derived from five test samples for each of the manufactured composite laminates.

3.7 Morphology and Fiber Volume Fraction

3.7.1 Optical Microscopy and Image Analysis

Optical Microscopy enables the visual characterization of fibre-reinforced material. It allows for the analysis of the voids content, size, shape, and spatial distribution (Little, Yuan and Jones, 2012) across the fibre-reinforced composite sample which can be indicative of the quality of the laminate as a function of the manufacturing process. For this work, the Olympus BX53M microscope shown in Figure 3-30(A) was employed.

To achieve good microscopic imaging, the surface cross-sections of the sample to be viewed were well prepared. The process begins with rectangular strips of 20 mm x 2 mm cross-sections cut from across the individual panels manufactured by the different processes described in section 3.4. To enable proper grinding and polishing, the cut sample is set in a transparent acrylic cold-mounting compound resin. With the aid of a Q50 semi-automatic preparation equipment, the resin-mounted sample undergoes three-stage preparation procedures. In the first stage, the resin-mounted sample was subjected to primary grinding on 320-grit silicon carbide grit paper with a 25N force and 150mm/min rotatory speed. The samples were subjected to further grinding utilising Plano cloth and Durasilk surfaces with 9µm and 6µm diamond abrasive solutions. The samples were then given a final polishing using a Chemcloth surface and 0.06µm silica colloidal solution. Upon completion, a high-quality mirror-like surface finish is observed on the surface of the sample as seen in Figure 3-30(B).

(A) (B)

Figure 3-30 Olympus BX53M Microscope setup (A) and polished glass/PFA composite samples (B).

The well-polished individual samples were then viewed at different magnifications with the respective images captured with the aid of the automated stitched image acquisition capabilities of the Olympus stream software. Further imaging analysis was performed for the determination of void content and fibre volume fraction using the ImageJ image processing software. To determine the percentage of fibre, shape, and location of porosity. The colour map image of the microscopic image was first transformed to an 8-bit grayscale image to return a binary image (Bodaghi *et al.*, 2016). This is followed by the application of a Gaussian filter to remove image blur and noise, and thresholding to identify areas with comparable greyscale values. Based on the processed images, the percentage of void and fibre content was determined. The void size was calculated from the area using equation 3.7 as suggested by Li et al. (2015).

$$D_e = \sqrt{\frac{4A}{\pi}} \qquad (3.7)$$

Where $D_e = Equivalent\ void\ diameter$

$A = is\ the\ area\ of\ the\ void$

According to Barraza et al. (2004), voids with an equivalent diameter greater than 50µm are categorized as large voids, whilst voids with an equivalent diameter less than 75µm are considered small voids. Medium voids were defined as voids with equivalent diameters ranging from 75µm to 150µm.

3.7.2 Determination of Fibre Volume Fraction

When evaluating the mechanical performance of fibre-reinforced polymer composites, the need for the fibre volume fractions is important. Destructive methods such as acid digestion and resin burn-off are common techniques usually employed for this purpose. For this work, attempts were made to utilize the acid digestion method for the determination of the fibre volume fraction. To accomplish this, 10mm x 10mm cross sections of the various manufactured panels are placed in a pressure vessel along with a mixture of 5 ml of Nitric acid and 5 ml of deionized water. The vessel is then inserted into a microwave digestion system (see Figure 3-30) and subjected to a digestion run at 160℃ for 60 minutes, following the recommendation by Pemberton, Edser and Gower (2020)

Figure 3-31 Microwave digestion system

The analysis of one of the results of the digestion process following the ASTM D 3171 standard (ASTM International, 1999) is presented in Table 3-1

Table 3-1 Evaluated constituent results from the acid digestion method.

Samples	Mass of sample before digestion (g)	Mass of Fibre after digestion (g)	Fibre Volume fraction (%)	Resin Volume Fraction (%)	Void Content (%)
Press Cure (CM5)					
CM5 (i)	1.5874	0.5416	24.37049	98.82197	-23.1925
CM5 (ii)	1.5784	0.5406	24.19237	97.52935	-21.7217
CM5 (iii)	1.5493	0.5412	24.84047	97.16836	-22.0088
Oven cure (OVC)					
OVC (i)	1.6514	0.643	27.50288	90.57729	-18.0802
OVC (ii)	1.6480	0.6488	27.88633	90.18871	-18.075
OVC (iii)	1.6505	0.6492	27.70517	89.73581	-17.441
Press Cure (CM10)					
CM 10 (i)	1.4304	0.6446	32.17092	82.35774	-14.5287
CM 10 (ii)	1.4495	0.65365	31.67377	80.98508	-12.6589
CM 10 (iii)	1.4592	0.62765	30.21172	84.05539	-14.2671

The results presented in Table 3-1 indicated a significantly low fibre volume content and a considerable negative voidage content for the samples. These findings strongly suggest errors in the results and therefore question the reliability of the method used for evaluating fibre volume content. For this reason, the fibre volume fraction was determined through image analysis using the optical microscopy method. The superior contrast difference between voids, fibre and the cured resin enhances the examination and evaluation of the constituent of the glass/PFA biobased composite.

Normalization

The mechanical properties of fibre-reinforced composites are largely dependent on the manufacturing process and the processing variable (Hosseini, 2015). Since the glass/PFA laminates produced by the two different methods have different fibre volume fractions, it is essential to normalise the fibre content before comparing their determined mechanical properties.

The normalized values were determined using equation 3.8 as suggested by Ghossein et al. (2020)

$$N\,V = Test\ property\ Value \times \frac{Chosen\ volume\ fraction}{volume\ fraction\ of\ Specimen} \qquad (3.7)$$

Where N V = Normalized Value

For this study, the determined mechanical property is normalised to an average value of 43.2 % by fibre volume fraction.

3.7.3 Scanning Electron Microscopy

The Scanning Electron Microscope (SEM) is a common investigative technique employed to study and perform fracture or failure analysis. Numerous studies (Chen, Poursartip and Fernlund, 2019; Benin *et al.*, 2020; Kufel, Para and Kuciel, 2021) have utilized this technique for surface morphology of fractured or failed specimens from different mechanical tests. The failure analysis on the fractured specimen from the tensile, flexural and interlaminar shear test of the biobased Glass/Polyfurfuryl composite samples manufactured for this work was performed on VEGA TESCAN 3 Scanning Electron Microscope shown in Figure 3-32.

Figure 3-32 VEGA TESCAN 3 Scanning Electron Microscopy

For each case, sections of the individual samples were first cut from the fractured surface and placed on metal stubs using double-sided carbon tabs. loaded and the corresponding fractured surface area was subjected to an electron beam emitted by a tungsten-heated filament electron cannon with an acceleration voltage of 20kV.

Chapter 4 Cure Kinetic Study

4.1 Introduction

Curing in polymeric thermosets is an irreversible process such that the degree of cure monotonously increases which ultimately leads to the material becoming rigid. As shown in Figure 4-1, curing thermosetting materials often entails exothermic chemical reactions that convert low molecular weight liquids to amorphous networks with infinite molecular weight (Ghaffari *et al.*, 2012; Masuelli, 2013) often referred to as polymerization (Sbirrazzuoli, 2019). The curing process is the most crucial component of the technical process involved in the manufacture of composite structures from prepregs. Its success is largely dependent on the success of the completion of the polymerization reaction of the embedded resin system. Therefore, accurate knowledge of the polymerization (cure) mechanism is necessary for the development and optimization of processing conditions (Temperature, Time, and Pressure). Vyazovkin et al. (2022) discussed in detail the mechanism of polymerization as it relates to thermosets, categorising it into two types: chain polymerization and step polymerization. To obtain the best qualities for the cured polymer or composite, it is crucial to control the polymerization reactions of thermoset materials. These complicated reactions can require numerous chemical and diffusion processes, which makes it particularly challenging to understand the reaction mechanism (Sbirrazzuoli, 2019).

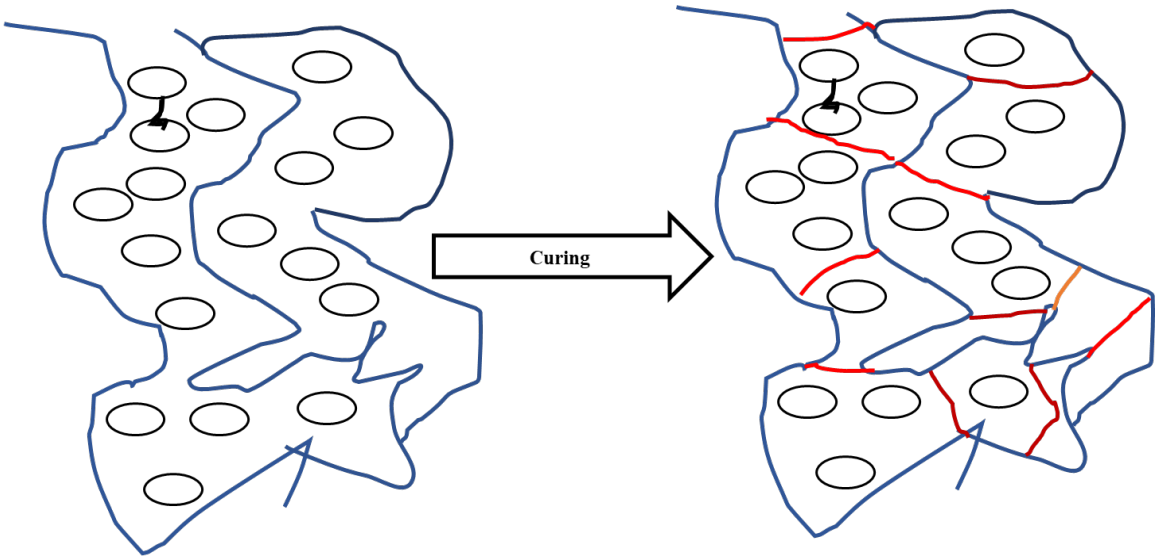

Figure 4-1 Illustration of polymerization during the curing process

As with most thermoset composites, manufacturing defects such as delamination, and warpage observed in the manufacture of polyfurfuryl alcohol-based composites arise from the

inadequacies of processing parameters. Therefore, a thorough understanding of the curing process is important, especially in terms of rapid manufacturing. The determination of appropriate process parameters for rapid manufacturing processes is mostly developed based on an appropriate understanding of the cure behaviour of the material during processing (Marefat Seyedlar, Imani and Mirabedini, 2017) and hence the necessity of cure kinetic studies. Sbirrazzuoli in (Sbirrazzuoli, 2021) underscored the importance of the knowledge of predictions of the extent of conversion or rate of reaction for a different time at a given isothermal temperature or varied temperature program for practical application.

In the study of curing kinetics of thermosetting resins, various techniques including, Dielectric Analysis, Thermogravimetry (TGA), Fourier-transform Infrared Spectroscopy (FTIR), Nuclear Magnetic Resonance (H NMR) Spectroscopy, and rheokinetic measurements (Rheometry) amongst others have been used. However, the application of the differential scanning calorimetry (DSC) technique remains the most commonly used. For resin or prepreg cure optimization studies from a manufacturing standpoint, the DSC technique is preferred due to the ease of obtaining kinetic information closely correlated to the conversion (degree of cure) as a function of time and temperature which are critical processing parameters of the real cure process.

Generally, in understanding the kinetics, phenomenological model equations are employed to analyse the cure reaction mechanisms through which optimal curing parameters can be determined. In broader terms, the phenomenological model equations may be categorized into two types based on their fitting mechanism namely (a) the Model-free kinetics (isoconversional) method and (b) the model-based fitting methods(Zhang *et al.*, 2011).

4.2 Theory of Cure Kinetics

Cure kinetics is the foundation and core of numerical simulation of thermoset composites to better understand the relationship between structure, performance and process (Liang *et al.*, 2022).The overall effect of the temperature and conversion on the reaction rate or degree of cure (α) per unit time $\frac{d\alpha}{dt}$, of a cure process may be described as a single step kinetic relationship (Domínguez, Grivel and Madsen, 2012)(Ghaffari *et al.*, 2012)(Newcomb, 2019) expressed as shown in equation *(4.1)*.

$$\frac{d\alpha}{dt} = k(T) \times f(\alpha) \qquad (4.1)$$

Here $k(T)$ is the rate coefficient which depends solely on the temperature and $f(\alpha)$ is the conversion function (also called kinetic function) which depends on the reaction mechanism (Fernández *et al.*, 2009). The rate coefficient $k(T)$ is defined with respect to temperature by the Arrhenius law (Hardis *et al.*, 2013) described in equation *(4.2)*

$$k(T) = A\ exp\left[-\frac{E_a}{RT}\right] \qquad (4.2)$$

Where A is the pre-exponential factor, E_a is the curing activation energy, R is the Universal gas constant and T refers to the Temperature.

Therefore, the overall kinetic relationship may be expressed by the combination of equations (1) and equation (*4.2) as* shown in equation *(4.3)*

$$\frac{d\alpha}{dt} = A\ exp\left[-\frac{E_a}{RT}\right] \times f(\alpha) \qquad (4.3)$$

Technically, the cure process is measured by the evolution of the degree of cure which is quantified over a range from 0 to 1. Thus, considering the reaction rate to be directly proportional to the heat flow (Lopez De Vergara *et al.*, 2014), (Ren *et al.*, 2016),(G.Liang, 2006). The heat flow rate profile output from the DSC experiments allow the conversion and reaction rate (dα / dt) to be obtained using equations *(4.4)* and *(4.5)* as follows:

$$\alpha = \frac{\Delta H_t}{\Delta H_{Tot}} \quad (0 \leq \alpha \leq 1) \qquad (4.4)$$

$$\frac{d\alpha}{dt} = \frac{1}{\Delta H_{Tot}}\left(\frac{d\Delta H_t}{dt}\right) \qquad (4.5)$$

Where the reaction enthalpy ΔH_t at a time (t) is obtained from DSC measurements and the overall enthalpy ΔH_{Tot} is determined by the integration of the peak from the DSC measurement at individual heating rates over a specified temperature range.

The expression in equation (3) is generic and valid for any cure cycle. Therefore, considering the reaction is studied under non-isothermal conditions, a general kinetic relationship for the analysis at different dynamic heating cycles is obtained using equation *(4.6)*.

$$\beta\frac{d\alpha}{dT} = A\ exp\left[-\frac{E_a}{RT}\right] \times f(\alpha) \qquad (4.6)$$

Where β is the heating rate, T is the Temperature and t refers to time.

4.3 Model Free Kinetics

The isoconversional principle which is used in this work to study the cure kinetics assumes that the reaction rate at a constant degree of cure (α) (Also referred to as the extent of conversion) is only a function of temperature (Sbirrazzuoli, 2020). When using the model-free isoconversional methods one needs to describe the kinetics of the process by using multiple single-step kinetic equations, each of which is associated with a certain degree of cure (α) (Vyazovkin and Wight, 1998; Vyazovkin and Sbirrazzuoli, 2006; Vyazovkin *et al.*, 2011). The model-free kinetic methods apply the isoconversional principle to calculate the conversion-dependent apparent activation energy of a process as well as the pre-exponential factor without the knowledge of the reaction mechanism (Stanko and Stommel, 2018). The solution is derived from the logarithmic derivative of equation (*1*) at a constant conversion (degree of cure) as presented in equation (4.7).

$$\left[\frac{\partial In\, d\alpha/dt}{\partial T^{-1}}\right]_{\alpha} = \left[\frac{\partial Ink(T)}{\partial T^{-1}}\right]_{\alpha} + \left[\frac{\partial Inf(\alpha)}{\partial T^{-1}}\right]_{\alpha} \qquad (4.7)$$

Since under isoconversional conditions the kinetic function $f(\alpha)$ has a constant value at constant conversion(α) (Jouyandeh *et al.*, 2019),(Mashouf Roudsari, Mohanty and Misra, 2014), equation *(4.7)* can be simplified for different heating rates (≡ *i*) in a non-isothermal DSC measurement as follows.

$$\left[\frac{\partial In(\beta_i(d\alpha/dt))}{\partial T^{-1}}\right]_{\alpha_i} = -\frac{E_a}{R} \qquad (4.8)$$

Where β_i is the heating rate, $\frac{d\alpha}{dt}$ is the reaction rate, T is the temperature under investigation, R is the universal gas and E_a is the activation energy. From the relationship above it is possible to obtain the activation energy at different conversions without assuming a kinetic function.

The Model-free kinetic modelling methods are subdivided into differential and integral methods. Advanced isoconversional methods like KAS, FWO, Friedman, and Starink are extensively exploited to evaluate the dependency of activation energy to the degree of conversion Two of the most simplistic approaches to kinetic analysis of thermal data discussed by the ICTAC Kinetics Committee (Vyazovkin *et al.*, 2011) are differential Friedman and the integral Ozawa Flynn Wall method. These were applied to this work due to suitability for non-isothermal temperature programs as well as evaluation capabilities of multi-step reactions. Furthermore, the Friedman method provides a non-approximate advantage in its calculations,

which aids in determining the true mechanism of a reaction, even though it may experience numerical instability (Sbirrazzuoli, 2019). The simplified temperature integral approximate derivation offered by the Ozawa Flynn wall method also provides an excellent evaluation of the reaction mechanism. Thus, providing a proper understanding through the different views of both methods.

4.3.1 Friedman's Method

Derived by the linearization of equation *(4.6)* at a specific degree of cure, the Friedmann method (Friedman, 1964) as reported by Lascano et al. (2019) is expressed as shown in equation *(4.9)*.

$$ln\frac{d\alpha}{dt} = \left(ln\,\beta\frac{d\alpha}{dT}\right)_{\alpha i} = ln[A\,f(\alpha)] - \frac{E_\alpha}{RT_{\alpha i}} \qquad (4.9)$$

Where β is the heating rate, A is the Pre-exponential factor, $f(\alpha)$ is the reaction model (kinetic function) which is considered constant, R is the gas constant and T is the temperature. With the reaction rates deduced from the experimental thermogram from DSC using equation (5), the value of the activation energy (E_a) for each defined conversion are determined from the slope of the linear fitting plot of the natural logarithm of $\frac{d\alpha}{dt}$ for the different heating rates against $\frac{1}{T}$. Based on this, a conversion range of α = 0.05 to α = 0.95 with an incremental step size of 0.05 as recommended by Lascano et al. (2019) is used to generate the plot.

The intercept of the plot defines the product of the term between the exponential factor (A) and the function of the reaction model. The value of $\ln[A\,f(\alpha)]$ and the evolution of activation energy (E_α) with conversion can be used to describe the kinetic behaviour (Wang, Laborie and Wolcott, 2005).

4.3.2 Ozawa Flynn Wall Method

The Ozawa Flynn Wall method proposed by Flynn and Wall and Ozawa using Doyle's approximation of the temperature integral (Ozawa, 1965; Flynn and Wall, 1966) is an isoconversional integral technique in which the curing rate at any degree of cure is dependent solely on the temperature (Marefat Seyedlar, Imani and Mirabedini, 2016). The method establishes a relationship between the degree of cure-dependent activation energy, heating rate, and the isoconversional temperature (Brown *et al.*, 2000). This is described by Jubsilp (Jubsilp, Takeichi and Rimdusit, 2011) in Equation (*4.10)*

$$ln\,\beta = ln\left(\frac{AE_\alpha}{R}\right) - ln\,g(\alpha) - 5.331 - 1.052\left(\frac{E_\alpha}{RT}\right) \quad (4.10)$$

$$Where\ g(\alpha) = \int_0^\alpha \frac{d\alpha}{f(\alpha)}$$

The $g(\alpha)$ is the integral function of the degree of cure (α), β the heating rate while T is the peak temperature for a specific degree of cure (α) determined from the individual experimental heat flow curve from the DSC. The activation energy is derived from the slope of the straight line when the heating rates (β) are plotted against the reciprocal of the peak temperature $\left(\frac{1}{T}\right)$.

In this work, the obtained conversion-dependent activation energies from both methods are compared to aid understanding and description of the cure mechanism of the biobased Glass/P prepreg.

4.4 Model Fitting Kinetics

The Model-fitting approach to cure studies is a commonly used technique employed in the kinetic modelling of materials. Although it has a huge area of application in solid-state kinetics (Savabieh *et al.*, 2019; Tarani *et al.*, 2019; Vasilopoulos, Skořepová and Šoóš, 2020; Mahmood *et al.*, 2021), it is also being used in polymerization kinetics(Abenojar *et al.*, 2018; Asadi, Jannesari and Arabi, 2019; Kuppusamy, Zade and Kumar, 2020). Model Fitting refers to fitting the rate equations (models) to the experimentally measured rate data (Vyazovkin *et al.*, 2022). This approach usually assumes that a particular reaction model represents the conversion dependence of the reaction rate (Yasnó *et al.*, 2021). The reaction model can be expressed in several empirical forms depending on the reaction mechanism. Literature has documented various reaction models used to describe different reaction mechanisms. Kamal-Sourour's autocatalytic model was chosen for this work. The selection of the model was based on its suitability for regular, autocatalytic, and multistep reactions as recommended by ICTAC Kinetics Committee recommendations (Vyazovkin *et al.*, 2022). The general kinetic expression of the curing process is described by Kamal and Sourour (Kamal and Sourour, 1973) in equations *(4.11)*

$$\frac{d\alpha}{dt} = k \propto^m (1-\propto)^n \quad (4.11)$$

Where k is a rate constant, α is the relative degree of reaction and the parameters m and n are constants independent of temperature. This is modified and expressed as shown in equation

(4.12). Where the chemical kinetics controls the reaction and the constants ($k_1 and\ k_2$) depends on temperature following the Arrhenius dependence, according to equation (4.3).

Substituting equation *(4.3)* into equation *(4.11)*

$$\frac{d\alpha}{dt} = \left(A_1 exp\frac{E_1}{RT} + A_2 exp\frac{E_2}{RT} \propto^m\right)(1-\propto)^n \qquad (4.13)$$

4.5 Model Free Vs Model Fitting Method

Although model fitting is a widely used method for analysing curing kinetics, its use of specific reaction models to evaluate kinetic parameters can result in inaccurate results, which model-free approaches can avoid (Ke, Wu and Chen, 2020). Examples of these differences were observed in the results of the studies by Hosseinpour et al. (2016) and Yan et al. (2020) where they concluded that the model-free method shows better prediction than the model-fitting method. The model-free kinetic methods offer a relatively simplistic approach to analysing the complexity of cure reactions of thermosetting resins by their ability to determine the activation energy of the reaction as a function of the degree of conversion without knowledge of an underlying kinetic model which is a major drawback of the model-based fitting method (Vyazovkin and Wight, 1999). Also, its modelling and predictive capabilities for other materials and resin types in both dynamic and isothermal conditions have been proven to be reliable as found in published studies [(Sbirrazzuoli, 2021),(Stanko and Stommel, 2018),(Budrugeac, 2019),(Ke, Wu and Chen, 2020), (Zhang *et al.*, 2011),(Domínguez, Grivel and Madsen, 2012),(Wang, Laborie and Wolcott, 2005),(Sbirrazzuoli *et al.*, 2009),(Cai, Chen and Liu, 2014)(Yan *et al.*, 2019)].

4.6 Kinetic Prediction of Isothermal Curing

Considering the model-free kinetic methods used for the analysis, the prediction of isothermal cure behaviour can be expressed by the relationship between the curing degree and the reaction time (Zhang *et al.*, 2011). The evolution of conversion at different isothermal temperatures and time may be determined by equation *(4.13)* (Sbirrazzuoli, 2021)

$$t_\alpha = \frac{1}{\beta e^{-E_\alpha/RT_{iso}}} \int_0^{T_\alpha} e^{E_\alpha/RT}\, dT \qquad (4.14)$$

Where t_α is the reaction time, $T_\alpha$is the experimental value of the temperature corresponding to the given conversion at the different heating rates, T_{iso} is the isothermal temperature. However, the equation does not take into account the variation of activation energy (E) with conversion (α) and may be suited for mechanisms where the activation energy is independent of the conversion (Budrugeac, 2019). Therefore, a modification of equation *(4.13)* for arbitrary temperature programs considering mechanism with activation energy varying with the conversion provides for isothermal predictions by the numerical solution of equation *(4.14)* (Sbirrazzuoli, 2021)

$$t_\alpha = \sum_{i=1}^{k} t_{\alpha,i} = \sum_{i=1}^{k} \frac{\int_{t_{\alpha,i-1}^{EET}}^{t_{\alpha,i}^{EET}} exp\left[-\frac{E_{\alpha,i}}{RT(t)}\right] dt}{\exp\left(-\frac{E_\alpha}{RT_{iso}}\right)} \tag{4.15}$$

Where $t_{\alpha,i}^{EET}$ is the Experimentally Estimated Time to reach a given conversion (α).

Based on the equation, simulated isothermal predictions (i.e., the extent of conversion vs. time curves at a given temperatures curves) can be obtained from the treatment of non-isothermal data.

Chapter 5 Kinetic Analysis and Cycle Optimization of Glass/PFA Prepreg

5.1 Introduction

Kinetic analysis is mainly used to elucidate the reaction mechanisms of the thermally activated process and to understand the transformation of reactants turn into products (Sbirrazzuoli, 2021). The objective of the kinetic analysis is to evaluate fundamental kinetic parameters such as the rate constant, activation energy, and reaction model (Vyazovkin *et al.*, 2020). These parameters are particularly important as it provides information on the mechanism of the curing process. The activation energy characterizes the minimum amount of energy required for a process and can be used to assess thermal stability, while the reaction model is used to explain the mechanisms of thermal processes (Hu *et al.*, 2018). From a composite processing and manufacturing perspective, kinetic analysis enables the understanding, development, simulation, and optimization of process parameters under different conditions. The concept and methods used to conduct these evaluations have been discussed in detail in chapter four. Therefore, in this chapter, we discuss the characterization and evaluation of the curing process of the bio-based Glass/PFA prepreg based on kinetic analysis to optimize its curing for rapid isothermal processes. The main objective of cure cycle optimization is to identify a time-temperature cycle that maximizes the thermal and mechanical properties of the prepreg.

To this end, the result of the Model-free kinetic (Friedman and Ozawa Flynn Wall) and the model-based kinetic methods applied to the experimental, non-isothermal, differential scanning calorimetry (DSC) data of the bio-based Glass/PFA prepreg is analysed and studied to have a full understanding of the reaction mechanism and to develop isothermal predictions of conversions (degree of cure). Taking advantage of the model-free kinetic method, the isothermal kinetic predictions that enable the analysis of the time-temperature relationship are employed to optimize the cure cycle using the Friedman model. Finally, the study of thermo-mechanical properties with the aid of a Dynamic mechanical analysis (DMA) of the prepreg during cure under the conditions of the manufacturer's recommended cycle and optimized cycle from the kinetic study is examined and discussed.

5.2 Evaluation of Cure Behaviour from Experimental DSC Measurement.

The normalized calorimetric measurement data of the non-isothermal DSC scan rates of 5°C, 10°C, 15°C and 20°C carried on the Glass/PFA Prepreg is shown in Figure 5-1. The integration of the exothermic peak of the individual dynamic curves from Figure 5-1 provides some vital cure information shown in Table 5-1.

Table 5-1 Cure reaction values for experimental DSC dynamic scans on Glass /PFA prepreg

Heating rate (°C /min)	Exothermic Temperature Range (°C)	Total Exothermic Heat (ΔH_{tot}) (J/g)	Peak Temperature (°C)
5	95-197	-273 ± 9	140
10	100 -202	-276 ± 11	150
15	104-222	-282.1 ± 7	160
20	114-214	-437 ± 10	166

Table 5-1 reveals the average exothermic heat of reaction of the Glass /PFA prepreg to be about 300 ± 9 J/g. This calculated value was found to be comparable with values obtained from similar studies of neat PFA resin (208 ± 21 - 284 ± 25 J/g) (Domínguez, Grivel and Madsen, 2012). However, it is noteworthy to mention that a substantial reaction enthalpy variation is noticed between the 20°C curves and the reaction enthalpy data of the other curves, this variation, in addition to the observed increase in reaction enthalpy value with corresponding heating rate is consistent with previous studies on PFA resin in which the catalyst content was varied (Domínguez, Grivel and Madsen, 2012; Falco, Nathanaël Guigo, *et al.*, 2018; Vargas-Hernández, Sulbarán-Rangel and Vázquez-Torres, 2020), as well as other resin systems (Jain, Choudhary and Narula, 2007; Zhang *et al.*, 2017; Lyu *et al.*, 2018). Although it is well known that in some commonly studied systems such as unsaturated polyester (Aktas *et al.*, 2015), Carbon/epoxy (Newcomb, 2019), polyurethane (Stanko and Stommel, 2018), phenolic resin (Zhang *et al.*, 2011) the enthalpy of reactions generally approaches a relatively constant value regardless of heating rate, the same has not been reported in the literature for PFA resin. In this study, the data spread between the reaction enthalpies for the different dynamic heating glass/PFA prepreg was found to be comparable to related literature data (Domínguez, Grivel and Madsen, 2012; Falco, Nathanaël Guigo, *et al.*, 2018).

Based on the calculated value of the average exothermic heat of reaction, it may initially suggest that the effect of the glass reinforcement may not significantly impact the overall cure kinetic of the Glass/PFA prepreg since no considerable difference in reaction enthalpy between the prepreg and neat resin is evident. The effect of variation of the different dynamic heat rates on the Glass/ PFA prepreg material is evident in the shift in the peak of the individual DSC thermogram. The peak of the exothermic curve for the various heating rates is observed to shift to a higher temperature at an increase in the heating rate at shorter periods. The same effect was reported for modified bismaleimide (Chandran *et al.*, 2012) and benzoxazine resins (Jubsilp, Takeichi and Rimdusit, 2011). This phenomenon may be attributed to the lag in curing response by the macromolecules of the resin in responding to the rapid temperature increase leading the prepreg material to extend the exothermic heat for polymerization (Drakonakis, Seferis and Doumanidis, 2013; Zolghadr *et al.*, 2019; Lascano *et al.*, 2021). Conversely, at a lower heating rate, the exothermic reaction occurs at a slightly lower temperature which is due to the sufficiency of time to allow for crosslink and diffusion which occurs during the curing reaction (Lascano *et al.*, 2019).

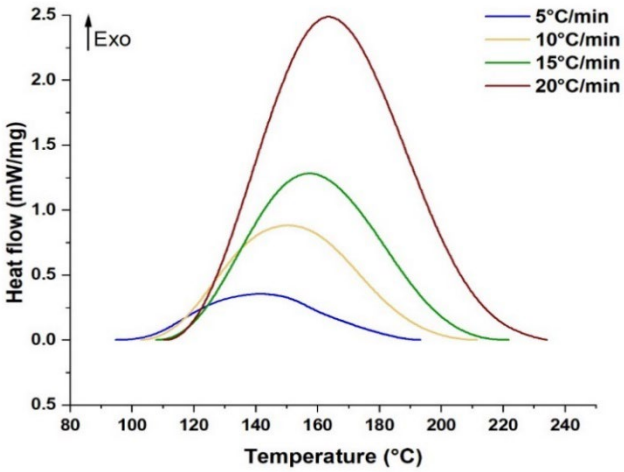

Figure 5-1 Normalized experimental measurement data from non-isothermal DSC scan.

The influence of this behaviour is validated in the conversion curve showing the degree of cure versus temperature and time in Figure 5-2. The exothermic temperature range for the different heating rates indicates that crosslinking during the curing process of the prepreg begins at temperatures above 90°C. The kinetic profile of these graphs exhibits a sigmoidal shape suggesting an autocatalytic reaction of crosslinking (Zhang *et al.*, 2017; Granado *et al.*, 2018; Jouyandeh *et al.*, 2020).

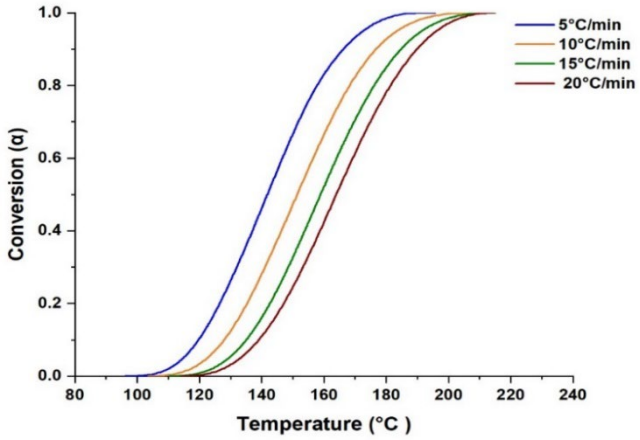

Figure 5-2 Plot showing the conversion as a function of temperature.

Furthermore, the temperature-dependent cure conversion rate profiles shown in Figure 5-3 are seen to be consistent for the different heating rates, thus suggesting a potential consistent reaction mechanism.

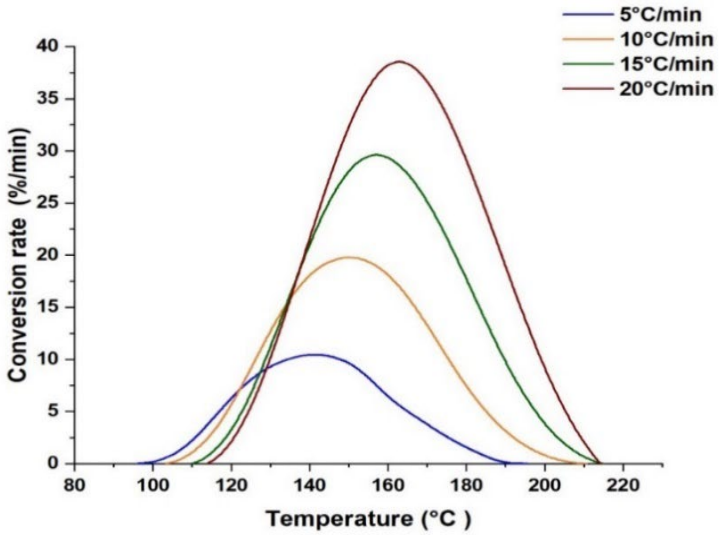

Figure 5-3 Conversion rate as a function of temperature for non-isothermal DSC tests.

5.3 Model-Free Kinetic Analysis

The Friedman (FR) and Ozawa Flynn Wall methods described in sections 4.3.1 and 4.3.2 were used to define the cure mechanism through the apparent activation energy on the degree of cure (α), during the entire cure process. The Friedman plot of $\ln d\alpha/dT$ vs T^{-1} extracted from the

values of the corresponding pair of α and T for each heating rate (as shown in Figure 5-2) is shown in Figure 5-4.

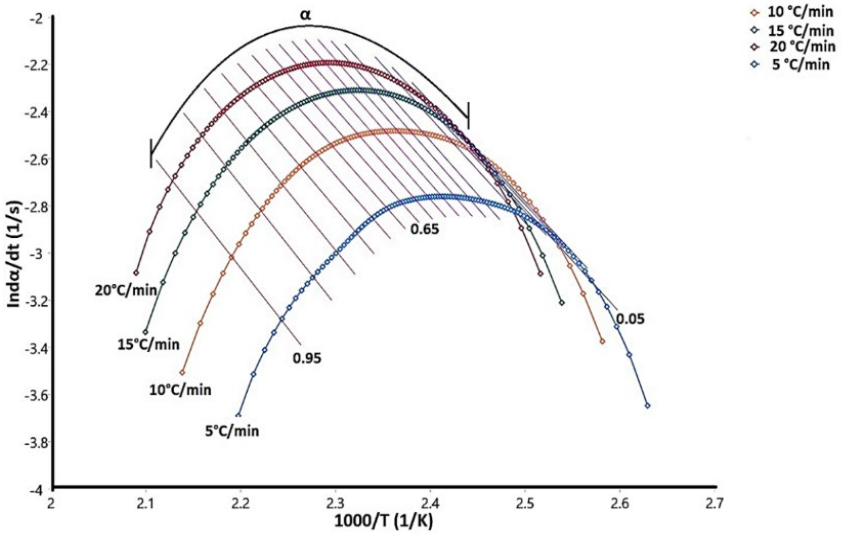

Figure 5-4 Friedman plot analysis of activation energy at various degrees of cure.

A similar plot was obtained for the Ozawa Flynn wall method derived from the plot of $\ln(\beta)$ vs T^{-1} as shown in Figure 5-5.

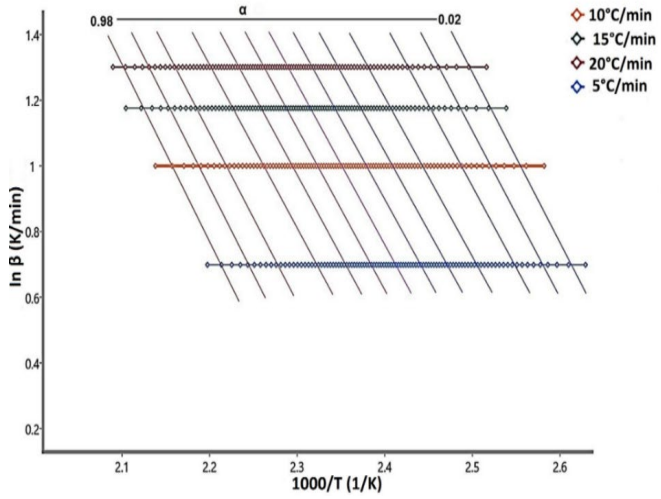

Figure 5-5 Ozawa-Flynn-Wall plot analysis of activation energy at various degrees of cure.

It is observed that the slope of the reaction rate for each of the applied heating rate cases is observed to be steeper than that of the isoconversional lines at the beginning of the reaction (right to left). This suggests an accelerated reaction which may be attributed to the autocatalytic

mechanism (Falco, Nathanaël Guigo, *et al.*, 2018) that induces the polymerization reaction (Lascano *et al.*, 2019).

5.4 Cure Reaction Mechanism and Activation Energy

The derived conversion-dependent activation energy plotted from Figure 5-4 and Figure 5-5 described by equation (9) and equation (10) respectively is shown with error bars that indicate the standard deviation for each calculated data point by the software in Figure 5-6. From both plots, a variation of the activation energy with the evolution of the degree of cure at any extent between 0 and 0.99 with a step change of 0.1 can be observed. The characteristic shape of the activation energy curve is reflective of the occurring crosslinking transitions during the curing process. Thus, indicative that the curing reaction of the glass/PFA prepreg exhibits a complex reaction process made up of several simultaneous and parallel steps (Moukhina, 2012) consequently, leading to effective change in the cure rate-limiting steps of the overall polymerization process (Falco, Nathanaël Guigo, *et al.*, 2018).

From the plot in Figure 5-6, the curing mechanism is observed to undergo various stages. At the beginning of the reaction, a decline in the activation energy from 92kJ/mol to 82kJ/mol is noticed at $\alpha \leq 0.1$ on the Friedman plot. A similar trend was also observed on the Ozawa Flynn wall plot with a decreased activation energy from 92 kJ/mol to 86 kJ/mol at $\alpha \leq 0.2.5$. This may be attributed to the effect of an autocatalytic mechanism similar to that reported for epoxy or modified epoxy (Murias *et al.*, 2015; Ma *et al.*, 2018; Wu, Zhou and Yu, 2018) and other resins (Zhang *et al.*, 2011; Karami *et al.*, 2020) observed in the comparable isoconversional model derived activation energy studies. The autocatalytic mechanism may have resulted from a balance between the concurrent initial main addition reaction (Zhang *et al.*, 2011) and condensation reaction as the formation of active species which begins the polymerization reaction (Guigo *et al.*, 2007; Lopez De Vergara *et al.*, 2014; Falco, Nathanaël Guigo, *et al.*, 2018). In agreement with the autocatalytic effect, the temperature effect on the viscosity of the prepreg contributes to this mechanism. The initial viscosity decrement caused by the increase in temperature of the B-stage cured prepreg at the start of the reaction leads to an increase in the rapid molecular collision of active species and mobility of existing polymer chains, resulting in a slow increase in molecular weight as crosslinking begins to occur. The activation energy (92kJ/mol to 82kJ/mol) at $\alpha \leq 0.2.5$ of the prepreg for both models of the prepreg was observed to be slightly higher than similar studies of that of neat PFA resin reported in the literature (Guigo *et al.*, 2007; Domínguez, Grivel and Madsen, 2012; Lopez De Vergara *et al.*,

2014; Falco, Nathanaël Guigo, *et al.*, 2018). Although the difference is found not to be very significant, it does highlight the possible effect of the reinforcement.

As the cure progresses with the increase in temperature, an appreciation in the activation energy 82kJ/mol to 89kJ/mol at $0.1 \geq \alpha \geq 0.45$ is seen for the Friedman plots (Figure 5-6). During this period, the generated active molecular species formed from the initial step reaction become predominant and interact leading to the formation of furfuryl alcohol oligomers via polycondensation reaction giving rise to the possible occurrence of evaporation of water and volatiles which is a by-product of the polycondensation reactions as the temperature increases during the curing process (Lopez De Vergara *et al.*, 2014),(Guigo *et al.*, 2007). As the reactions evolve, the conversion increasingly develops, and the growing molecular chain continuously increases the molecular weight which notably enhances the viscosity of the reaction. Local motion within the available free volume improves the movement of the chain segment, allowing the reaction to continue. These complexities in the chemical interactions occur simultaneously at the molecular level requiring more energy due to the increase in viscosity. It is noteworthy to remark that the increase in the activation energy observed during this phase was not evident in similar studies to that of neat PFA resin reported in the literature (Guigo *et al.*, 2007; Domínguez, Grivel and Madsen, 2012; Lopez De Vergara *et al.*, 2014; Falco, Nathanaël Guigo, *et al.*, 2018). The neat resins exhibited lower and constant activation energy over the discussed conversion range. Thus, the glass fibre reinforcement may have contributed to the increase in activation energy at this stage by restricting the mobility of active molecules and polymer chains as they consolidate to form a structured network, requiring more energy for the cure reaction to progress.

Progressively, as the temperature increased, the constant activation energy of 88.5 kJ/mol was observed on the Friedman plot (figure 5-6) within the range of α between 0.45 to 0.55 indicating the occurrence of a potential single reaction cure mechanism, thereby validating the discussed mechanism change. The cure behaviour for α between 0.55 to 0.67 revealed by the Friedman model signifies a change in the mechanism. A decline in the activation energy from 88.5 kJ/mol to 87.5 kJ/mol on the Friedman plot was observed. The decline signals the event of the gelation process taking place. This means that the molecular weight approaches maximum and all the monomers are connected by at least one chemical bond (Witold, Joshua and Goodman, 2014). At this stage the low molecular mobility induces a reduction in the overall reaction rate, transforming the reaction from a kinetic to a diffusion-controlled regime (Guigo *et al.*, 2007; Falco, Nathanaël Guigo, *et al.*, 2018).

Beyond this point, a sharp increase in activation energy from 88.5 kJ/mol to 100.5 kJ/mol for α between 0.67 to 0.95 is observed on the Friedmann plot, revealing another change in the cure mechanism. This phase may be attributed to the reactivation of a subsequent chemical process as the remaining gelled chain segment crosslinks as the system approaches the glass transition with increasing temperature. Ostensibly, this occurs at about 165°C and 173°C as seen in figures 11 and 12 and is further described in section 4.5. A similar activation energy increase observed in the study of the neat PFA resin by Guigo et al. (2007) explained the phenomena by the contribution of further Diels-Alder cycloaddition to the cure rate.

The entire process culminates at about $\alpha > 0.95$. At this point, the built-up glass transition temperature of the system tends to exceed the cure temperature allowing for vitrification. The system is characterized by constrained molecular mobility due to the diffusion regime associated with the vitrification phenomenon, thus leading to a decrease in activation energy as seen in the Friedman plot (Figure 5-6).

A comparison between both models used for analysis shows the plot profile of the conversion-dependent activation energy is observed to follow a comparable profile to Friedman's plot as seen in Figure 5-6. Although significant deviations could be observed along with the conversion, they may be attributed to errors due to the error introduced by the calculation method. For example, the approximation error synonymous with the Ozawa Flynn wall model. Individual error bars for both models which indicate the overall error are shown inset of Figure 5-6. The Friedman's profile of the Glass/PFA prepreg activation energy shows a similar trend when compared to related isoconversional kinetic methods used to analyse neat polyfurfuryl alcohol resin reported in the literature. (Rivero *et al.*, 2011),(Lopez De Vergara *et al.*, 2014),(Domínguez, Grivel and Madsen, 2012),(Falco, Nathanaël Guigo, *et al.*, 2018).

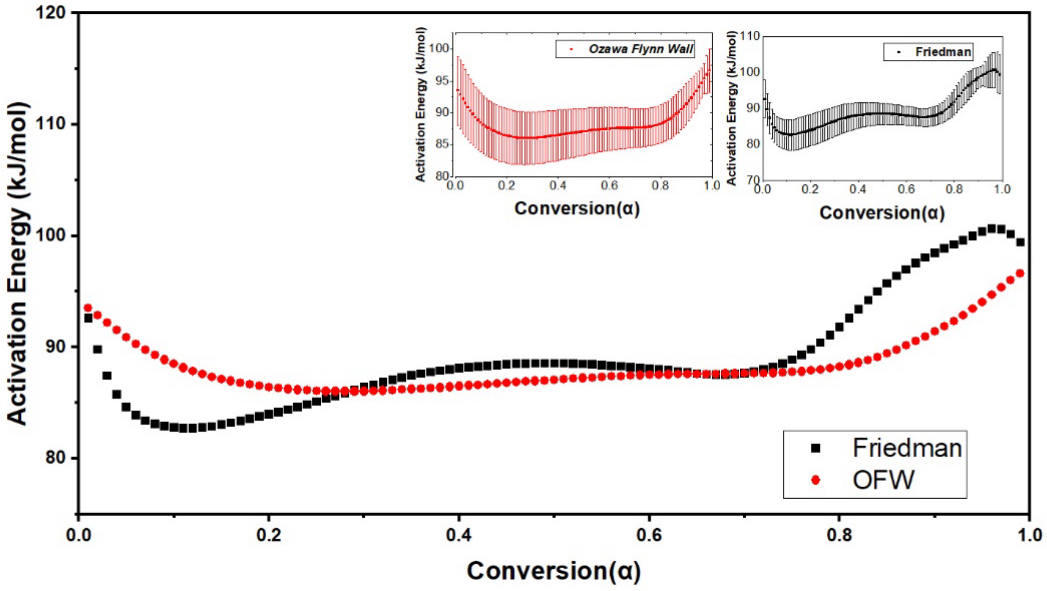

Figure 5-6 Activation energy dependence on conversion using Friedman's and Ozawa-Flynn-Wall plots (Inset: Individual plots with error bars)

The average activation energy of the biobased Glass/PFA prepreg estimated by the Friedman method was 88 ± 4.9 kJ/mol. This value was found to be slightly higher than that reported for neat PFA resins in related literature as shown in Table 5-2. This phenomenon may be attributed to a combination of either the higher activating energy required due to the higher viscosity of the resin achieved from the initial B-stage curing or the influence of the concentration of the activating catalyst in the resin system. The effect of the presence of fibre reinforcement may also be a contributing factor.

Table 5-2 Comparison of activation energy obtained in present study to other studies.

Parameters	**Present study**	**(Rivero *et al.*, 2011)**	**(Guigo *et al.*, 2007)**	**(Lopez De Vergara *et al.*, 2014)**
Resin	Glass/PFA prepreg	PFA Resin	PFA Resin	PFA Resin
Model-free method	Friedman	Kissinger	Kissinger	Ozawa Flynn wall
Activation Energy (E_a)	88 ± 4.9 kJ/mol	72.5 kJ/mol	73 kJ/mol	79.83 kJ/mol

5.5 Model Fitting Kinetic Analysis

From the model free kinetic analysis in section 5.4, the clear observation of the variation of the activation energy with the evolution of the conversion (degree of cure) reveals the complexity of the reaction that occurs during the curing process of the biobased Glass/PFA prepreg. From the model-fitting kinetics perspective, these complexities are evident in the appearance of reaction steps with their activation energy and reaction type. The revealed mechanism of the biobased Glass/PFA prepreg from the isoconversional models shows that the cure mechanism which drives the curing process predominantly constitutes of autocatalytic reaction. For this reason, the Kamal-Sourour autocatalytic model was fitted with the experimental data to describe the curing process. Using a nonlinear regression method with the aid of Origin Pro software (Trial version) the conversion rate – degree of cure plot obtained from the experimental data of the individual heating rate using equations 4.4 and 4.5 was fitted with the Kamal -Sourour model. Table 5-3 presents the obtained kinetic fitting parameter result.

Table 5-3 Kinetic parameters obtained using the Kamal-Sourour model based on dynamic experimental data.

	Kinetic Parameters					
Heating rates	A_1	E_1	A_2	E_2	(m)	(n)
5℃	1.61159	127.13402	2.49391	52.88773	0.60017	0.72304
10℃	1.61862	97.15918	3.66927	50.53638	0.60464	0.69334
15 ℃	1.39082	109.60482	4.76186	48.90127	0.651	0.73579
20 ℃	1.71931	98.47092	5.53633	47.9486	0.64582	0.75849
Mean	1.62251	108.09	4.11	50.06	0.6254	0.727

Thus, from Table 5-3, the model-based equation for the curing of the glass/PFA prepreg can be represented by

$$\frac{d\alpha}{dt} = \left(1.62\ Exp\frac{108.09}{RT} + 4.11\ Exp\frac{50.06}{RT} \propto^{0.63}\right)(1-\propto)^{0.73} \quad (5.1)$$

To validate the model, the experimental results are compared with the model in equation (14), as shown in Figure 5-7. It is seen that the model equation is in good agreement with the experimental results showing a correlation coefficient of 0.98.

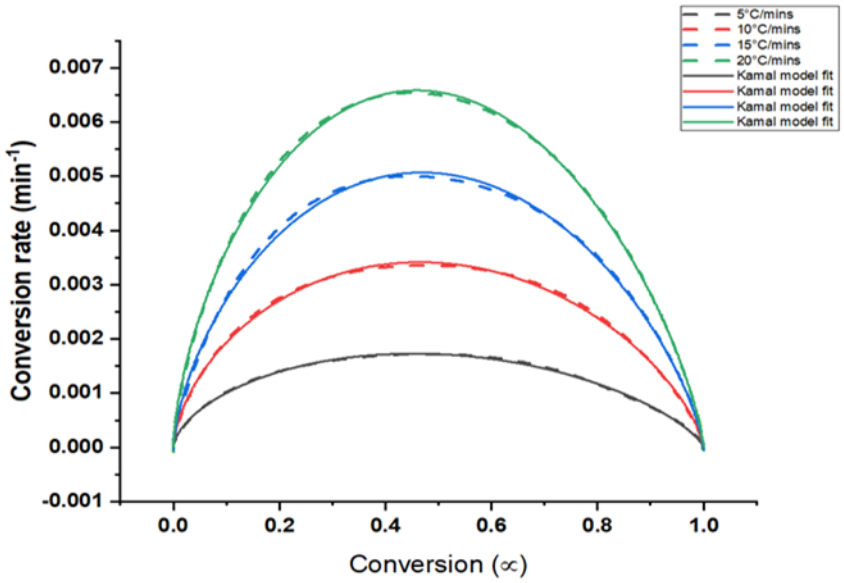

Figure 5-7 Comparison of experimental values and the Kamal Model

For further model validation, the activation energy derived by the isoconversional method was compared to that obtained by the model fitting equation. It was revealed that the average of the sum of the calculated activation energies E1 and E2 from the model correlate quite well with a difference of about 9 kJ/mol to that obtained by the Friedman model of the isoconversional method.

Despite, the agreement between the experimental data and the Kamal-Sourour model, it is worth noting that the equation may not be a fully sufficient representation of the curing process as it assumes the curing as a function of chemical reactive kinetics throughout the process without taking into account the other process such as diffusion which also occurs toward the end of the reaction. This drawback contributes to its limitation for the isothermal predictions.

5.6 Isoconversional Kinetic Model Validation

A comparison between the predicted conversion (degree of cure) of the individual kinetic models and experimental data is very helpful in determining the reliability of the models and by extension the choice model for isothermal prediction. The simulated conversion curve results from the Friedman kinetic model presented in Figure 5-8 exhibited an excellent fitting with each of the experimental data with a correlation coefficient of 0.998. A slight bias between the curves was observed at the beginning of the reaction at $\alpha < \sim 0.2$. This may be expected due to the limitations of differential computations of very small conversion interval steps

decrement or noise smoothing. On the other hand, significant deviations were observed from α < 0.8 in the comparison between the Ozawa Flynn wall model predicted conversion curves and the experimental data as shown in Figure 5-9. Beyond this range, the deviation diminishes. This is corroborated by a correlation coefficient of 0.851. The observed deviation may be attributed to the computational errors as highlighted earlier.

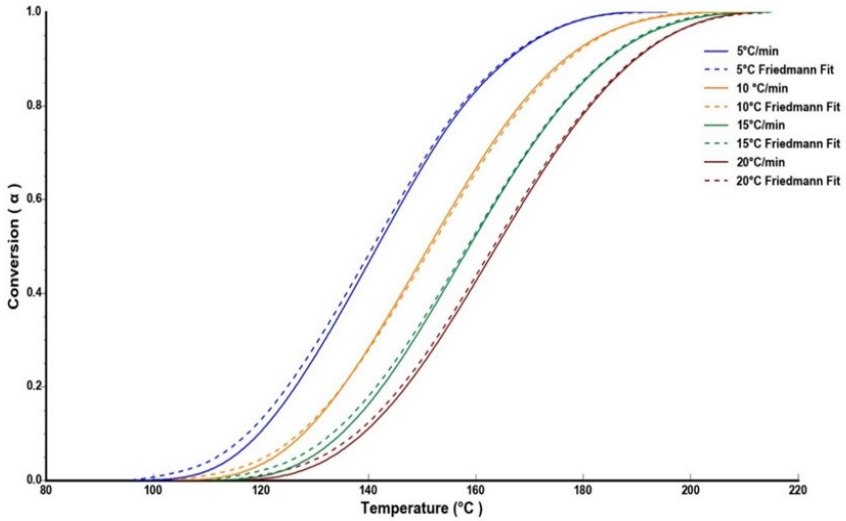

Figure 5-8 The conversion fit showing the agreement between the experimental data and Friedman's Model

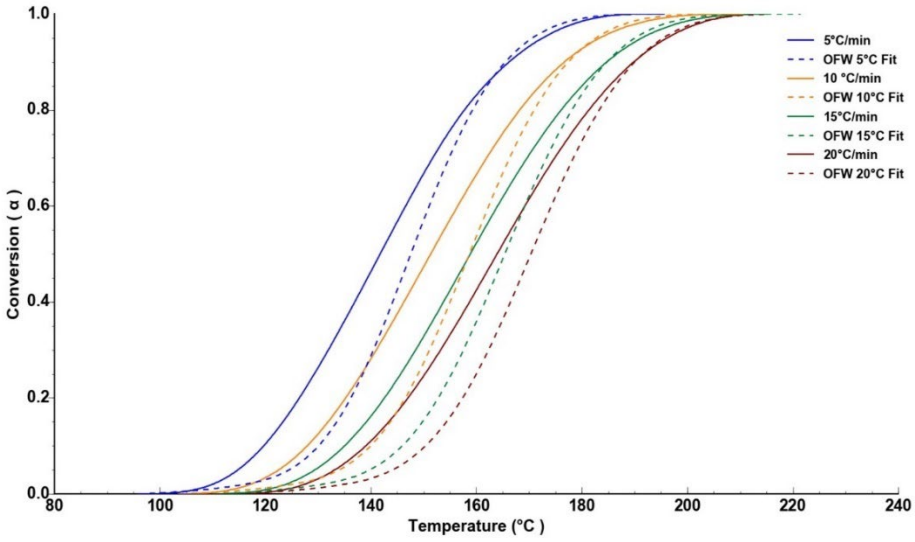

Figure 5-9 The conversion fit plot showing limited agreement between the experimental data and Ozawa Flynn Wall Model

Overall, despite the observed limitations, both models may be used to evaluate the apparent activation energy, however, results from the Friedmann model provide better accuracy and hence are preferred for isothermal kinetic predictions of Glass/PFA prepreg.

5.7 Kinetic Prediction of Curing Degree of the Glass/PFA Prepreg under Isothermal Conditions

Kinetic predictions are well-known techniques used to assess the kinetic behaviour of materials outside the temperature domain in which the kinetic parameters were measured experimentally (Vafayan *et al.*, 2013). From the conclusion drawn from the previous section, the Friedman model proved better reliable for analysis based on the validity of its fit to the non – isothermal experimental data. As a result, time-dependent - conversion curves for isothermal temperatures were predicted using equation (14), based on Friedman's model. Figure 5-10 presents the simulated conversion curves of the biobased Glass /PFA prepreg for a range of predictive isothermal temperatures and their corresponding cure time as a function of the degree of cure using the Friedman model. To compare and validate the model's predictions, experimental runs of two isothermal temperatures (120°C and 160°C) were performed for 30 minutes and 100 minutes, respectively, as suggested by the predictions in Figure 5-10. Figure 5-11 shows a very good agreement between the observed curves of both isothermal runs (120°C and 160°C) and the predicted curve from the model. Thus, demonstrating the validity of the modelling methodology. According to the model, the manufacturer's recommended cycle of an isothermal dwell for 1 hour at 130°C after an initial ramp up at 2°C from room temperature, which potentially achieves cure in a total time of 112.5 minutes, could be optimized to achieve over a 97 per cent degree of cure in 30 minutes if processed in an isothermal condition such as in a compression moulding. The consideration of the results is however independent of other processing factors such as compaction pressure, and void content. Furthermore, factors such as part thickness and complexity of profile may also make it difficult for uniform isothermal conditions to be maintained throughout the part and these must be taken into account. Ultimately, timesaving is particularly important at an industrial level, especially where rapid manufacturing is essential.

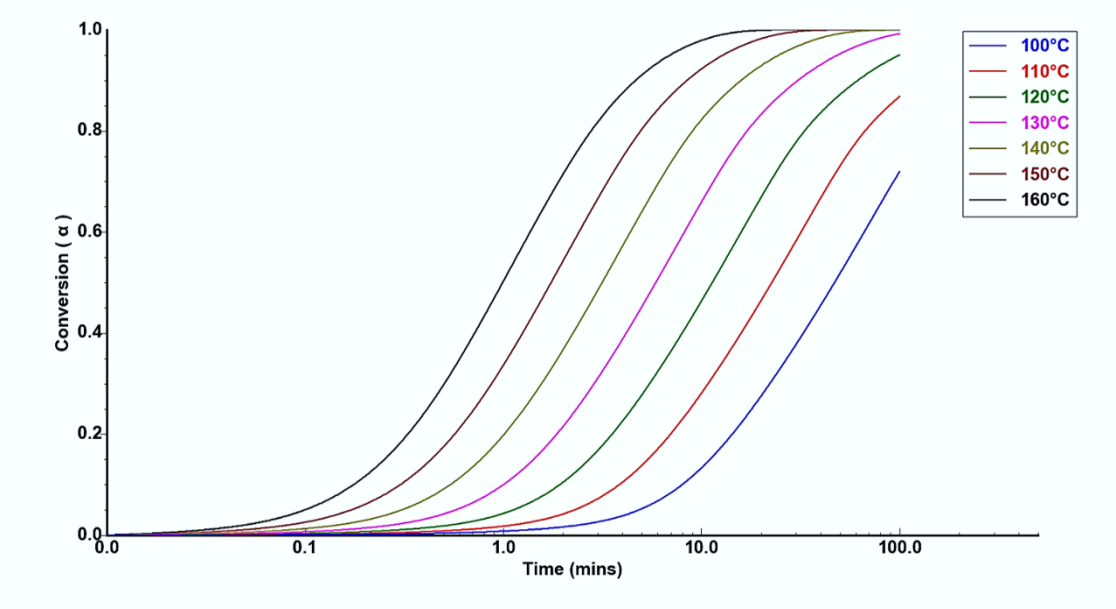

Figure 5-10: Predicted conversion curves for isothermal temperatures as a function of time.

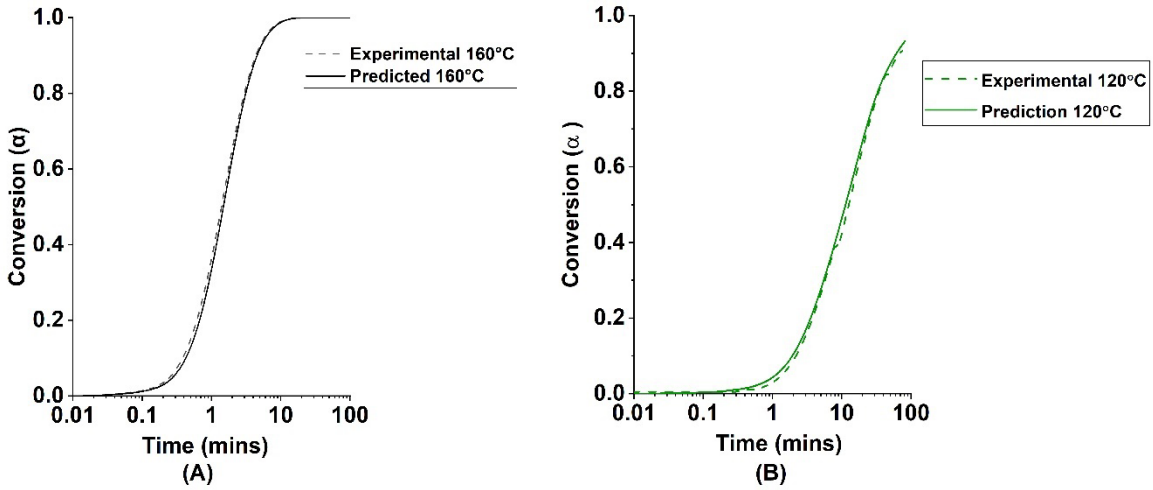

Figure 5-11 Comparisons between isothermal predictions and experimental data at different temperatures. (A) 160°C (B) 120°C

5.8 Dynamic Mechanical Analysis on the Cure Study of the Glass/PFA Prepreg

The viscoelastic behaviour of the uncured bio-based prepreg gave good insight into the relationship between the structural evolution and the curing transitions. From Figure 5-12, it can be seen that the increase in temperature leads to an initial decline in the storage modulus. This is due to the initial relaxation within the macromolecule of the resin because the material is already in a B-stage cured state causing chain mobility. Subsequently, a further increase in temperature results in an increase in the tan delta curve. Thus, indicating rapid agglomeration of the chain network giving rise to a corresponding increase in stiffness of the material which is seen with the corresponding increase in the storage modulus. This is seen to continue till the tan delta reaches its peak at about 120°C and subsequently begins to decline. An initial decline is observed in the storage modulus; however, this changes as it is seen to increase shortly afterwards. This is indicative of two possible scenarios, either the rest of the molecular reaction is continued by a diffusion control mechanism or alternately, the cure cycle is not sufficient to achieve a complete cure.

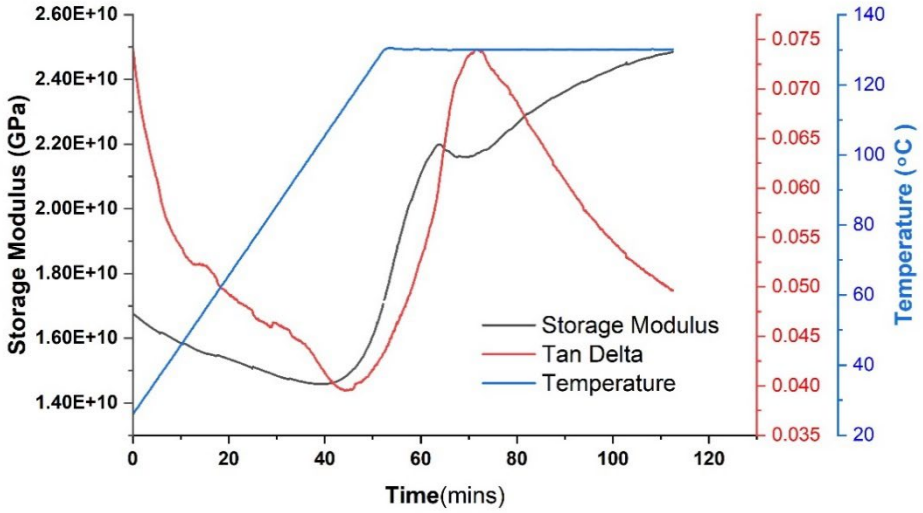

Figure 5-12 The DMA curve of the curing of the Glass reinforced PFA prepreg.

Based on this understanding, the DMA analysis of the pocket-cured samples using the manufacturer cure cycle and the model optimized cycle reveals the plots of the tan delta and storage modulus as a function of temperature as seen in figures (5-13 and 5-14). The temperature at the peak of the tan delta curve revealed the glass transition temperature (Tg) of

the manufacturer cycle (130°C at 2°C followed by isothermal dwell at 130°C for 1 hour) to be at about 165°C while that of the optimized cycle (Isothermal at 160°C for 30 minutes) predicted by the model is observed at about 173°C. The peak height of the tan delta values for both cases is seen to be very low with the sample from the model-optimized cycle even lower. Thus, suggesting good fibre matrix adhesion (Shanmugam and Thiruchitrambalam, 2013) which culminates in a rigid network structure aiding good load-bearing capacity. The storage modulus of the kinetic model predicted optimized cured sample (Figure 5-14) exhibited a value of 7 GPa which is noticed to be higher than that of the manufacturer cycle (Figure 5-13)

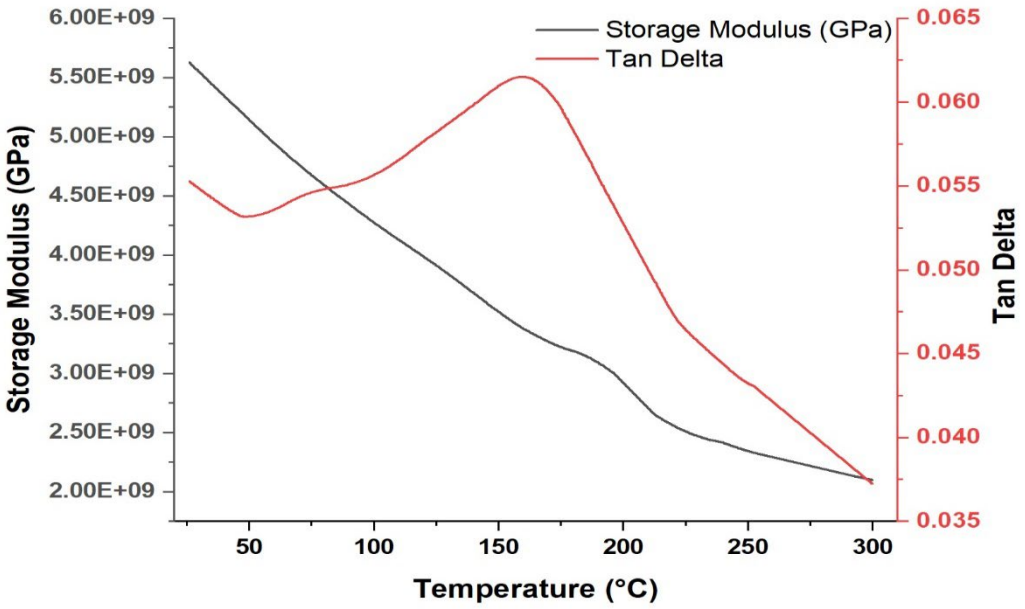

Figure 5-13 Storage modulus and tan delta plot of cured Glass/PFA prepreg using the manufacturer cure cycle.

which had a value of 5.6 GPa. However, they both showed a steep decline in value with the increase in temperature. This trend is quite expected considering the thickness size (0.24 mm) in relation to the fibre content of the pocket-cured sample. From the above discussed, it is evident that the kinetic model optimized cycle presents a relatively better result in comparison to that obtained from the manufacturer's recommended cycle. This further validates the predictive capability of a model-free kinetic approach to cure cycle optimization.

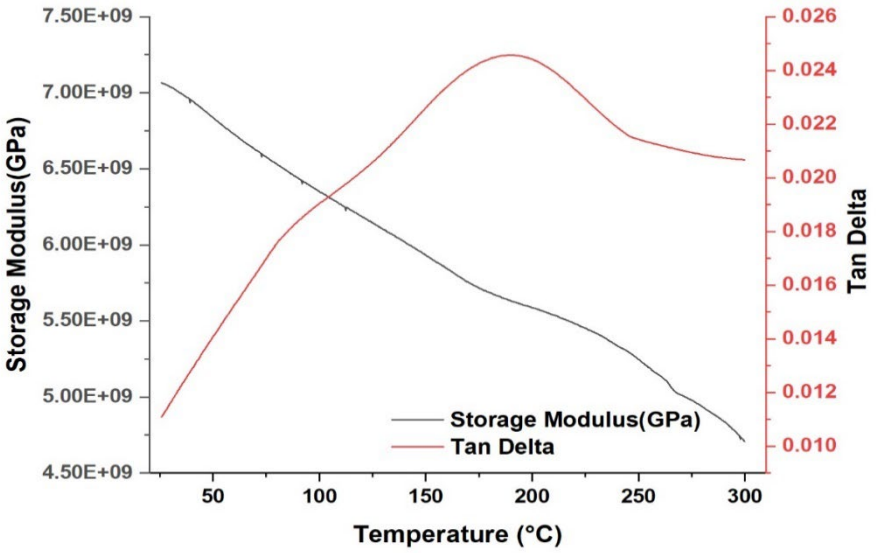

Figure 5-14 Storage modulus and tan delta plot of cured Glass/PFA prepreg using the kinetic model predicted optimized cure cycle.

5.9 Summary

In this chapter, the cure reaction behaviour of the biobased Glass/Polyfururyl Alcohol prepreg was studied employing non-isothermal DSC analysis using a model-free and model-fitting kinetic approach. The cure mechanism was analysed through the activation energy dependence on conversion using the Friedman and Ozawa Flynn wall method, to understand the curing mechanism and to find out the practical limits for a possible reduction in cure time using faster heating rates during curing. The curing mechanism of the biobased glass/PFA prepreg was found to exhibit a complex reaction process made up of several simultaneous and parallel step cure mechanisms. To validate the model, a comparison was made between both models and a temperature conversion plot from dynamic experimental data. The Friedman method which exhibited an excellent fit (R =0.998) with the experimental data was proven to be more accurate for analysis and isothermal prediction. The average value of the activation energy of the biobased glass/PFA prepreg was determined to be 88 ± 4.9 kJ/mol which was found to be slightly higher in value compared to previous work on neat PFA resin. The increase may be attributed to the effect of the glass reinforcement in the prepreg. Furthermore, the viscoelastic behaviour during the curing process was analysed and found to follow the established pattern described by the model. The results from the kinetic analysis enabled Friedman's algorithm to predict the relationship between conversion (degree of cure) and time-temperature which

allows for cure cycle optimization for isothermal curing conditions. This is evident in the reduction of curing time by about 50% during Glass/PFA composites manufacture. Finally, DMA analysis of the pocket-cured composite using the predicted optimized cure cycle and the manufacturer-recommended cure cycle was employed to further validate the kinetic prediction capability of the model. The findings of this study demonstrate the effectiveness of a simple model-free kinetic approach for the cure cycle optimization of composite prepregs for manufacturing processes.

Chapter 6 Experimental Results and Discussion

6.1 Introduction

The characterization of the cure kinetics of the glass/PFA prepreg conducted in Chapter 5 suggests an optimum cure cycle that halves the processing time making it suitable for rapid manufacture by a compression moulding technique. The DMA analysis revealed that the optimized cycle exhibited better thermo-mechanical characteristics compared to the manufacturer's cycle. Despite the success of the kinetic analysis, it is important to state that the study considered only time-temperature parameters and did not consider curing pressure, which is an important manufacturing parameter. During the curing process, pressure contributes to the consolidation of the prepreg plies and the expulsion of excess resin and air bubbles from the laminate (Hernández *et al.*, 2013). This parameter is very important because insufficient pressure could lead to void formation or poor infiltration effect within the reinforcement limiting the overall property of the cured laminate. Excessive pressure, on the other hand, could bleed out the resin while restricting the diffusion and collision of molecules of the resin resulting in weak adhesion, fibre distortion and an overall laminate with poor mechanical and thermal properties Hence, to establish a suitable rapid cure procedure for the Glass/PFA prepreg, it is necessary to evaluate the effect of pressure on thermal and mechanical properties of the cured biobased Glass/PFA composite for the selection of an optimal pressure parameter suitable for the developed optimized cycle. Literature has documented numerous techniques for finding the optimum pressure relative to other parameters for composite manufacturing. This includes the application of the design of experiment methods (Tharazi *et al.*, 2017; Zhijun *et al.*, 2019), genetic algorithm, finite element, and numerical simulation method (Dolkun *et al.*, 2018). However, due to the limitations of our manual hydraulic press, only 5 and 10-bar pressure were evaluated for comparison in finding the optimal pressure suitable for the optimised cure cycle of the glass/PFA Prepreg as established by a kinetic study.

For this reason, individual set samples were manufactured utilising the compression moulding technique (hot press) using the optimized cycle at 5 and 10 bar, respectively. Similarly, another set of samples was manufactured by the vacuum bagging and oven curing method using the manufacturer's recommended cycle as detailed in section 3.2. For ease of understanding, Table 6.1 details the sample specimen designation and their cure parameter.

Table 6-1 Sample designation and cure parameters for Glass/PFA laminate manufacturing

Sample Code	Manufacturing Method	Cure Temperature (°C)	Cure Pressure (bar)	Total Manufacturing Time (mins)
OVC	Vacuum bag /Oven	130 (Ramp and Dwell)	-1	112
CM 5	Hot Press	160 (Isothermal)	5	30
CM10	Hot Press	160 (Isothermal)	10	30

In this chapter, the results of the mechanical and thermal characterization of glass/PFA laminates produced with two different processes are presented. Mechanical (Flexural, Tensile and interlaminar shear strength testing) and thermal (glass transition temperature) evaluation was performed on individual samples of the manufactured plates. The result of samples from the plates made at two different pressures through the hot press using the optimized cycle from the kinetic study (CM5 and CM10) was compared to the results of samples from panels made by a vacuum bag oven curing process using the prepreg manufacturer curing cycle.

6.2 Examination of Manufactured Composite Laminate

The Glass/PFA composite panel were manufactured using the Vacuum-bag/Oven curing method and the Compression moulding process (Hot-press). The manufacturing procedure of both methods has been discussed in detail in section 3.4. Following through the techniques of both processes, cured panels from which samples for mechanical and thermal characterization described in sections 3.4.1 and 3.4.2 were produced. Figures 3-16B, 3-19A and B show the images of the Glass/PFA panel manufactured using the vacuum bagging/oven curing process and images of the Glass/PFA composite panel manufactured using the compression moulding (Hot Press) using the optimized cycle from the kinetic study at 5 bar and 10 bar, respectively.

6.2.1 Examination of Composite Laminate Quality

To assess the quality of the manufactured laminates to gain a thorough understanding of the process-induced microstructure variations, through thickness cross-sections of hot press and oven-manufactured individual panels were examined under an optical microscope, as described in section 3.7, Figure 6-1 presents representative optical macro and microscopic image view of the cross-section of the individual manufactured panels by the different processes.

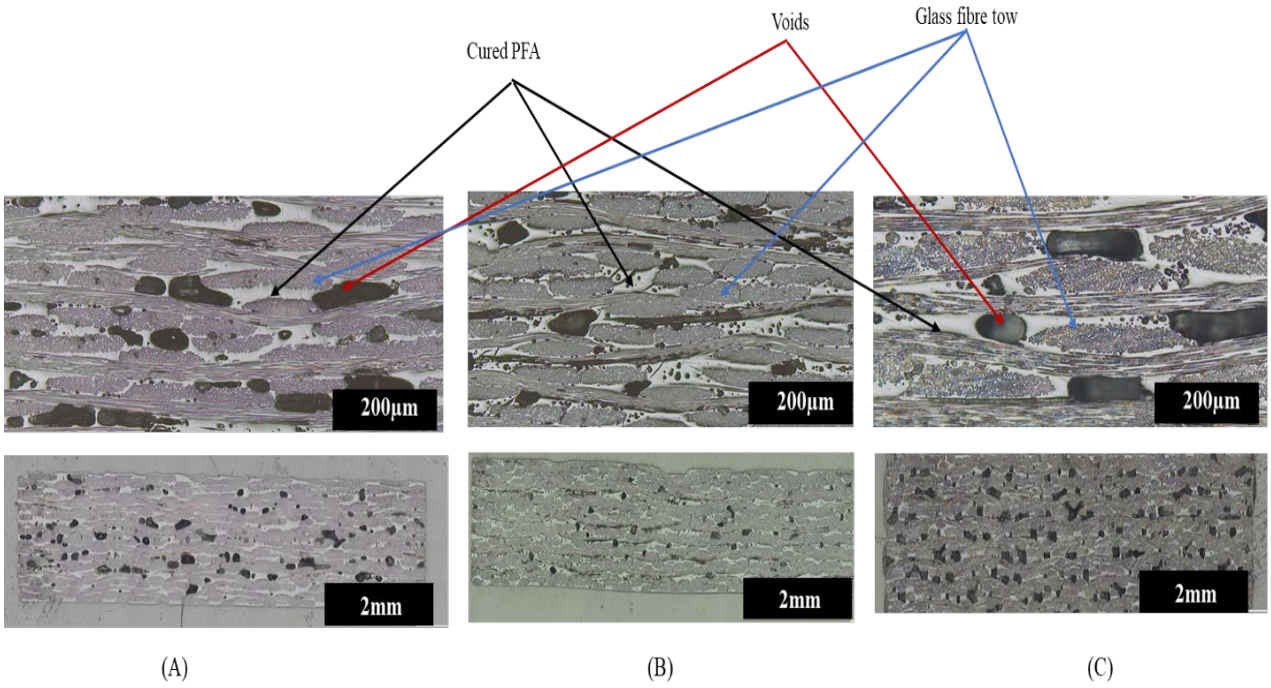

Figure 6-1 Cross-sectional view of panels manufactured by different processes (A) OVC panel (B) CM5 panel (B) CM10 panel.

For the three differently manufactured panels, the constituent laminate glass fibre tows, cured polyfurfuryl alcohol resin and voids can be distinctively seen at 100X magnification as indicated by the arrows in Figure 6-1. The polyfurfuryl alcohol matrix phase is seen as the muted grey background, whereas the darker grey elliptical objects correspond to the twill glass fibres aligned in the direction perpendicularly to the cross-section. The black spot on the images shows the voids within the laminates. It could be observed for the individual samples that the voids predominately appeared resin-rich zone and sparsely between the yarns or at the interface between the fibre despite the difference in the manufacturing process and pressure conditions. The proximity of the inter and intralaminar fibre two within the individual composite samples highlights the effect of the different manufacturing consolidation pressures. For all cases, the cured laminate had an equal number of layers and stacking sequences.

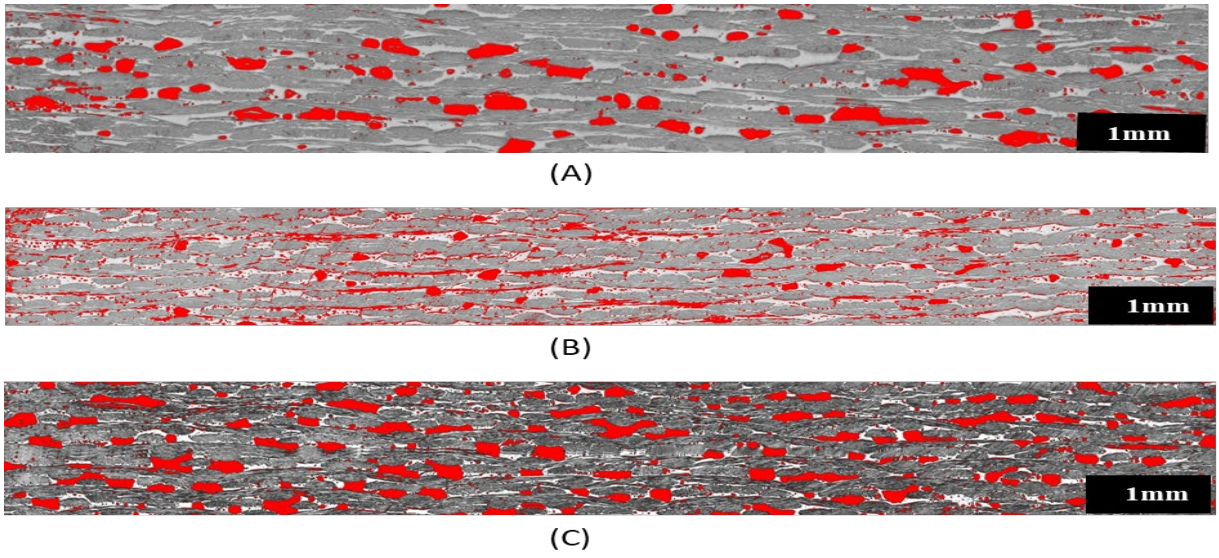

Figure 6-2 Representative void distribution (a) OVC sample (b) CM 5 sample (c) CM10 sample.

Typically, the formation of voids in composites is produced by the entrapment of air during the layup process or by volatiles inside the resin or resin fibre interface during curing (Mehdikhani *et al.*, 2019). They are generally considered to have a detrimental effect on the mechanical properties of fibre-reinforced composite materials. Figure 6-2 depicts optical microscope images of the distribution (form and size) of voids (red area) within typical specimens cut from the various laminates. In all instances of the laminates, void formation was mostly observed within the PFA matrix, indicating the evaporation of water, a consequence of the polycondensation reaction in the form of moisture during the curing process (Oishi *et al.*, 2013). Analyzing and evaluating the images of the various laminates with Image J's thresholding function reveals the percentage voidage and fibre content, as well as the void equivalent diameter. Presented in Table 6-2 are the laminates produced using various methods and pressure conditions as well as the calculated constituent composition. At the same level of image magnification, voids are more visible on the OVC and CM10 samples than on the CM5 sample as shown in Figure 6-2. As shown in the table specimens of the different laminates were analysed and the results indicated that the void content of the oven-manufactured sample (OVC) was about 16.3% while hot press manufactured laminates (CM 5 and CM 10) were 10.9% and 17.8% respectively.

Table 6-2 Constituent content of the different manufactured laminates.

	OVC	CM5	CM10
Manufacturing Method	Vacuum Bag /Oven Curing	Hot Press	Hot Press
Curing Pressure	-0.98 bar (Vacuum)	5 bar	10 bar
Void Content (V_c) (%)	16.3	10.9	17.8
Fibre Volume Fraction (V_f) (%)	39.2	43.4	47.2
Void Equivalent Diameter D_e (µm)	12	2	9

Voidage in the three laminates (OVC, CM5, and CM10) was observed to have an irregularly elliptical shape, with varying levels of flatness appearing primarily in the resin-rich region between the fibre towsTop of Form (see Figure 6-2). According to the determined equivalent void diameter shown in Table 6-2, the void sizes of OVC laminates are approximately 83.3% larger than those of CM5 and 25% larger than those of CM10. The effect of the manufacturing process's consolidation pressure may be regarded as one of the most principal factors significantly influencing void size. Similar phenomena were observed by Anderson and Altan, in their work on the effect of laminate edge conditions on the formation of micro-voids in composite laminates (Anderson and Altan, 2015). Relatedly, the fibre volume fraction of the OVC laminate was determined to be 39.2 % while that of the compression moulded laminates (CM5 and CM10) was calculated to be 43.2% and 47.2% respectively. Visible fibre bundles from the images in Figures 6-5 B and C exhibit a high level of compaction that rapidly reveals the pressure's effects. In addition, there are fewer apparent resin-rich areas in the CM5 and CM10 samples, which can be attributed to the higher pressure that led the plies to nest and the tows to compact. These two effects are consistent with the greater fibre volume percentage of samples produced by hot pressing.

For the OVC sample, the observed spatially distributed voids may be primarily caused by the nucleation and development of entrapped fast-vaporized wet and volatiles, which are formed as a byproduct of the polymerization reaction during the curing process under vacuum. With the hot press-produced sample (CM5), the combined effect of steady compaction pressure and periodic degassing by elevating the top platen as the resin's dynamic viscosity changes during the curing process, allowing volatile escapes, suggests a positive contribution allowing for better bonding and reduced voids with more flat shapes. This was alluded to by Resch-Fauster et al. (2018), where a comparable method was utilized. In the case of the CM10 sample,

however, the higher pressure may have caused resin bleeding, allowing the migration of resin and voids into the gap between the warp and weft structure of the glass reinforcement, while simultaneously confining the flow zone. Consequently, this explains the dry, fibre-rich appearance visible on the face, as well as the increased fibre proportion. Moreover, the impact of high compaction pressure on through-thickness resin flow at the interlaminar level is visible in the observed ply waviness.

6.3 Thermomechanical Properties Characterization of Cured Laminate

The viscoelastic behaviour of the biobased Glass/PFA composites was studied with the help of DMA and the TMA. Results from the DMA analysis of a cured laminate enable the determination of the temperature-dependent properties of storage modulus and the glass transition temperature of the laminate. The storage modulus indicates the state of the cure and the final stiffness of the cured sample, whereas the glass transition temperature is a good candidate for correlation with mechanical properties because it is highly dependent on the cure cycle and corresponds to an essential physical property used in structural design. (Gernaat *et al.*, 2009). The tan delta plot of a DMA analysis is a ratio of viscose to elastic response of a material to applied stress or strain as a function of temperature. It is also referred to as the measure of the ratio of the loss modulus to the storage modulus during one cycle of oscillation (Gupta and Singh, 2018). It provides useful information on the state of the material being investigated. For example, the peak of the Tan delta curve is interpreted to give the glass transition temperature (T_g) of a given material. In relation to a temperature range, it shows the molecular transitions which occur in a material thus providing information on the damping properties of composite materials. According to John and Anandjiwala (John and Anandjiwala, 2009), damping property in fibre-reinforced composites is majorly affected by (a) the nature of matrix and fibre (b) the nature of interphase (c) frictional damping due to slip in the unbound regions between fibre and matrix interface or delamination and (d) damping due to energy dissipation in the area of matrix cracks and broken fibres.

Another thermomechanical characterization technique employed to characterize the biobased Glass/PFA composites was the application of the Thermomechanical Analyzer (TMA). This technique was employed to measure the glass transition temperature as well as to understand the dimensional change associated with the relaxation of stress stored in a material as a function of temperature.

6.3.1 Dynamic Mechanical Analysis (DMA) Characterization

Conducting a dynamic mechanical analysis test revealed several temperature-dependent parameters of laminated composites, such as storage modulus, loss modulus, and tan delta. These thermo-mechanical properties characterize stored elastic energy and the energy expended as the material undergoes forms of mechanical straining. These properties are considerably influenced by filler features, i.e., cure cycle, manufacturing processes, weight fractions, the dispersion state of fillers in the matrix, geometry and adhesion between reinforcement and matrix (Hossain *et al.*, 2020). Figure 6-3 displays the storage-dependent temperature plot obtained from the DMA run ranging from 25 to 300 °C conducted at a heating rate of 2°C/min on biobased Glass/PFA panel (OVC), which was manufactured using the recommended cure cycle provided by the prepreg manufacturer and Glass/PFA panels (CM5 and CM10) manufactured by hot press, utilizing the optimized cure cycle derived from the kinetic study of the prepreg, as described in section 3.3.3

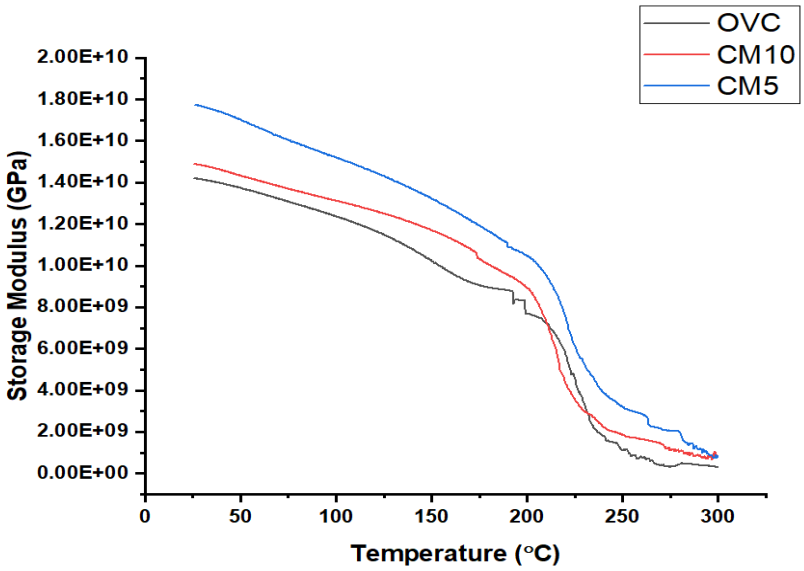

Figure 6-3 Storage modulus vs Temperature plot for OVC, CM5, and CM10 laminates.

For all the cases of the manufactured panels, the storage modulus at 25 °C has been presented in Table 6-3. It is observed that in all cases of the laminate, the storage modulus begins to decline as the temperature increases. In a glassy state, the rate of decline was lower, but as the temperature approached the glass transition, the rate increased. The decrease is ascribed to increased chain mobility of the polymer or the cooperative a-relaxation of PFA chains, which is often associated with the glass transition (Falco, Nathanael Guigo, *et al.*, 2018). This

phenomenon is not uncommon, as it has been observed to be synonymous with polyfurfuryl alcohol resin in literature (Deka, Misra and Mohanty, 2013; Asaro *et al.*, 2019; Menager *et al.*, 2019; Ipakchi *et al.*, 2020; Marefat Seyedlar, Imani and Mirabedini, 2021). For the oven-manufactured sample (OVC) this decline is observed up to about 173℃ where a step decrease in the storage modulus is seen with a corresponding increase in the tan delta. Similarly, the onset of the storage modulus is observed for the CM5 and CM10 at 180℃ and 200 ℃ respectively. Also, the storage modulus of all the samples in the rubbery condition was observed not to have risen not rise indicating full curing (Ma *et al.*, 1995). A comparison between the magnitude of the storage modulus observed at 25℃ as determined in Table 6-3, shows the CM5 sample possessed the highest storage modulus value amongst the three samples investigated. The storage modulus value of the CM5 sample at 25℃ was about 19% higher than both the OVC and CM10 samples. The difference in the storage modulus values may be attributed to varied volume-free rigid chain structures or lower densities of the crosslinks which culminate in smoother stress transfer between the chains (Falco, Nathanael Guigo, *et al.*, 2018; Meng *et al.*, 2020). In fact, according to Ünal et al. (2017) the projection of crosslink density distinguished between a glassy condition and a rubbery plateau. To validate this reason, the Flory theory for rubbery elasticity (Mashouf Roudsari, Misra and Mohanty, 2017; Meng *et al.*, 2020) was used to calculate the crosslink densities of the three different samples. This is expressed using equation *(6.1)*

$$v_e = \frac{E'}{3RT} \tag{6.1}$$

$V_e = Crosslink\ density$

E' = $Elastic\ modulus\ value\ at\ T\ (MPa)$

$R = Gas\ constant\ \ of\ value\ 8.3144\ \ J/K/mol$

T = *Temperature at which the storage modulus and tan delta do not change in the rubbery state in Kelvin(K).*

From the storage modulus and tan delta plots against temperature in Figures 6-3 and 6-4, the rubbery plateau showed it peaked at about 50℃ above the glass transition temperatures for the

respective samples. Therefore, $T = T_g + 80$ was applied to the equation. A summary of the calculated crosslink densities is presented in the thermal property in Table 6-8

Table 6-3 Thermal properties summary of OVC, CM5, and CM10 samples from DMA analysis.

Sample	OVC	CM5	CM10
$\boldsymbol{Storage\ modulus\ E'_{glass}\ at\ 25℃\ (GPa)}$	14.99	17.731	14.19
$\boldsymbol{Glass\ transition\ Temperature(T_g)(℃)}$	173	200	184
$\boldsymbol{Storage\ modulus\ E'\ at\ (T_g + 80℃)\ (MPa)}$	1750	131	700
$\boldsymbol{Crosslinking\ \ density\ V_e\ (\times 10^3 mol^{-3})}$	11.1	13.8	11.4

The effect of the crosslinking density is better understood by the analysis of the glass transition temperature(T_g) of the panels. The glass transition temperature(T_g) was evaluated by the peak of the tan delta-temperature curve of the individual sample. As shown in Figure 6-4, the tan delta plot reveals a distinct peak which is followed by multiple peaks at elevated temperatures. These peaks may suggestively be interpreted as noise which may be due to loss of dimensional stability as the sample was observed to be loosed on the clamps of the DMA up on completion of the run for all cases of the sample. The distinctive peak observed on all the samples was suggestively indicative of the composite having a homogeneous network structure. A similar phenomenon was reported in (Wang *et al.*, 2018). In terms of the glass transition temperature(T_g) , this was observed at about 202℃ for CM5 sample which is 18 and 26℃ higher than the OVC and CM10 samples. The difference can be associated with the crosslinking densities calculated earlier. Clearly, from Table 6-3, it is evident that the CM5 panel exhibited a 9.3% and 31.5% increase in crosslinking density compared to that of the OVC panel and the CM10 panel, respectively. Thus, accounting for the higher glass transition temperature recorded by the CM5 sample which in effect translates to better mechanical properties as evident in the higher elastic modulus value. Increasing the crosslinking density is known to lead to corresponding in mechanical property of a material (Hanifpour *et al.*, 2019) as the stress value demand for the failure of such material would increase (Safranski and Gall, 2008)

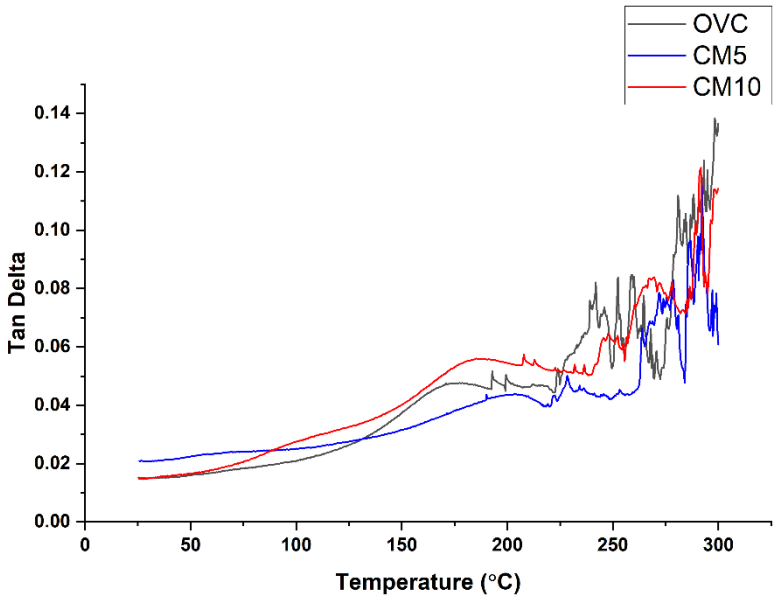

Figure 6-4 Tan delta vs Temperature plot for OVC, CM5, and CM10 laminates

The variation of tan delta manufactured laminates (OVC, CM5 and CM10) as a function of temperature is presented in Figure 6-4. It was observed that the peak intensity decreased with the shift in glass transition temperature(T_g) to higher temperatures for the different curves. The CM5 sample shows a tan delta peak height of 0.043 which is lower than the 0.055 and 0.047 recorded by the OVC and CM10 samples, respectively. The reduction in the intensity of the tan delta peak is attributed to the restriction of mobility of the polyfurfuryl alcohol molecular chains (Deka, Misra and Mohanty, 2013), which is a result of excellent interfacial adhesion between glass fibre reinforcement and the polyfurfuryl alcohol matrix resulting in increased stiffness. This phenomenon is further explained by the corresponding broader width of the curve observed in the CM5 tan delta plot as compared to that of the OVC and CM10 samples which is suggestive of efficient stress transfer between the glass fibre and matrix. The resultant effect of this is evident in the evaluated mechanical property of the laminates.

6.3.2 Thermomechanical Analysis (TMA) Characterization

From the results of the DMA analysis of the three investigated panels (OVC, CM5 and CM10) detailed in section 6.4.1, a series of multiple clustered peaks were seen immediately after the glass transition temperature was observed on the tan delta-temperature curve. In addition, a visual examination of the test specimen upon completion of the DMA test revealed a loss of specimen rigidity between the DMA equipment clamp fixtures. For this reason, the thermomechanical Analysis (TMA) investigation was conducted, to determine the dimensional

stability response of the investigated laminates (OVC, CM5 and CM10) as well as their glass transition temperature for comparison with that obtained from the DMA analysis. The TMA analysis was performed on the z-direction of each sample as described in section 3.3.3.

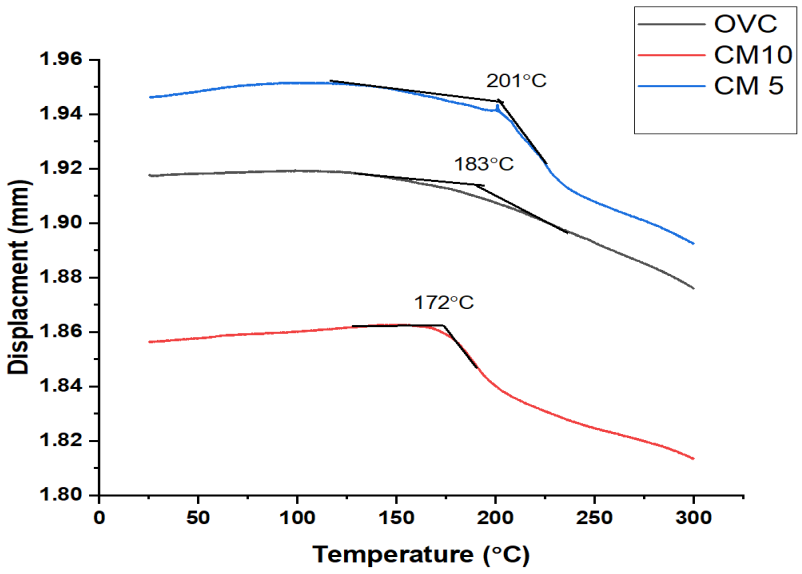

Figure 6-5 Displacement vs Temperature plot for OVC, CM5, and CM10 laminates.

Figure 6-5 shows the combined plot of the displacement against temperature for three laminates. The shape of the profile was observed to be similar for all the laminates which is indicate the similarity in the occurrence of segmental motion of the molecular chain network structure as a function of temperature. Based on the plot, the glass transition temperature(T_g) is determined as the intersection drawn by tangents to the slopes in the glassy and rubbery regions as seen in Figure 6-5. The glass transition temperature (T_g) of the OVC, CM5 and CM10 were evaluated to be 183°C, 201°C and 172°C respectively. This is in good agreement with that obtained from the DMA analysis in section 6.4.2.

The dimensional behaviour of the manufactured laminates was investigated when subjected to an increase in temperature. In all cases of the laminate, it is noticed that the composite maintained limited displacement indicating good dimensional stability between room temperature 25°C and the respective glass transition temperature(T_g).Beyond the observation of the glass transition temperature(T_g), a decline is observed relative to the displacement with the corresponding increase in temperature. This behaviour is suggestive of shrinkage occurring (Haris *et al.*, 2021). Similar behaviour was reported for the pineapple leaf/kenaf fibre reinforced by (Asim *et al.*, 2019). This can be explained as a result of the shrinking of the

porosity of the sample caused by the effect of load on the material at its glass transition temperatures corresponding to the rubbery region. In molecular terms, as the biobased glass/PFA sample is heated to its glass transition temperature, the molecular motion capacity is elevated enough to begin to unfreeze the molecular chains, which leads to the collapse of excess free volume which reduces the density consequently causing the relaxation of inherent frozen internal stress in the material which leads to the molecular chains to shrink to undisturbed size (Li *et al.*, 1997). Hence, resulting in a dimensional loss. This is noticed to be accompanied by a loss in the mechanical stiffness of the material which is evident in the reduction in the storage modulus as observed in the DMA plot.

6.4 Comparison between DMA Analysis from Kinetic Study and Experimental DMA Result

The DMA analysis performed on the biobased Glass/PFA prepreg in section 5.8 determined the glass transition temperature*s* (T_g) values to be 163℃ and 173℃ for the cured prepreg when simulated using the manufacturer-recommended cycle and optimized cure cycle from the kinetic study, respectively. Comparing the values to those obtained from actual experimental using the same cycle, the manufactured laminate (OVC) using the recommended cure cycle showed a 19℃ increase in glass transition temperature*s* (T_g) whereas the laminate (CM5) manufactured using the optimized cycle from the kinetic study showed a 27℃ increase in glass transition temperature*s* (T_g). On the other hand, the CM10 laminate manufactured using the same optimized cure cycle with a 10bar pressure recorded 173℃ as its glass transition temperature*s* (T_g) which is the same as the obtained from the analysis of the prepreg. The observed difference in glass transition temperature values was quite expected taking into account that the analysis performed in section 5.8 was conducted using a single ply of the prepreg. Based on this, it is seen that the concept of the kinetic study corroborates the experimental work, hence validating the optimization technique.

6.5 Mechanical Characterization of Laminates

Fibre-reinforced composites are particularly susceptible to the external loads to which they are subjected, such as stress or load. Therefore, to investigate a material response to loads of varying kinds, they are subjected to mechanical property tests. The flexural, tensile, and short beam tests are fundamental and efficient methods for evaluating the mechanical properties of materials. To perform a comparison between the mechanical properties of manufactured

laminates produced by the two different techniques using the different cure cycles described in section 3.4, a tensile, flexural and shear strength test was performed on samples of the individual laminates. The evaluation of the results is presented and discussed below.

6.5.1 Evaluation of Tensile Properties

The tensile test was conducted according to the ASTM 3039 standard as described in section 3.5.1 whereby the strength and modulus tensile strength and modulus were computed. The test was performed on five specimens per manufactured sample. The obtained representative stress against strain plot for each panel is shown in Figure 6-6

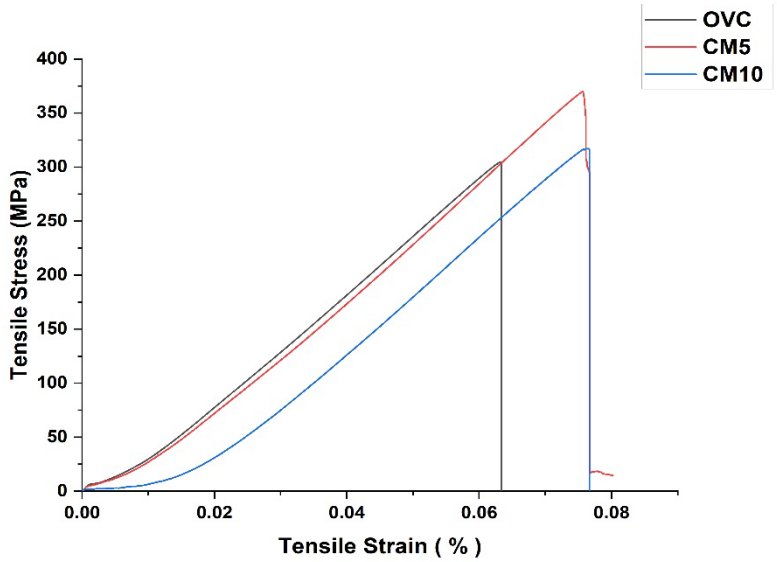

Figure 6-6 Representative tensile stress-strain plot of OVC, CM5, and CM10 specimens.

The individual profile of the glass/PFA plot in figures 6-6 shows similarity in the tensile behaviour irrespective of the difference in cure parameter or process. The shape of the stress-strain plot is observed to be similar to that obtained for the tensile investigation of the flax/PFA composite reported by Palumbo et al. (2019). Two distinct regions are observed to define the characteristic tensile behaviour of the Glass/PFA material when subjected to mechanical tensile stress. Upon the application of stress on the sample, an initial linear behaviour is observed which may be attributed to the stress relaxation of the matrix's molecular chains as it advances along the direction of pull (Zheng *et al.*, 2020). This linear phase defines the elastic region of the material by which its average tensile modulus is determined. The linearity observed in the elastic region continues as the stress is applied until it peaks at a maximum which is prompted by the catastrophic laminate failure which is evident by a sharp drop denoting the failure region. Also seen was the percentage elongation of the Glass/PFA remains averagely the same for all

the samples. The linear region is indicative of the linear deformation of the reinforcement and matrix while the drop in the failure region may be attributed to the resultant effects of micro damage within the inter and intralaminar fibre-matrix interface prompted by the crack propagation which occurs through the matrix leading to abrupt catastrophic fibre pull failure. This is further aided by the brittle nature of cured polyfurfuryl alcohol resin (Mohajeri and Pazokifard, 2015; Kubouchi *et al.*, 2016; Marefat Seyedlar, Imani and Mirabedini, 2021). The mechanical properties of tested samples from panels manufactured by the oven and hot press method, in terms of average values of the breaking load, tensile strength, tensile modulus, and percentage strain at break are summarized in Table 6-4. The tensile modulus of each tested sample was determined by evaluating the ratio between the change in stress and the change in strain from the slope of the individual stress-strain plot between 0.01% and 0.04% strain. The results in Table 6-4 were computed from the selected four best samples from five tested samples. To reduce the impact of deviations and improve the comparison between the different laminates, the results were normalized to an average fibre volume fraction of 43.2% using equation 3.7 as detailed in section 3.7.2

Table 6-4 Summary of tensile properties from stress-strain curves of each panel.

Test Sample	Average Breaking Load (N)	Break strain (%)	Average Tensile Strength (MPa)	Normalized Tensile Strength (MPa)	Average Tensile Modulus (GPa)	Normalized Tensile Modulus (GPa)
OVC	16358 ± 560	6.2	307 ± 13	339 ± 13	15 ± 0.57	16 ± 0.57
CM5	19114 ± 589	7.5	376 ± 9	375 ± 9	18 ± 0.23	17 ± 0.23
CM10	16339 ± 441	7.3	318 ± 7	292 ± 7	15 ± 0.89	14 ± 0.89

According to Table 6-4, the hot-pressed manufactured sample (CM5) exhibited the highest average tensile strength and modulus properties values of 376 ± 9 MPa and 18 ± 0.23 GPa compared to the OVC and CM10 sample which showed tensile strengths of 307 ± 13 and 318 ± 7.16 and moduli values of 15 ± 0.57 and 15 ± 0.89 GPa respectively. A comparison of the normalized results as shown in Figures 6-7 demonstrates that the average tensile strength for the CM5 sample increased by 10.25 % compared to the OVC samples and 28.42 % relative to the CM10 samples. In terms of tensile modulus, the CM5 sample showed a 6.25 %

improvement over the OVC sample and a corresponding 21.43 % increment over the CM10 samples. The results also revealed the impacts of curing pressure on both hot-press-manufactured samples (CM5 and CM10), as the CM5 sample, which was manufactured utilising a 5bar pressure, exhibited superior tensile properties. Thus, indicating that it is the optimal pressure parameter best suited for the optimised cure cycle developed from the kinetic analysis discussed in chapter five for the hot-press manufacture of the glass/PFA composite.

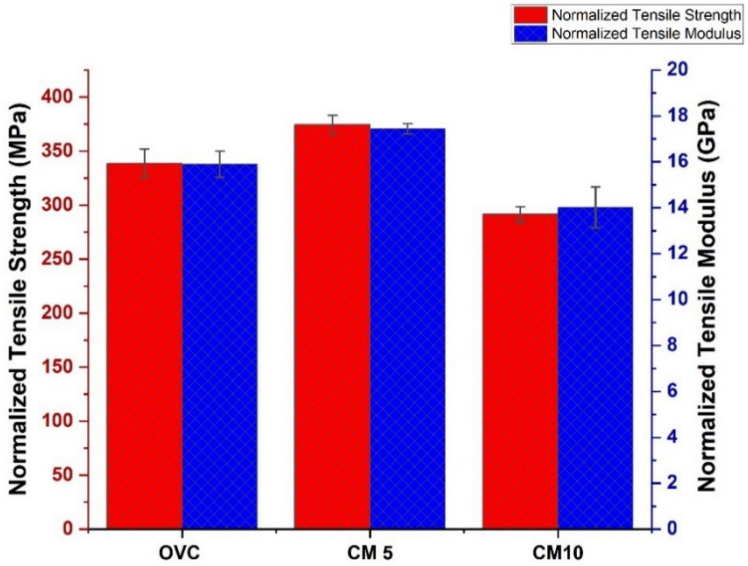

Figure 6-7 Normalized tensile properties of the oven and hot press manufactured laminate.

Comparing the effect of the manufacturing process on the tensile properties of Glass/PFA from Figure 6-7 shows that laminates manufactured by the compression moulding method possess higher tensile properties than the oven-cured sample. However, this is subjective to applied compaction pressure, although as observed in the case of the CM10 sample and OVC sample the difference between their tensile properties was significantly small. The relative similarity in the tensile property value of the glass/PFA was observed by Al-Maqdisi (2016) who reported 23.17 GPa and 336 MPa as tensile modulus and strength values, respectively. Although in his case, the tested laminate was manufactured by a compression moulding process using a staggered cure cycle with a total processing time of two hours. Other related cases in literature report higher tensile property values. For example, the tensile strength and modulus of the composite were reported to be 750 MPa and 46 GPa on tested laminate manufactured by pultrusion method according to C. C.M. Ma et al. (1995). Crossley, Schubel and Stevenson (2014) reported 850 MPa and 36.5GPa as tensile strength and modulus values recorded on

samples manufactured by vacuum assisted resin moulding (VARTM) method. The effect of the manufacturing method is significant to the achievable tensile property. The impressive result of the analysis of the tensile test on manufactured glass/PFA panels demonstrates the adequacy of the optimized cure cycle developed from the kinetic study of the Glass/PFA prepreg.

6.5.2 Tensile Failure Mode Analysis

Upon completion of the tensile test, the failure modes of the fractured specimens were visually examined and classified based on the type, area, and location of the damages in accordance with the acceptable failure locations designation as recommended by the ASTM D3039 standard shown in Figure 6-8. As described in Figures 6-8, the first letter of the code corresponds to the characteristics of the failure mode. The second denotes the area of failure whilst the third indicates the location of the failure. Diverse failure modes are typically observed when fibre-reinforced polymer composites are subjected to various types of severe load conditions. The types and modes of failure are influenced by a variety of factors. Usually, the mechanism of fracture and propagation involves failure of the matrix phase, failure of the reinforcing phase, and failure at the constituent material interface.

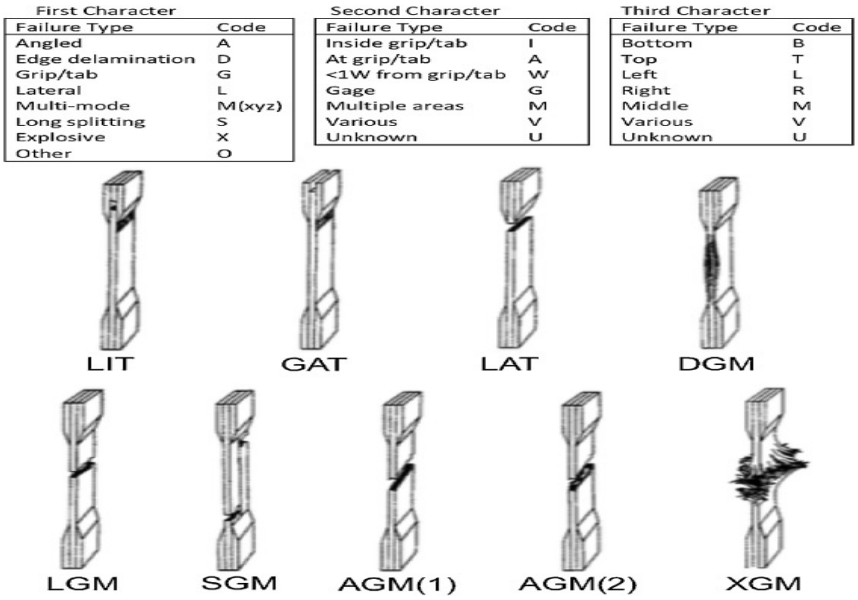

Figure 6-8 Modes of failure described by ASTM 3039 Standard (ASTM International, 2010)

Figure 6-9 shows images of the fractured OVC and CM5 specimens after the tensile test. A visualization of the fractured tensile test specimen to the corresponding failure modes as per the ASTM 3039 standard is detailed in Table 6-5 for the OVC sample.

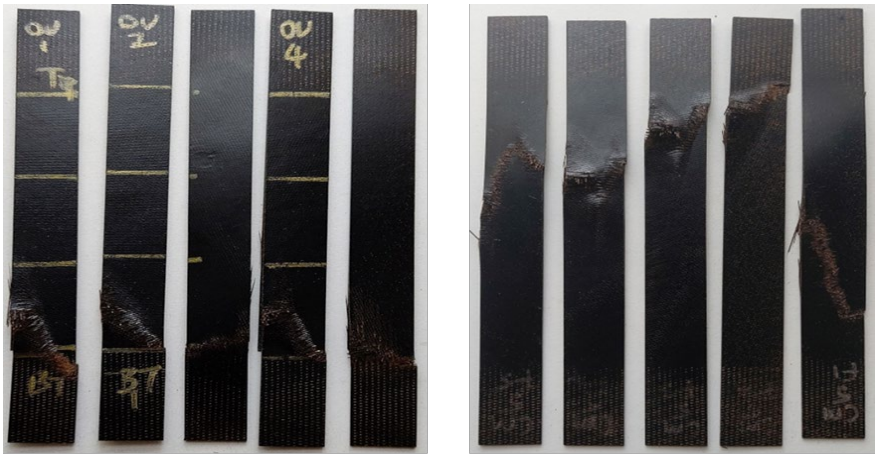

(A) (B)

Figure 6-9 Fractured specimen after tensile test of (A) OVC test coupons (B) CM5 test coupons.

From Table 6-5, the fracture mode was observed to be uniform across the five tested specimens. It shows that the fracture type was a constituent of a multi-mode failure type which occurred at the width from the grip.

Table 6-5 Mode of failure in OVC cured sample according to ASTM 3039 (ASTM International, 2010)

Test Coupon	Mode of failure (ASTM code)	Failure Type (First Character)	Failure Area (Second Character)	Failure Location (Third Character)
OVC S1	MWB	Multi-mode	W from grip/tab	Bottom
OVC S2	MWB	Multi-mode	W from grip/tab	Bottom
OVC S3	MWB	Multi-mode	W from grip/tab	Bottom
OVC S4	MWB	Multi-mode	W from grip/tab	Bottom
OVC S5	MWB	Multi-mode	W from grip/tab	Bottom

The failure mode of the CM5 sample as detailed in Table 6-6, showed the fracture mode was to be uniform across only three of the tested specimens while the similarity was observed with

the remaining two. It showed that the fracture type was a combination of multi-mode failure, propagating mainly from the gauge of the coupon and occurring at the middle.

Table 6-6 Mode of failure in CM5 cured sample according to ASTM 3039 (ASTM International, 2010)

Test Coupon	Mode of failure (ASTM code)	Failure Type (First Character)	Failure Area (Second Character)	Failure Location (Third Character)
CM5 S1	MGM	Multi-mode	Gauge	Middle
CM5 S2	MWT	Multi-mode	W from grip/tab	Top
CM5 S3	MWT	Multi-mode	W from grip/tab	Top
CM5 S4	MGM	Multi-mode	Gauge	Middle
CM5 S5	MGM	Multi-mode	Gauge	Middle

As shown in Table 6-7, the CM10 samples predominantly displayed lateral failure, as observed in Figure 6-10, primarily occurring at the bottom section.

Figure 6-10 Fractured CM10 test coupons (A) and cross-section of damaged CM10 coupon (B) after tensile testing.

Table 6-7 Mode of failure in CM10 cured sample according to ASTM 3039 (ASTM International, 2010)

Test Coupon	Mode of failure (ASTM code)	Failure Type (First Character)	Failure Area (Second Character)	Failure Location (Third Character)
CM10 S1	MGM	Multi-mode	Gauge	Middle
CM10 S2	LAT	Lateral	At Grip//Tab	Bottom
CM10 S3	LAT	Lateral	At Grip//Tab	Bottom
CM10 S4	LAT	Lateral	At Grip//Tab	Bottom
CM10 S5	MGM	Multi-mode	At Grip//Tab	Middle

From a visual examination of the test coupons in Figures 6-9 and 6-10, the interpreted failure is evident that the mode of fracture type was reasonably consistent across all of the tested coupons. Except for CM10 samples, all other coupons from the other laminates (CM5 and OVC) failed due to multimode-type failure. The multimode failure type observed on the tested coupons can be suggested to be a combination of an angular type of fracture which occurs explosively that leads to edge-type delamination seen at observed at the edge. In reality, the process is a rapid occurrence successive of failure mechanisms throughout the fracture process. As the stress corresponding to the tensile load increases, the material strains proportionally. At the fibre architecture-resin interface, early stress relaxation occurs; however, as the stress level rises, microcracks develop beginning at the fibre/matrix interface of the outermost composite layer as shown in Figure 6-11A. Fractures in fibre-reinforced polymer composites typically begin in the resin progressively leading to debonding between fibre and resin structure, ultimately resulting in failure (Bhat *et al.*, 2019). Similarly, the microcrack within the cured polyfurfuryl alcohol resin structure within the composite progresses from the outer edge toward the centre at an angle. This is observed on a Scanning Electron Microscope (SEM) as shown in Figure 6-11A.

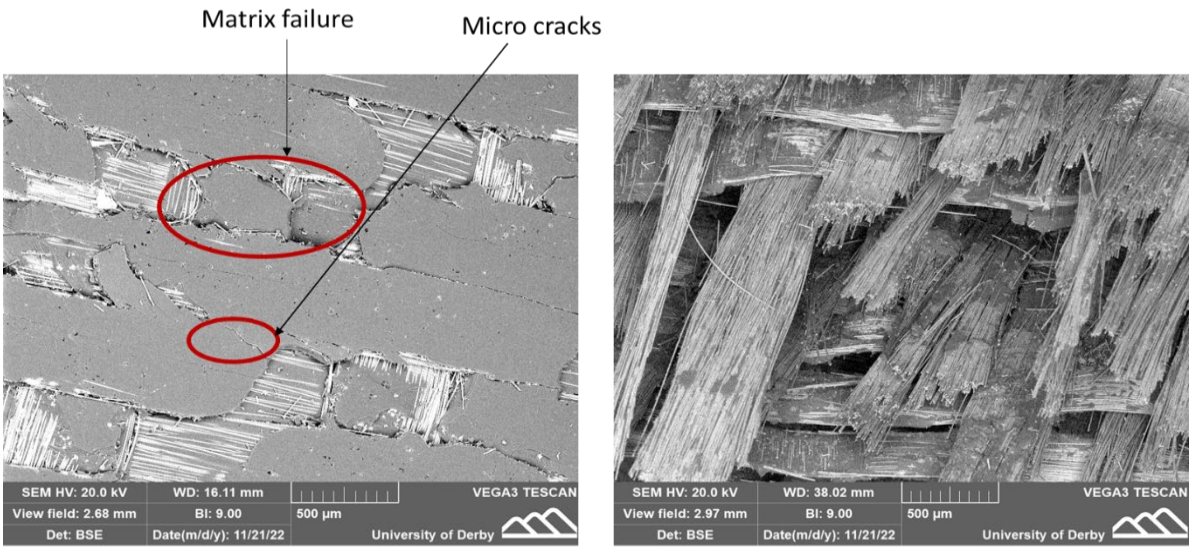

(A) (B)

Figure 6-11 SEM images of fractured tensile coupon: (A) PFA matrix failure due to micro-cracks, (B) Glass fibre failure.

The same was observed by Fairlie and Njuguna (Fairlie and Njuguna, 2020) who noted that angular rupture was observed on their composite specimen after the tensile test propagated from the outer edge. This may be due to the stress concentration from the combination of tensile and shear stress at the interlaminar mid-plane of the material, which results in an explosive failure as seen at a micro and macro level (Figure 6-11B and Figure 6-10B) followed by edge-type delamination observed along the gauge length. This is evident by the drop in stress from a maximum observed in the stress-strain plots in Figures 6-3. The delamination failure is developed generally due to excessive inter-laminar stresses generated at the interface between plies. Figure 6-12 presents the Scanning Electron Microscope (SEM) images of fractured surfaces of the different laminates.

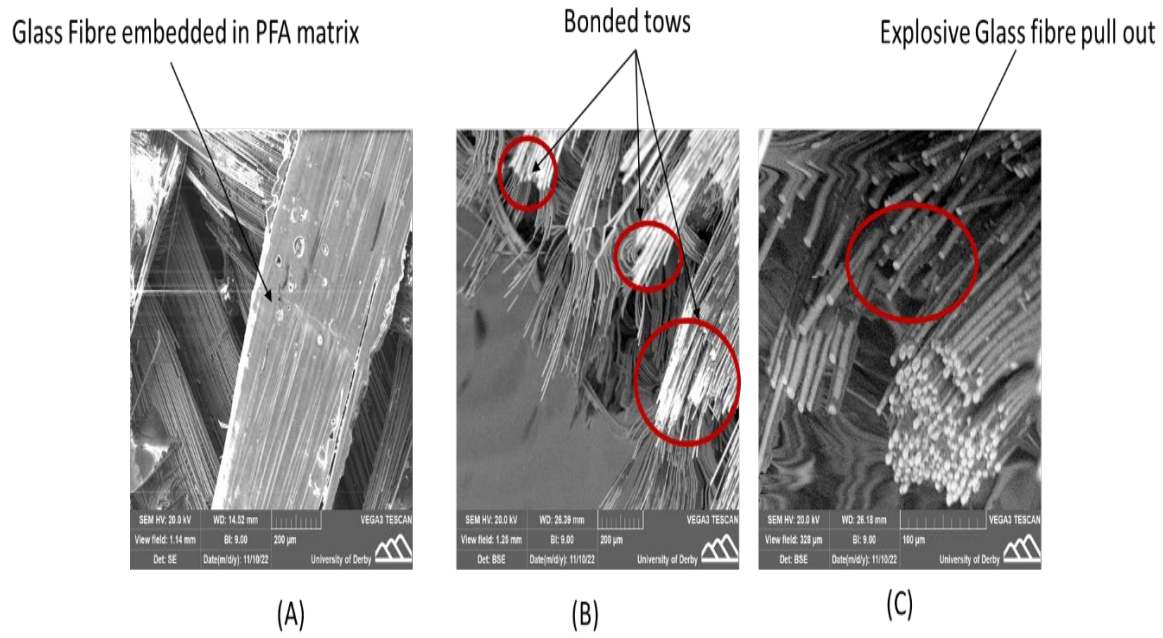

Figure 6-12 SEM images of fractured tensile specimens: (A) OVC, (B) CM5, and (C) CM10.

Comparing the fracture mode observed from the different panels to the individual manufacturing method used, it can be seen from Figure 6-12 that the fibres in the OVC sample (Figure 6-12A) were properly embedded in the PFA resin confirming the low fibre volume fraction (39.2%) recorded on section 6.2.1. Therefore, it can be deduced that the level and distribution of voids within the laminates contributed significantly to the propagation of failure under tensile load. Figure 6-12B reveals that the fibres on CM5 remain bound in tows, showing strong adhesion between the fibre matrix interface at both inter and intralaminar levels. This may be largely contributed to by the application of a compaction pressure of 5 bar during curing thus accounting for the superior tensile properties. The observed failure mechanism in the CM5 specimens was predominantly lateral in contrast to the OVC sample which exhibited delamination after initial fibre pulls upon failure. The fractured CM10 sample clearly shows a disintegrated glass fibre pull out with limited PFA matrix on the surface (Figure 6-12C), which is consistent with the high-volume fraction achieved relative to the 10bar compaction pressure applied during curing. The catastrophic failure and comparative poor tensile characteristics suggest that the pressure may have been a tad excessive, which may have resulted in extensive bleeding of the resin.

6.5.3 Evaluation of Flexural Properties

With the aid of the flexural test method described in section 3.5.2, the bending deformation resistance of biobased Glass/PFA composites manufactured by the two methods with different curing cycles was tested and evaluated. In performing a flexural test, compression, tension, and shearing phenomena are experienced simultaneously by the material, five specimens were examined for each test panel.

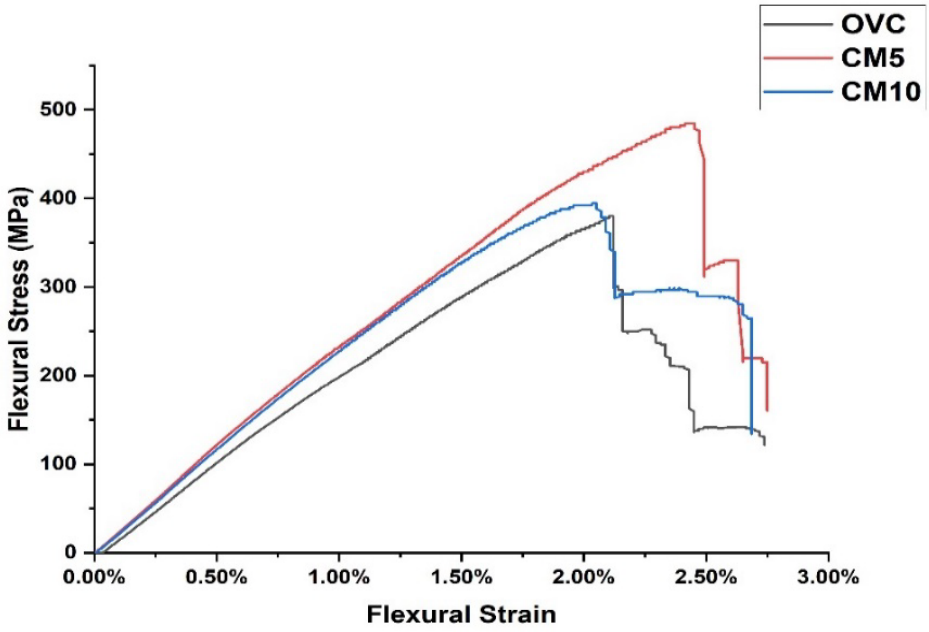

Figure 6-13 Representative flexural stress-strain plot of OVC, CM5, and CM10 specimens.

Figures 6-13 show the average representation of the stress-strain curves for the three panels (OVC, CM5, and CM10) generated from the force-displacement plot of each test. The strain value was computed from the displacement of the crosshead. On all tested samples, it is seen that the stress increased almost proportionally with the strain until an initial abrupt drop in stress caused by the failure of the sample followed by a continued drop in a stepped manner indicating the possibility of delamination after initial failure. The average flexural properties obtained from the flexural stress-strain plot in Figures 6-13 were evaluated and presented in Tables 6-8.

Table 6-8 Flexural properties summary of OVC, CM5, and CM10 panels.

Test Sample	Average Flexural Strength (MPa)	Normalized Flexural Strength (MPa)	Average Flexural Modulus (GPa)	Normalized Flexural Modulus (GPa)
OVC	391	429 ± 9	21 ± 0.28	23 ± 0.28
CM5	487 ± 8	485 ± 8	24 ± 0.23	24 ± 0.23
CM10	394 ± 4	359 ± 3	21 ± 0.61	20 ± 0.61

From Table 6-8, the flexural strength of the benchmark biobased Glass/PFA sample (OVC) manufactured using the prepreg's manufacturer-recommended cure cycle was determined to be 391 MPa, whereas the biobased Glass/PFA panels (CM5 and CM10) manufactured by hot press using the optimised cure cycle derived from the prepreg's kinetic study possessed flexural strengths of 487 ± 8 MPa and 394 ± 4 MPa, respectively. Similarly, the OVC panel was a flexural modulus of 21 ± 0.28 GPa, and CM5 and CM10 panels exhibited flexural moduli of 24 ± 0.23 GPa and 21 ± 0.61 GPa, respectively. The results showed consistency similar to what was reported in (Al-maqdasi, 2016). For comparison purposes, the flexural raw results were normalized as in the earlier case (tensile results) to an average volume fraction of 43.2%. The normalized flexural results are presented in Figure 6-14.

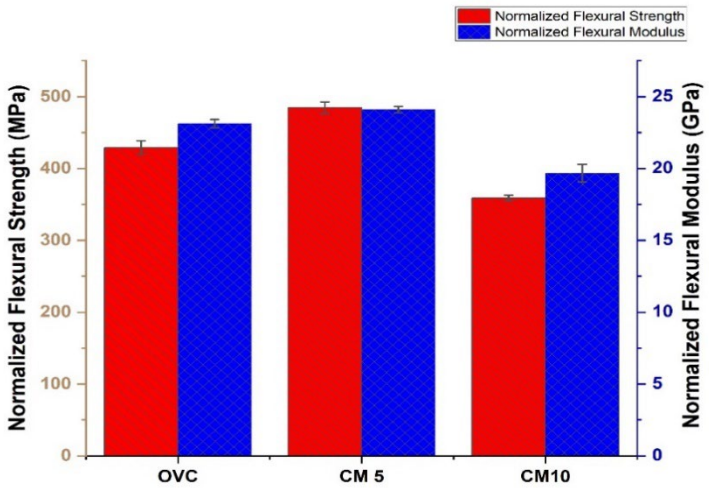

Figure 6-14 Normalized flexural properties comparison of oven and hot press manufactured laminate.

The chart shows that the Glass/PFA panel (CM5) manufactured by hot press using the optimised cure cycle derived from the prepreg's kinetic study exhibited the highest flexural properties. It was found to be 13.04% and 4.35% better than the OVC laminate in flexural strength and modulus, respectively. In comparison to the CM10 laminate, it showed a 35.9% increase in flexural strength while a 20% superiority was observed for its flexural modulus. The increase in flexural strength of the CM5 sample suggests good impregnation of the polyfurfuryl alcohol resin into the glass fibre which may be attributable to the cure cycle in combination with an adequate compaction pressure during the manufacturing process which provides excellent interfacial adhesion between fibre and resin leading on to lower porosity and better resistance to bending deformation. The results give credence to the outcome thermomechanical analysis discussed in section 6.3 suggesting the relationship between the molecular crosslinking density and the high glass transition temperature recorded for the CM5 contributes to its better mechanical performance. A similar phenomenon has been reported in a study of the mechanical properties of bio-epoxy network (Mashouf Roudsari, Misra and Mohanty, 2017).

6.5.4 Flexural Failure Analysis

To examine the effect of the manufacturing process and condition on the laminates, and the failure mechanism of the laminates, scanning electron microscopy was performed on the fractured surface of the different laminates. The scanning electron microscopic images are shown in Figure 6-15

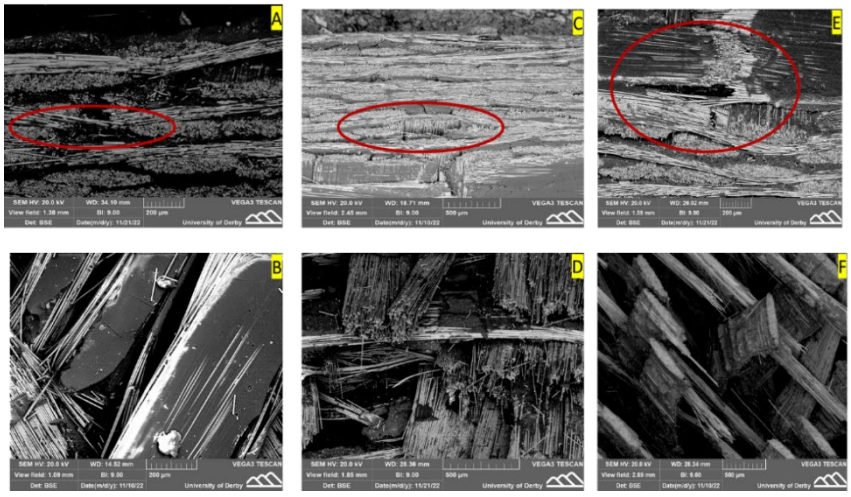

Figure 6-15 SEM images of fractured surfaces of OVC (A, B), CM5 (C, D), and CM10 (E, F) samples after the flexural test.

When the load is applied to a sample, the surface layers are involved there is a transfer of force which occurs between the fibres and polymer matrix. For all the samples, the failure as seen in Figures 6-15(A)(C)(E) (area circled in red) was initiated by a micro crack in the PFA matrix due to compressive stress which is further propagated along the layers within of the laminate aided by the distribution of void across the specimen. This brittle nature of the resin micro-cracks leads to debonding between the warp or weft glass fibre tow and the PFA matrix interface. The failure mechanism in bending was similar to that observed in tension. As shown in Figure 6-15(F), the CM10 exhibited poor interfacial bonding as the glass fibres are seen to be clean with limited matrix accounting for the extensive fibre pull-out during failure. A similar failure mechanism in bending has been reported for graphene-modified glass/epoxy composites (Wang *et al.*, 2016). In the case of the OVC sample, Figure 6-15B, no kinking or twisting of the glass fibres was observed under compression, rather the failure observed may be attributed to the porosity distribution across the laminate due to the evident voids as shown in Figure 6-15A. The effect of optimal curing pressure in the CM 5 laminate which accounts for the high fibre volume fraction and comparatively lower void content account for the superior flexural properties it exhibited. Hence, packed cured inter and intralaminar tows are observed in Figure 6-15D. Overall, the failure mechanism found for Glass/PFA composites under bending, regardless of the manufacturing method, is consistent with the literature. (Ipakchi *et al.*, 2020)

6.5.5 Evaluation of Interlaminar Shear Strength

The short beam shear (SBS) test is designed to generate interlaminar shear indirectly through bending and is the most popular method to characterize the apparent interlaminar shear strength of fibre-reinforced composites (ASTM International, 2003). The short beam test was performed on the three sets of manufactured samples oven manufactured sample OVC and CM5 and CM10. Five specimens of each type of laminate were evaluated and the best four results were selected for calculations. The average representative force-displacement curve was obtained from the short beam test performed on the three laminates (OVC, CM5 and CM10) samples as presented in Figures 6-16.

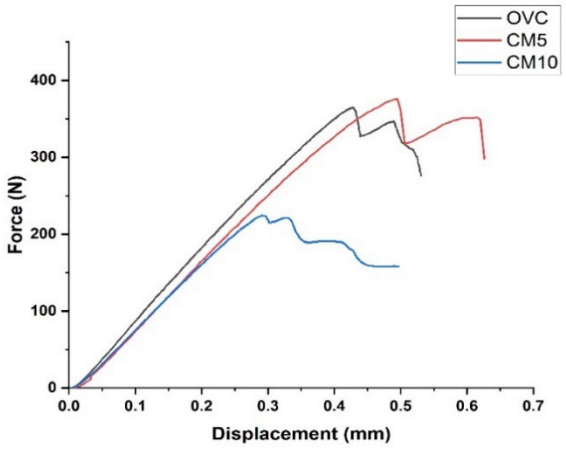

Figure 6-16 Force-displacement plot of OVC, CM5, and CM10 laminates

For all the case, it can be observed that all the curves rise linearly during the early stage of loading and then drops. The plot shows that the average maximum shear load of the OVC specimen is 366.8 N, while that of the CM5 and CM10 is 370.6 N and 229.6 N, respectively. The OVC sample fails after a displacement of 0.44 mm, but the CM5 and CM10 fail after 0.48 mm and 0.29 mm, respectively, with no visible plastic deformation. The average interlaminar shear strength (ILSS) was computed for each laminate and found that the OVC sample had an interlaminar shear strength of 29 ± 1.7 MPa, while the CM5 and CM10 samples had 32 ± 2 and 20 ± 0.8 MPa, respectively. The actual results were normalised to the average fibre volume fraction stated in section 3.7.2 for comparative validity. Figure 6-17 illustrates a comparison of the normalised ILSS of the different laminates.

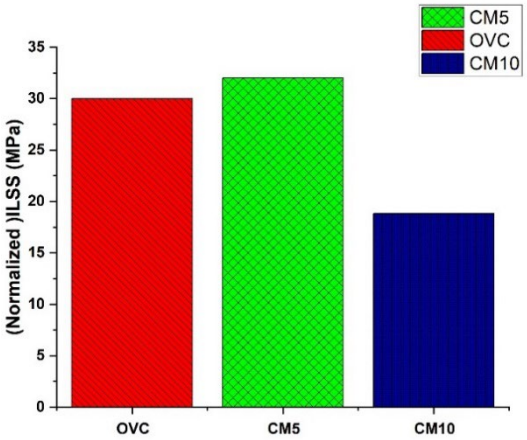

Figure 6-17 Interlaminar shear strength comparison of OVC, CM5, and CM10 laminates.

The chart shows a 10.34% increase in hot press-manufactured composite laminates processed by the optimized cure cycle with 5 bar compaction pressure to the standard oven-manufactured sample (OVC). Compared with the CM10 sample it showed a 60.6 % increase. Although interlaminar shear strength depends on several factors such as fibre volume fraction, fibre array pattern, mechanical properties of the fibre, and matrix (Sun *et al.*, 2019), the increased interlaminar shear strength (ILSS) in the CM 5 sample could be attributed to the optimized cure cycle (temperature, time and pressure) which allows for better interfacial bonding between resin matrix and the fibres during the gelation and vitrification stage of the during the prepreg curing.

6.5.6 Interlaminar Shear Failure Analysis

For a better understanding of the fracture morphology of the samples were investigated under a Scanning Electron Microscope. Figure 6-18 shows the SEM micrographs of the post-failure surfaces of the various laminates.

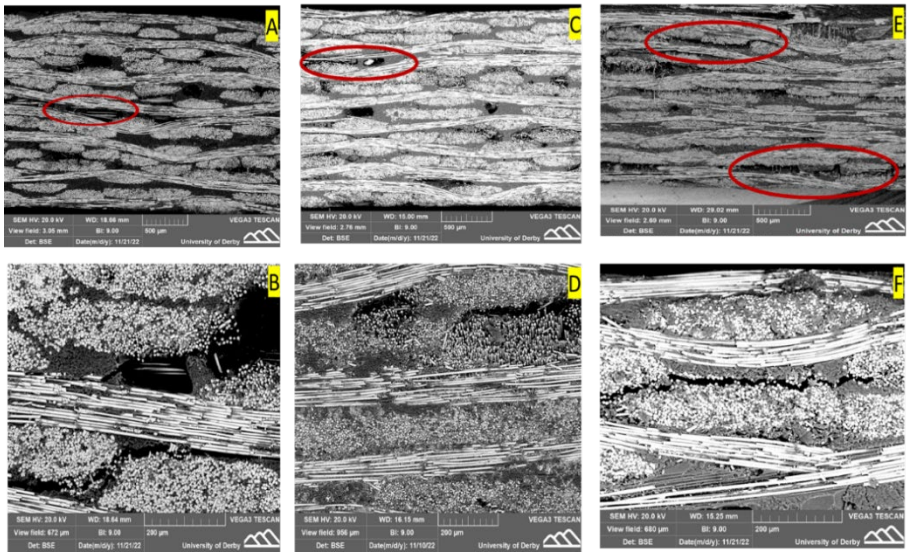

Figure 6-18 SEM images of fractured ILSS samples: OVC (A and B), CM5 (C and D), CM10 (E and F).

Figures 6-18 (A), (C), and (D) show, respectively, the fractured Interlaminar shear strength test surfaces of the OVC, CM5, and CM10 laminates. The SEM images reveal that the microstructure of the samples is made up of plies of glass fibres bound together by the PFA matrix in both weft and warp direction (Figure 6-18 (A) (C)and (D)) with a well-defined interface. Observation of the failed OVC sample from the compression side indicated microcracking began at the top, leading to debonding at the intra and interlayer along the weft

direction (Figure 6-18(B)) within the laminate as the load progresses downward. Clearly, the presence and distribution of voids along the same plane enhances the crack's prop ensity to propagate. A similar failure mechanism was observed for the CM5 and the CM10 samples (Figures 6-18 (B)(D)(F)), however, with the CM5 laminate, its densely packed glass fibre with good interfacial adhesion with the PFA resin (Figure 6-18C) and optimal fibre volume fraction accounts for its failure at a higher load with an average displacement which is 16.3 and 36.2% better average displacement in comparison to the OVC and CM10 sample. The same cannot be said for the CM10 laminate which fails predominantly within the intra-layer as seen in Figure 6-18F.

6.6 Summary

The results of an investigation into the mechanical and thermo-mechanical properties of the biobased Glass/PFA laminate produced by different manufacturing processes using the manufacturer-recommended cure cycle for the prepreg and the optimised cycle derived from the kinetic study are discussed. The plots of storage modulus and tan delta against temperature obtained by the DMA analysis of the manufactured laminates (OVC CM5, CM10) revealed that the CM5 sample had a higher storage modulus and glass transition temperature (T_g) than the OVC and CM10 samples. The crosslinking density, which evaluates the distance between the glassy and rubbery states, was calculated and compared for the three samples. The CM5 sample demonstrated a greater degree of crosslinking, consequently showcasing its outstanding thermomechanical characteristics. The glass transition temperature (T_g) obtained from the DMA analysis was compared to that obtained from the TMA analysis, and it was found to be consistent across the three samples. The TMA analysis also revealed the occurrence of shrinkage in the glass/PFA composite which also corroborated the noisy DMA signal observed at elevated temperature. Furthermore, the CM5 sample outperformed the OVC and CM10 samples which relatedly accounts for the observed superior mechanical properties.

The mechanical properties of bio-based Glass/PFA composites manufactured using two different processes and cure cycles were analysed. Tensile, flexural, and apparent shear strength properties were evaluated and discussed. The results for the tensile and flexural strengths of the OVC, CM5, and CM10 panels are as follows: OVC panel - 307 MPa (tensile), 391 MPa (flexural); CM5 panel - 376 MPa (tensile), 485 MPa (flexural); CM10 panel – 318 MPa (tensile), 394 MPa (flexural). The CM5 and CM10 Glass/PFA panels exhibited tensile and flexural moduli of 18 and 24 GPa, respectively, while the OVC panel showed moduli of

15 GPa (tensile) and 23 GPa (flexural). Additionally, the short beam test revealed apparent shear strength values of 29 MPa, 32 MPa, and 20 MPa for the OVC, CM5, and CM10 panels, respectively. Normalizing these results to an average fibre volume fraction of 43.2% for comparison shows the hot press manufactured laminate (CM5) using the optimized cure cycle with 5bar pressure to have better mechanical properties than the standard oven-manufactured laminate (OVC) and the hot press manufactured laminate with 10 bar pressure (CM10). It outperformed the OVC and CM10 panels in tensile strength by 10.25 and 28.42% and in tensile modulus by 6.25 and 21.43% respectively. Its compressive property also showed a 13.04 % and 35.9% superiority in flexural strength, corresponding to a 4.35% and 20 % increase in flexural moduli, respectively. In the matrix-dominated interlaminar shear strength test, the CM5 panel revealed a 7% improvement in interlaminar shear strength compared to the OVC panel, validating its improved compressive property. The relationship between the mechanical and thermomechanical properties as a function of the laminates (OVC, CM5, CM10) manufactured based on the recommended cycle and the optimized cure cycle developed from the kinetic study at different compaction pressure is shown in Figure 6-15

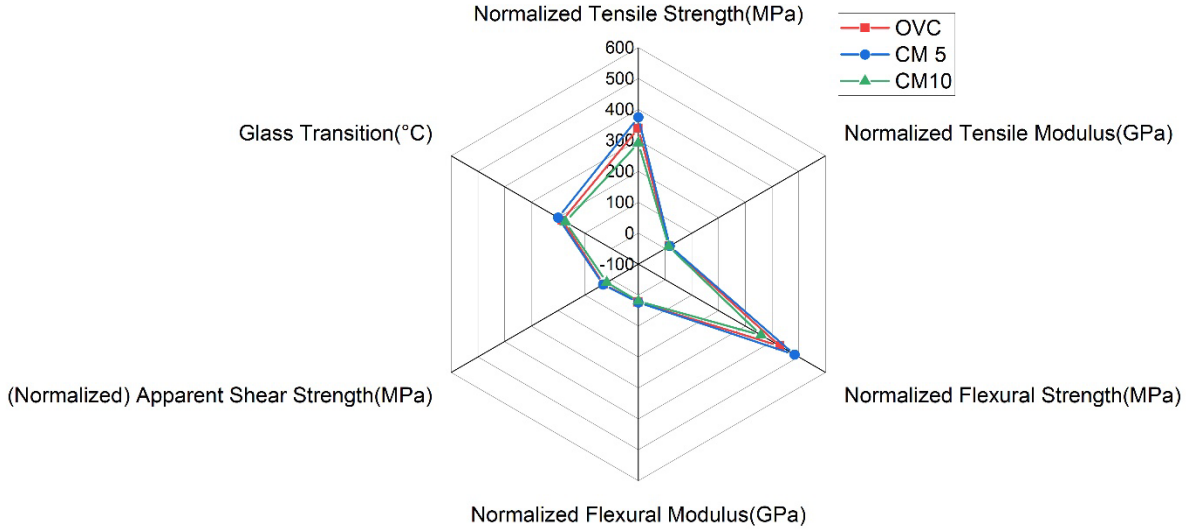

Figure 6-19 Mechanical and thermomechanical analysis summary of OVC, CM5, and CM10 laminates.

Overall, it is evident that the thermo-mechanical and mechanical properties of the 5bar hot-pressed cured biobased Glass/ PFA laminate using the optimized cure cycle from the kinetic study were observed to be sufficiently superior to those of vacuum bag /oven-cured samples panel manufactured using the hot-press possessed better or comparable mechanical properties to that manufactured using the vacuum bagging/oven curing process. In addition, a comparative

analysis of the mechanical properties suggests that the pressure of 5 bar was the optimal consolidation pressure combination together with the optimized cure cycle for rapid manufacturing of Glass/PFA composites using the hot press.

Chapter 7 Conclusion, Recommendation and Future Work

7.1 Conclusion

This research aims to provide insight into the curing mechanism of biobased glass-reinforced polyfurfuryl alcohol-based prepreg to establish an optimised curing cycle for the rapid production of biobased glass-reinforced polyfurfuryl alcohol composites with comparable qualities. A comprehensive literature study on the synthesis, manufacture and previously published mechanical properties was conducted to give a solid framework to understand the resin and its fibre-reinforced application.

The cure reaction mechanism of the glass/PFA prepreg was investigated using both isoconversional (model-free) and model-based kinetics studies. Four experimental non-isothermal cure datasets generated from a Dynamic Scanning Calorimetry (DSC) analysis of uncured glass/PFA prepreg were fitted with the Friedman and Ozawa Flynn wall isoconversional models. The resultant conversion-dependent activation energy plot demonstrated that the cure mechanism exhibited a complex reaction process involving multiple simultaneous and parallel steps. It was established that the average activation energy for the entire reaction was 88 4.9 kJ/mol, which is approximately 18.9 per cent higher than the activation energy reported in the literature for the pure polyfurfuryl alcohol resin. Both models were evaluated for reliability, and the Friedman model was found to be reliable for isothermal prediction because of its excellent fit to the degree of cure (Conversion) – time /temperature plot derived from the experimental cure dataset. Relatedly, model-fitting classical models of cure kinetics are commonly used to fit measurement data acquired from non-isothermal measurements. Hence, the correlation between the curing rate, temperature, and time, is developed into an equation which reflects the curing kinetics of the system. The Model fitting kinetic method employed the Kamal-Sourour autocatalytic model to develop a model that describes the curing process based on an assumption that the dominant reaction which occurs during the curing was autocatalytic as a result the resultant equation has excellently fitted the plot of the reaction rate against the degree of a cure curve.

Furthermore, the time-dependent - conversion curves for cure isothermal temperature were predicted using the kinetic prediction equation based on the Friedman model. For comparison and validation of the generated isothermal predictive curves from the model, experimental runs of two isothermal temperatures (120°C and 160°C) were performed for 30 minutes and 100 minutes, respectively, as suggested by the isothermal temperature-time prediction curve. The

results showed good agreement between the observed curves of both experimental isothermal runs (120°C and 160°C) and the predicted curve from the model. The model was applied to optimize the cure cycle of Glass/PFA for which it predicted complete cure was achievable at 30 minutes if cured at an isothermal temperature of 160℃ compared to the prepreg manufacturer's recommended cure temperature of 130 ℃ for 60 minutes.

Further, cure analysis on the uncured Glass/PFA prepreg was conducted on a Dynamic Mechanical Analyzer (DMA) for the thermomechanical property comparison between the manufacturer's recommended cure cycle of 130°C for a total processing time of 112.5 minutes, and the kinetic study-developed optimised cure cycle of 160°C held isothermally for 30 minutes. The investigation showed that the sample cured using the kinetic study's optimized cure cycle had a 4 per cent higher glass transition temperature when compared to the sample cured using the manufacturer's suggested cure cycle. The storage modulus value of the sample cured using the optimised cure cycle from the kinetic research was observed to have shown improvement, recording a value of 7.3 GPa compared to the sample cured using the manufacturer's recommended cure cycle, which recorded a value of 5.6 GPa.

From an experimental point of view, the biobased Glass/PFA composite panels were manufactured using the conventional oven and the compression moulding (hot press) technique. The glass/PFA manufacturer's recommended oven cure cycle was used for manufacturing the composite panel using the oven process while to investigate the suitability of the optimized cure cycle from the cure kinetic study for rapid manufacturing, panels were made using compression moulding (Hot Press) using the optimized cycle at 5 bar and 10 bar pressure.

Evaluation of the thermal properties of the different manufactured panels through a DMA analysis revealed both panels manufactured by the compression moulding technique using the optimized cure cycle from the kinetic study (CM5 and CM10) exhibited glass transition temperatures of 194℃ and 230℃ respectively. This was found to be higher than the 174℃ recorded by the oven manufacture panel (OVC). Also, a lower tan delta curve was observed for the CM5 and CM10 samples compared to the OVC samples. Thus, alluding to potentially better mechanical properties. This was evident in the evaluation of the mechanical properties which revealed that the CM5 panel showed a 10.25% and 13.04% increase in tensile and flexural strength compared to the OVC panel. It also showed a 10.34% higher apparent shear strength compared to the OVC panel. In conclusion, a manufacturing cure cycle of 160 ℃ held

isothermally for 30 mins under a compaction pressure of 5 bar was found the most suitable for rapid manufacture of the glass/PFA prepreg while maintaining comparable laminate quality. Hence, with the aid of cure kinetic analysis, the biobased Glass/PFA prepreg was successfully optimized for rapid manufacturing. This is of great significance as with a little further research and scaling up, this could encourage the use of biobased material which from a sustainability point of view would largely contribute to the global reduction of dependence on fossil fuels as well as the reduction in carbon emissions. Furthermore, the time saving achieved with this process improves and enhances industrial volume productivity and the commercial viability of the material.

7.2 Limitation to study

The aim and objective of this study were met, and it was demonstrated that, within the parameters of the two pressures taken into account, the optimised manufacturing isothermal cure cycle of 160 °C held for 30 minutes applied at 5 bar of compression moulding pressure is the most suitable cure cycle for the rapid manufacturing process to produce well-consolidated composite Glass/PFA laminates with comparable mechanical and thermal properties to standard vacuum bagged and oven cured equivalent. Although the success provided for the reduction of the processing time by over half providing for quick manufacturing suitability, there was some limitation to the findings of the research. Some of these include.

I. Experimental data acquisition for cure kinetic

Despite the success achieved by the Friedman and Ozawa Flynn wall isoconversional models, The experimental data used for the analysis was limited to dynamic or non-isothermal runs from conventional Dynamic scanning calorimetry (DSC). This is a result of the ramp-up challenge encountered when acquiring true isothermal data with conventional DSC. This limited the study to the use of non-isothermal experimental data for analysis. Although experimental data from dynamic runs are adequate for most cure kinetic analysis, the application of a combination of both dynamic and isothermal experimental data is necessary to provide a more robust kinetic analysis for kinetic predictions. The use of temperature-modulated Dynamic Scanning Calorimetry (DSC) is a suggested alternative for very good and accurate isothermal experimental data acquisition for cure kinetic modelling.

II. Content characterization

A major drawback to this work was the inability to evaluate the constituent content of the panels produced by the various method using the different parameters for adequate comparison. The uncertainty surrounding the actual density value of the neat pure resin impregnated into the glass fibre prevented the evaluation of the volume constituent content. Attempts were made using the acid digestion method; however, the result was proven invalid as large negative void contents were recorded. Although the Optical microscopy method was used, it does have its limitations. Hence other content characterisation investigation methods such as X-tomography may be employed.

III. Hot-press equipment.

Since the compression moulding technique was carried out with the aid of a laboratory scale in-house manufactured hot press, there was an inherent limitation to the equipment by design. Firstly, due to peculiar design issues with the equipment uneven temperatures distribution uniformity over the surface of the platens which potentially affects the laminate quality. In addition, the hot press design setup allows for pressure from the ram of the hydraulic press to be applied at the centre of the top platen which potentially leads to uneven pressure distribution across the platen since the ram is acting as a point load rather than a supposedly a uniform distributed load across the platen.

The limitation of achieving a colour press manual hydraulic press being manually operated limits the investigation of lower compaction pressure range below 5 bar.

This study was mainly focused on areas of cure cycle optimization within a limited pressure range. However, for a robust result comprehension, it would be worthwhile to perform research studies on the effect of compaction creep and compaction speed.

7.3 Recommendation and Future Work

In a fast-changing world where the need for sustainability and net zero carbon is at the heart of material selection and product development, there remains a growing need for research and development in biobased material with the capability for rapid manufacturing. The application of cure kinetic modelling and thermal analysis is one of the developed techniques employed for optimization analysis. This is immensely helpful in industrial applications where the need for a reduction in manufacturing time is critical. For fibre-reinforced polyfurfuryl alcohol materials, several areas of research need to be uncovered to fully characterize and process its composites. Although this research work was focused and limited to the cure kinetic analysis

and kinetic prediction for optimization of the cure cycle of the Glass/PFA, its findings should be considered as a basis for future research.

Research considerations based on this work for the future could include:

- Expanding the fundamental of this work by further development of the model fitting equation based on the addition of rheology studies to understand the diffusion kinetic regime, actual gelation, and vitrification boundary relative to the glass transition temperature under dynamic or isothermal conditions which can be analysed using cure viscosity and diffusion models to develop a Time-Temperature-Transformation (TTT) diagram which can aid further cure cycle optimization.
- Thermal analysis and investigation through rheological studies on the rate and duration of degassing process as a function of temperature during the compression moulding manufacturing process fibre reinforced PFA. This is essential as it contributes to the void content and overall quality of the laminate.
- Further mechanical property characterization can include impact testing and analysis, and fracture toughness.

Broader-related research areas in which further work may be considered include:

I. Finite Element Modelling and Simulation Data of the Resin and the Reinforced Composite.

Despite the enormous experimental work by researchers on the various properties of the PFA resin and its fibre-reinforced composite, data, or analysis on its micro or macro mechanics is yet to be seen in the literature. Therefore, numerical, and finite element analysis on subject areas such as impact damage and failure would be very helpful in the analysis and mechanical properties prediction of the biobased Glass/PFA prepreg.

II. Fatigue and Creep Properties and Analysis

Unlike other traditional fibre-reinforced composites such as glass epoxy, studies on the fatigue or creep behaviour of PFA resin-based composites have yet to be reported. Research in this area would contribute to the understanding of this behaviour, allowing for the prediction of long-term properties to assess the viability and long-term durability of these materials. This would be helpful and would encourage broader structural application towards structural application.

III. Fabrication of Thick Composite.

Generally, the fabrication of very thick fibre-reinforced composite may prove somewhat difficult. Moreso, owing to the challenges of water (moist) release during the curing of the PFA resin since energy diffuses from the surface to the bulk by conduction, there exists a high potential risk of having water (Moist) generated during curing trapped in between the numerous layers causing potential defects to the laminate.

IV. Fibre Hybridization

Fibre hybridization and resin blending have been one of the techniques used to modify and improve the properties of fibre-reinforced composites for applications. Jawaid and Abdul Khalil (Jawaid and Abdul Khalil, 2011) in their reviewed and detailed the success of fibre hybridization in the improvement of different mechanical properties of natural fibre composites. Interestingly, to the best of the author's knowledge, there has not been any documented study on a hybridized fibre /polyfurfuryl resin composite, e.g., glass/flax with the PFA resin. This could be explored as a route to improve the properties of PFA-based composite.

References

Abenojar, J. *et al.* (2018) 'Kinetics of curing process in carbon/epoxy nano-composites', *IOP Conference Series: Materials Science and Engineering*, 369(1). doi: 10.1088/1757-899X/369/1/012011.

Ahmad, E. E. M., Luyt, A. S. and Djoković, V. (2013) 'Thermal and dynamic mechanical properties of bio-based poly(furfuryl alcohol)/sisal whiskers nanocomposites', *Polymer Bulletin*, 70(4), pp. 1265–1276. doi: 10.1007/s00289-012-0847-2.

Aktas, A. *et al.* (2015) 'A cure modelling study of an unsaturated polyester resin system for the simulation of curing of fibre-reinforced composites during the vacuum infusion process', *Journal of Composite Materials*, 49(20), pp. 2529–2540. doi: 10.1177/0021998314549820.

Al-maqdasi, Z. (2016) *Competitive Bio-based Composites for Sandwich Structure Applications*. Luleå University of Technology. doi: 10.13140/RG.2.1.2004.9525.

AL-Rekabe, J. M., Saleh, H. M. and Hanoosh, W. S. (2020) 'Synthesis, Chemical Resistance and Thermal Behavior of Polyfurfural Alcohol', *IOP Conference Series: Materials Science and Engineering*, 928, p. 052015. doi: 10.1088/1757-899x/928/5/052015.

Anderson, J. P. and Altan, M. C. (2015) 'Effect of laminate edge conditions on the formation of microvoids in composite laminates', *AIP Conference Proceedings*, 1664(June). doi: 10.1063/1.4918431.

Apolinario, G. *et al.* (2016) 'Effects of water ageing on the mechanical properties of flax and glass fibre composites: Degradation and reversibility', *RILEM Bookseries*, 12, pp. 183–196. doi: 10.1007/978-94-017-7515-1_14.

Arnold, E. . *et al.* (2009) 'Next Generation Sustainable Composites : Development and Processing of Furan-Flax Biocomposites', in *17th International Conference on Composite Materials.* Edinburgh: British Composite Soicety, pp. 27–31. Available at: http://www.iccm-central.org/Proceedings/ICCM17proceedings/Themes/Materials/NATURAL FIBRE COMPOSITES/D9.13 Arnold.pdf.

Asad, M. Z., Mahmood, A. and Shah, S. T. H. (2020) 'Phenol-furfural resin/montmorillonite based high-pressure green composite from renewable feedstock (Saccharum munja) with improved thermo-mechanical properties', *Polymers*, 12(7), pp. 1–14. doi: 10.3390/polym12071562.

Asadi, F., Jannesari, A. and Arabi, A. (2019) 'Epoxy siloxane/ZnO quantum dot nanocomposites: Model-fitting and model-free approaches to kinetic analysis of non-isothermal curing process', *Progress in Organic Coatings*, 135(June), pp. 270–280. doi: 10.1016/j.porgcoat.2019.06.006.

Asaro, L. *et al.* (2019) 'Development of low environmental impact protective coatings based on a furan resin and cellulose nanocrystals', *Progress in Organic Coatings*, 133(April), pp. 229–236. doi: 10.1016/j.porgcoat.2019.04.035.

Asim, M. *et al.* (2019) 'Dynamic and thermo-mechanical properties of hybridized kenaf/PALF reinforced phenolic composites', *Polymer Composites*, 40(10), pp. 3814–3822. doi: 10.1002/pc.25240.

Assarar, M. *et al.* (2011) 'Influence of water ageing on mechanical properties and damage events of two reinforced composite materials: Flax-fibres and glass-fibres', *Materials and Design*, 32(2), pp. 788–795. doi: 10.1016/j.matdes.2010.07.024.

ASTM International (1999) 'ASTM D 3171-99 - Standard Test Methods for Constituent Content of Composite Materials', *ASTM Book of Standards*, 76(February), pp. 1–10.

ASTM International (2003) 'Standard Test Method for Short-Beam Strength of Polymer Matrix Composite Materials and Their Laminates', *Annual Book of ASTM Standards*, 3(2), pp. 136–140.

ASTM International (2010) 'Standard Test Method for Tensile Properties of Polymer Matrix Composite Materials'. , West Conshohocken, PA. doi: 10.1520/D3039_D3039M-08.

Asyraf, M. R. M. *et al.* (2022) 'Product Development of Natural Fibre-Composites for Various Applications: Design for Sustainability', *Polymers*, 14(5). doi: 10.3390/polym14050920.

Bachmann, J., Hidalgo, C. and Bricout, S. (2017) 'Environmental analysis of innovative sustainable composites with potential use in aviation sector—A life cycle assessment review', *Science China Technological Sciences*, 60(9), pp. 1301–1317. doi: 10.1007/s11431-016-9094-y.

Barraza, H. J. *et al.* (2004) 'Porosity reduction in the high-speed processing of glass-fiber composites by Resin Transfer Molding (RTM)', *Journal of Composite Materials*, 38(3), pp. 195–226. doi: 10.1177/0021998304038649.

Behzadfar, A., Imani, M. and Farahmandghavi, F. (2019) 'Shelf-life of polyfurfuryl alcohol resin: an accelerated rheokinetics study', *Polymer Bulletin*, 76(11), pp. 5903–5918. doi: 10.1007/s00289-019-02692-4.

Belgacem, M. N. and Alessandro, G. (2003) 'Furan-Based Adhesives', in Pizzi, A. and Mittal, K. L. (eds) *Handbook of Adhesive Technology*. Second. New York: CRC Press, p. 615. doi: https://doi.org/10.1201/9780203912225.

Belgacem, M. N. and Gandini, A. (2003) *Furan Based Adhesives*. Second Edi, *Handbook of Adhesive Technology, Revised and Expanded*. Second Edi. Edited by A. Pizzi and K. L. Mittal.

Benin, S. R. *et al.* (2020) 'Mechanical characterization of prosopis juliflora reinforced polymer matrix composites with filler material', *Materials Today: Proceedings*, 33, pp. 1110–1115. doi: 10.1016/j.matpr.2020.07.190.

Bhat, R. *et al.* (2019) 'Mechanical testing and microstructure characterization of glass fiber reinforced isophthalic polyester composites', *Journal of Materials Research and Technology*, 8(4), pp. 3653–3661. doi: 10.1016/j.jmrt.2019.06.003.

Bobrowski, A. and Grabowska, B. (2012) 'The impact of temperature on furan resin and binders structure Artur Bobrowski, Beata Grabowska.', *Metallurgy and Foundry Engineering*, 38(1), p. 73. doi: 10.7494/mafe.2012.38.1.73.

Bodaghi, M. *et al.* (2016) 'Experimental characterization of voids in high fibre volume fraction composites processed by high injection pressure RTM', *Composites Part A: Applied Science and Manufacturing*, 82, pp. 88–99. doi: 10.1016/j.compositesa.2015.11.042.

Bosq, N. *et al.* (2015) 'Thermomechanical behavior of a novel biobased poly(furfurylalcohol)/silica nanocomposite elaborated by smart functionalization of silica nanoparticles', *Polymer Degradation and Stability*, 118, pp. 137–146. doi: 10.1016/j.polymdegradstab.2015.04.018.

Brown, M. E. *et al.* (2000) 'Computational aspects of kinetic analysis Part A: The ICTAC Kinetics Project-data, methods and results', *Thermochimica Acta*, 355(1–2), pp. 125–143. doi: 10.1016/S0040-6031(00)00443-3.

Budrugeac, P. (2019) 'Comparison between model-based and non-isothermal model-free computational procedures for prediction of conversion-time curves of calcium carbonate

decomposition', *Thermochimica Acta*, 679(July), p. 178322. doi: 10.1016/j.tca.2019.178322.

Burket, C. L. *et al.* (2006) 'Genesis of porosity in polyfurfuryl alcohol derived nanoporous carbon', *Carbon*, 44(14), pp. 2957–2963. doi: 10.1016/j.carbon.2006.05.029.

Carotenuto, G. and Nicolais, L. (1998) 'Furfuryl alcohol-based resin as matrix for high performance composites', *Advanced Composites Letters*, 7(4), pp. 105–109. doi: 10.1177/096369359800700402.

Carus, M. (2015) 'Biocomposites in the Automotive Industry, markets and environment. bio!car', *Biobased Materials for Automotive Applications Conference*, 11, pp. 16–17. Available at: https://epaper.bioplasticsmagazine.com/issue-04-2015/63071353.

Chandran, M. S. *et al.* (2012) 'Cure Kinetics and Activation Energy Studies of Modified Bismaleimide Resins', *ISRN Polymer Science*, 2012(i), pp. 1–8. doi: 10.5402/2012/309861.

Chate, G. R. *et al.* (2018) 'Modeling and optimization of furan molding sand system using design of experiments and particle swarm optimization', *Proceedings of the Institution of Mechanical Engineers, Part E: Journal of Process Mechanical Engineering*, 232(5), pp. 579–598. doi: 10.1177/0954408917728636.

Chen, C., Poursartip, A. and Fernlund, G. (2019) 'Effect of Cure Pressure on Void Content and Interlaminar Shear Strength of Interlayer Toughened Composite Laminates', *Conference: 11th Canadian – International Conference on Composites 2019*, (July).

Chinthapalli, R. *et al.* (2020) *Biobased Building Blocks and Polymers - Global Capacities, Production and Trends, 2018-2023*, *Industrial Biotechnology*. doi: 10.1089/ind.2019.29179.rch.

Corma Canos, A., Iborra, S. and Velty, A. (2007) 'Chemical routes for the transformation of biomass into chemicals', *Chemical Reviews*, 107(6), pp. 2411–2502. doi: 10.1021/cr050989d.

Crossley, R. J. *et al.* (2012) 'Development and Processing of a Sustainable Fully Bio Derived Polyfurfuryl Alcohol Matrix Flax', in *ECCM15 - 15TH EUROPEAN CONFERENCE ON COMPOSITE MATERIALS*. Venice ,Italy, pp. 24–28.

Crossley, R., Schubel, P. and Stevenson, A. (2014) 'Furan matrix and flax fibre as a sustainable renewable composite: Mechanical and fire-resistant properties in comparison to phenol, epoxy and polyester', *Journal of Reinforced Plastics and Composites*, 33(1), pp. 58–68. doi: 10.1177/0731684413502108.

Das, P. P. and Chaudhary, V. (2021) 'Moving towards the era of bio fibre based polymer composites', *Cleaner Engineering and Technology*, 4. doi: 10.1016/j.clet.2021.100182.

Deka, H., Misra, M. and Mohanty, A. (2013) 'Renewable resource based "all green composites" from kenaf biofiber and poly(furfuryl alcohol) bioresin', *Industrial Crops and Products*, 41(1), pp. 94–101. doi: 10.1016/j.indcrop.2012.03.037.

Deka, H., Mohanty, A. and Misra, M. (2014) 'Renewable-resource-based green blends from poly(furfuryl alcohol) bioresin and lignin', *Macromolecular Materials and Engineering*, 299(5), pp. 552–559. doi: 10.1002/mame.201300221.

Dolkun, D. *et al.* (2018) 'Optimization of cure profile for thick composite parts based on finite element analysis and genetic algorithm', *Journal of Composite Materials*, 52(28), pp. 3885–3894. doi: 10.1177/0021998318771458.

Domínguez, J. C., Grivel, J. C. and Madsen, B. (2012) 'Study on the non-isothermal curing kinetics of a polyfurfuryl alcohol bioresin by DSC using different amounts of catalyst', *Thermochimica Acta*, 529, pp. 29–35. doi: 10.1016/j.tca.2011.11.018.

Domínguez, J. C. and Madsen, B. (2014) 'Chemorheological study of a polyfurfuryl alcohol resin system-Pre-gel curing stage', *Industrial Crops and Products*, 52, pp. 321–328. doi: 10.1016/j.indcrop.2013.11.006.

Domínguez, J. C. and Madsen, B. (2015a) 'Development of new biomass-based furan/glass composites manufactured by the double-vacuum-bag technique', *Journal of Composite Materials*, 49(24), pp. 2993–3003. doi: 10.1177/0021998314559060.

Domínguez, J. C. and Madsen, B. (2015b) 'Development of new biomass-based furan/glass composites manufactured by the double-vacuum-bag technique', *Journal of Composite Materials*, 49(24), pp. 2993–3003. doi: 10.1177/0021998314559060.

Drakonakis, V. M., Seferis, J. C. and Doumanidis, C. C. (2013) 'Curing Pressure Influence of Out-of-Autoclave Processing on Structural Composites for Commercial Aviation', *Advances in Materials Science and Engineering*, 2013, pp. 1–14. doi: 10.1155/2013/356824.

Džalto, J., Medina, L. and Mitschang, P. (2014) 'Volumetric interaction and material characterization of flax/furan bio-composites', *KMUTNB International Journal of Applied Science and Technology*, 7(1), pp. 11–21. doi: 10.14416/j.ijast.2014.01.004.

Eisenreich, N. (2008) 'New classes of Engineering Composites Materials from Renewable

Resources', *Report for EU 6th Framework Programme, IntegratedProject*, pp. 1–31.

Elejoste, P. A. *et al.* (2022) 'Development and Characterisation of Sustainable Prepregs with Improved Fire Behaviour Based on Furan Resin and Basalt Fibre Reinforcement', *Polymers*, 14(9). doi: 10.3390/polym14091864.

Eseyin, A. E. and Steele, P. H. (2015) 'An overview of the applications of furfural and its derivatives', *International Journal of Advanced Chemistry*, 3(2), p. 42. doi: 10.14419/ijac.v3i2.5048.

Fairlie, G. and Njuguna, J. (2020) 'Damping properties of flax/carbon hybrid epoxy/fibre-reinforced composites for automotive semi-structural applications', *Fibers*, 8(10), pp. 1–15. doi: 10.3390/fib8100064.

Falco, G., Guigo, Nathanaël, *et al.* (2018) 'FA polymerization disruption by protic polar solvents', *Polymers*, 10(5), pp. 1–14. doi: 10.3390/polym10050529.

Falco, G., Guigo, Nathanael, *et al.* (2018) 'Opening Furan for Tailoring Properties of Bio-based Poly(Furfuryl Alcohol) Thermoset', *ChemSusChem*, 11(11), pp. 1805–1812. doi: 10.1002/cssc.201800620.

Fam, A., Eldridge, A. and Misra, M. (2014) 'Mechanical characteristics of glass fibre reinforced polymer made of furfuryl alcohol bio-resin', *Materials and Structures/Materiaux et Constructions*, 47(7), pp. 1195–1204. doi: 10.1617/s11527-013-0122-5.

Fan, Z., Santare, M. H. and Advani, S. G. (2008) 'Interlaminar shear strength of glass fiber reinforced epoxy composites enhanced with multi-walled carbon nanotubes', *Composites Part A: Applied Science and Manufacturing*, 39(3), pp. 540–554. doi: 10.1016/j.compositesa.2007.11.013.

Fernández, R. *et al.* (2009) 'Kinetic studies of the polymerization of an epoxy resin modified with rhodamine B', *Thermochimica Acta*, 493(1–2), pp. 6–13. doi: 10.1016/j.tca.2009.03.015.

Fink, J. K. (2013) *Reactive Polymers: Fundamentals and Applications*. 2nd edn. Elsevier Science & Technology Books. Available at: https://app.knovel.com/web/view/khtml/show.v/rcid:kpRPFAAC1P/cid:kt011FWQH4/viewerType:khtml/?view=collapsed&zoom=1&page=1&q=furfural to furfuryl alcohol.

Fitzgerald, A. *et al.* (2021) 'A life cycle engineering perspective on biocomposites as a solution for a sustainable recovery', *Sustainability (Switzerland)*, 13(3), pp. 1–25. doi:

10.3390/su13031160.

Flynn, J. H. and Wall, L. A. (1966) 'General Treatment of the Thermogravimetry of Polymer', *Journal of research of the National Bureau of Standards. Section A, Physics and chemistry*, 70 A(6), pp. 487–523. doi: 10.6028/JRES.070A.043.

Foruzanmehr, M. *et al.* (2016) 'Degradation characteristics of new bio-resin based-fiber-reinforced polymers for external rehabilitation of structures', *Journal of Composite Materials*. doi: 10.1177/0021998315590262.

Fowler, P. A., Hughes, J. M. and Elias, R. M. (2006) 'Biocomposites: technology, environmental credentials and market forces', *Journal of the science of food and agriculture*, 86(December 2005), pp. 1781–1789. doi: 10.1002/jsfa.2558.

Friedman, H. L. (1964) 'Kinetics of thermal degradation of char-forming plastics from thermogravimetry', *Journal of Polymer Science Part C: Polymer Symposia*, 6(1), pp. 183–195.

G.Liang, K. C. (2006) 'Cure kinetics and rheology characterization of soy-based epoxy resin system', *Journal of Applied Polymer Science*, 102(4), pp. 3168–3180.

Gagani, A. I. *et al.* (2019) 'A novel method for testing and determining ILSS for marine and offshore composites', *Composite Structures*, 220(January), pp. 431–440. doi: 10.1016/j.compstruct.2019.04.040.

Gandini, A. and Belgacem, M. N. (1997) 'Furans in polymer chemistry', *Progress in Polymer Science (Oxford)*, 22(6), pp. 1203–1379. doi: 10.1016/S0079-6700(97)00004-X.

Gernaat, C. *et al.* (2009) 'Correlation between viscoelastic and mechanical properties for an out-of-autoclave polymer composite', *International SAMPE Technical Conference*, (Clc).

Ghaffari, M. *et al.* (2012) 'The kinetic analysis of isothermal curing reaction of an epoxy resin-glassflake nanocomposite', *Thermochimica Acta*, 549, pp. 81–86. doi: 10.1016/j.tca.2012.09.021.

Ghossein, H. *et al.* (2020) 'Characterization of mechanical performance of composites fabricated using innovative carbon fiber wet laid process', *Journal of Composites Science*, 4(3). doi: 10.3390/jcs4030124.

Gill, P., Moghadam, T. T. and Ranjbar, B. (2010) 'Differential scanning calorimetry

techniques: Applications in biology and nanoscience', *Journal of Biomolecular Techniques*, 21(4), pp. 167–193.

Granado, L. *et al.* (2018) 'Kinetic regimes in the curing process of epoxy-phenol composites', *Thermochimica Acta*, 667(July), pp. 185–192. doi: 10.1016/j.tca.2018.07.019.

Guigo, N. *et al.* (2007) 'Chemorheological analysis and model-free kinetics of acid catalysed furfuryl alcohol polymerization', *Physical Chemistry Chemical Physics*, 9(39), pp. 5359–5366. doi: 10.1039/b707950h.

Guigo, N. *et al.* (2009) 'New insights on the thermal degradation pathways of neat poly(furfuryl alcohol) and poly(furfuryl alcohol)/SiO2 hybrid materials', *Polymer Degradation and Stability*, 94(6), pp. 908–913. doi: 10.1016/j.polymdegradstab.2009.03.008.

Guigo, N. *et al.* (2010) 'Eco-friendly composite resins based on renewable biomass resources: Polyfurfuryl alcohol/lignin thermosets', *European Polymer Journal*, 46(5), pp. 1016–1023. doi: 10.1016/j.eurpolymj.2010.02.010.

Guigo, N. and Sbirrazzuoli, N. (2018) 'Thermal Analysis of Biobased Polymers and Composites', in Vyazovkin, Sergey, Nobuyoshi Koga, C. S. (ed.) *Handbook Of Thermal Analysis and Calorimetry Recent Advances, Techniques and Applications Recent Advances, Techniques and Applications*. Second. John Fedor, p. 399.

Gupta, M. K. and Singh, R. (2018) 'Flexural and Dynamic Mechanical Analysis (DMA) of Polylactic Acid (PLA) Coated Sisal Fibre Reinforced Polyester Composite', *Materials Today: Proceedings*, 5(2), pp. 6109–6114. doi: 10.1016/j.matpr.2017.12.216.

Gurunathan, T., Mohanty, S. and Nayak, S. K. (2015) 'A review of the recent developments in biocomposites based on natural fibres and their application perspectives', *Composites Part A: Applied Science and Manufacturing*, 77, pp. 1–25. doi: 10.1016/j.compositesa.2015.06.007.

Hanifpour, A. *et al.* (2019) 'Poly(furfuryl alcohol) bioresin-modified LY5210 epoxy thermosets', *Journal of Polymer Research*, 26(8), pp. 1–9. doi: 10.1007/s10965-019-1876-4.

Hans Hoydonckx, I. E. *et al.* (2015) 'Polyfurfuryl Alcohol Thermosets Resins in Fire Resistant Composite Applications', in *20th International Conference on Composite Materials Copenhagen, 19-24th July 2015*. Copenhagen.

Hardis, R. *et al.* (2013) 'Cure kinetics characterization and monitoring of an epoxy resin

using DSC, Raman spectroscopy, and DEA', *Composites Part A: Applied Science and Manufacturing*, 49, pp. 100–108. doi: 10.1016/j.compositesa.2013.01.021.

Haris, N. I. N. *et al.* (2021) 'Dynamic Mechanical Properties and Thermal Properties of Longitudinal Basalt/Woven Glass Fiber Reinforced Unsaturated Polyester Hybrid Composites', *Polymers*, 13, pp. 1096–1098. doi: https://doi.org/10.3390/polym13193343.

Hatakeyama, T. and Hatakeyama, H. (2005) *THERMAL PROPERTIES OF GREEN POLYMERS Hot Topics in Thermal Analysis and Calorimetry*. Available at: http://ebooks.springerlink.com.

He, L. *et al.* (2012) 'Effects of Polymerization Conditions on the Properties of Poly(furfuryl alcohol) Composite Membranes', *Journal of Applied Polymer Science*, 124(4), pp. 3383–3391. doi: 10.1002/app.35356.

Heinze, S. and Echtermeyer, A. T. (2018) 'A practical approach for data gathering for polymer cure simulations', *Applied Sciences (Switzerland)*, 8(11), pp. 1–31. doi: 10.3390/app8112227.

Hernández, S. *et al.* (2013) 'Optimization of curing cycle in carbon fiber-reinforced laminates: Void distribution and mechanical properties', *Composites Science and Technology*, 85, pp. 73–82. doi: 10.1016/j.compscitech.2013.06.005.

Holtzer, M. *et al.* (2020) 'Environmental impact of the reclaimed sand addition to molding sand with furan and phenol-formaldehyde resin—a comparison', *Materials*, 13(19), pp. 1–12. doi: 10.3390/ma13194395.

Holtzer, M., Dańko, R. and Kmita, A. (2016) 'Influence of a Reclaimed Sand Addition to Moulding Sand with Furan Resin on Its Impact on the Environment', *Water, Air, and Soil Pollution*, 227(1). doi: 10.1007/s11270-015-2707-9.

Hossain, M. K. *et al.* (2020) 'Evaluation of Thermo-Mechanical Properties of Carbon / Epoxy Amino-Functionalized Graphene Nanoplatelet Composite', pp. 1–10. doi: 10.33552/GJES.2020.04.000591.

Hosseini, N. (2015) *Experimental And Micromechanical Analysis Of Flax And Glass Reinforced Bio-Based Composites*. North Dakota State University of Agriculture and Applied Science By. doi: 10.4324/9781315721606-101.

Hosseinpour, A. *et al.* (2016) 'Investigation of the cure kinetics of an epoxy resin by

advanced isoconversional and model-fitting methods', *AIP Conference Proceedings*, 1713(March 2016). doi: 10.1063/1.4942315.

Hu, H. *et al.* (2020) 'Polyfurfuryl alcohol assisted synthesis of Na2FePO4F/C nanocomposites as cathode material of sodium ion batteries', *Journal of Electroanalytical Chemistry*, 867, p. 114187. doi: 10.1016/j.jelechem.2020.114187.

Hu, S. *et al.* (2018) 'Initiation mechanisms and kinetic analysis of the isothermal decomposition of poly(α-methylstyrene): A ReaxFF molecular dynamics study', *RSC Advances*, 8(7), pp. 3423–3432. doi: 10.1039/c7ra12467h.

Hubert, P. *et al.* (2017) 'Out-of-autoclave prepreg processing', in Zweben, C. H. and Beaumont, P. (eds) *Comprehensive Composite Materials II*. 2nd edn. Elsevier Ltd., pp. 63–94. doi: 10.1016/B978-0-12-803581-8.09900-8.

Ipakchi, H. *et al.* (2020) 'Bio-resourced furan resin as a sustainable alternative to petroleum-based phenolic resin for making GFR polymer composites', *Iranian Polymer Journal (English Edition)*, 29(4), pp. 287–299. doi: 10.1007/s13726-020-00793-w.

Iroegbu, A. O. *et al.* (2020) 'Sustainable Chemicals: A Brief Survey of the Furans', *Chemistry Africa*, 3(3), pp. 481–496. doi: 10.1007/s42250-020-00123-w.

Iroegbu, A. O. and Hlangothi, S. P. (2018) 'Effects of the Type of Catalyst on the Polymerisation Mechanism of Furfuryl Alcohol and its Resultant Properties', *Chemistry Africa*, 1(3–4), pp. 187–197. doi: 10.1007/s42250-018-0017-5.

Iroegbu, A. O. and Hlangothi, S. P. (2019) 'Furfuryl Alcohol a Versatile, Eco-Sustainable Compound in Perspective', *Chemistry Africa*, 2(2), pp. 223–239. doi: 10.1007/s42250-018-00036-9.

Jain, R., Choudhary, V. and Narula, A. K. (2007) 'Studies on the curing kinetics of epoxy resins using mixture of nadic/or maleic anhydride and 4,4'-diaminodiphenyl sulfone', *Journal of Thermal Analysis and Calorimetry*, 90(2), pp. 495–501. doi: 10.1007/s10973-006-7793-x.

Jawaid, M. and Abdul Khalil, H. P. S. (2011) 'Cellulosic/synthetic fibre reinforced polymer hybrid composites: A review', *Carbohydrate Polymers*, 86(1), pp. 1–18. doi: 10.1016/j.carbpol.2011.04.043.

Jia, Y. and Fiedler, B. (2018) 'Influence of furfuryl alcohol fiber pre-treatment on the

moisture absorption and mechanical properties of flax fiber composites', *Fibers*, 6(3). doi: 10.3390/fib6030059.

John, M. J. and Anandjiwala, R. D. (2009) 'Chemical modification of flax reinforced polypropylene composites', *Composites Part A: Applied Science and Manufacturing*, 40(4), pp. 442–448. doi: 10.1016/j.compositesa.2009.01.007.

John, M. J. and Sabu, T. (2012) 'Nanocomposites from Furanic Derivatives', in *Natural Polymers, Volume 2 - Nanocomposites*. 1st edn. Royal Society of Chemistry, pp. 150–184. doi: 10.1039/9781849735315-00150.

Jouyandeh, M. *et al.* (2019) 'Protocol for nonisothermal cure analysis of thermoset composites', *Progress in Organic Coatings*, 131(January), pp. 333–339. doi: 10.1016/j.porgcoat.2019.02.040.

Jouyandeh, M. *et al.* (2020) 'Nonisothermal cure kinetics of epoxy/MnxFe3-xO4 nanocomposites', *Progress in Organic Coatings*, 140(September 2019), p. 105505. doi: 10.1016/j.porgcoat.2019.105505.

Jubsilp, C., Takeichi, T. and Rimdusit, S. (2011) 'Polymerization kinetics', in Ishida, H. and Agag, T. (eds) *Handbook of Benzoxazine Resins*. Elsevier, pp. 157–174. doi: 10.1016/B978-0-444-53790-4.00052-7.

Kamal, M. R. and Sourour, S. (1973) 'Kinetics and thermal characterization of thermoset cure', *Polymer Engineering & Science*, 13(1), pp. 59–64. doi: 10.1002/pen.760130110.

Kandola, B. K., Ebdon, J. R. and Chowdhury, K. P. (2015) 'Flame retardance and physical properties of novel cured blends of unsaturated polyester and furan resins', *Polymers*, 7(2), pp. 298–315. doi: 10.3390/polym7020298.

Kandola, B. and Krishnan, L. (2014) 'Fire performance evaluation of different resins for potential application in fire resistant structural marine composites', *Fire Safety Science*, 11, pp. 769–780. doi: 10.3801/IAFSS.FSS.11-769.

Karami, Z. *et al.* (2020) 'A comparative study on cure kinetics of layered double hydroxide (Ldh)/epoxy nanocomposites', *Journal of Composites Science*, 4(3). doi: 10.3390/jcs4030111.

Katiyar, R. and Shobhit, S. (2017) 'Studies on Furan Polymer Concrete', *International Research Journal of Engineering and Technology*, 04(05), pp. 721–727.

Kherroub, D. E., Belbachir, M. and Lamouri, S. (2015a) 'Study and Optimization of the Polymerization Parameter of Furfuryl Alcohol by Algerian Modified Clay', *Arabian Journal for Science and Engineering*, 40(1), pp. 143–150. doi: 10.1007/s13369-014-1512-x.

Kherroub, D. E., Belbachir, M. and Lamouri, S. (2015b) 'Synthesis of poly(furfuryl alcohol)/montmorillonite nanocomposites by direct in-situ polymerization', *Bulletin of Materials Science*, 38(1), pp. 57–63. doi: 10.1007/s12034-014-0818-3.

Kim, M. G. *et al.* (1998) 'Furfuryl alcohol emulsion resins as co-binders for urea-formaldehyde resin-bonded particleboards', *Wood and Fiber Science*, 30(3), pp. 238–249.

Kubouchi, M. *et al.* (2016) 'Biopolymers', 6(3), p. 4568.

Kufel, A., Para, S. and Kuciel, S. (2021) 'Basalt/glass fiber polypropylene hybrid composites: Mechanical properties at different temperatures and under cyclic loading and micromechanical modelling', *Materials*, 14(19). doi: 10.3390/ma14195574.

Kumar, R. (2016) 'A Review on Epoxy and Polyester Based Polymer Concrete and Exploration of Polyfurfuryl Alcohol as Polymer Concrete', *Journal of Polymers*, 2016, pp. 1–13. doi: 10.1155/2016/7249743.

Kumar, R. and Anandjiwala, R. D. (2012) 'Alternative fuels from waste cellulosic substrates and poly furfuryl alcohol', *Fuel*, 93, pp. 703–705. doi: 10.1016/j.fuel.2011.09.038.

Kumar, R. and Anandjiwala, R. D. (2013) 'Compression-moulded flax fabric-reinforced polyfurfuryl alcohol bio-composites:Mechanical and thermal properties', *Journal of Thermal Analysis and Calorimetry*, 112(2), pp. 755–760. doi: 10.1007/s10973-012-2623-9.

Kuppusamy, R. R. P., Zade, A. and Kumar, K. (2020) 'Time-temperature-cure process window of epoxy-vinyl ester resin for applications in liquid composite moulding processes', *Materials Today: Proceedings*, 39(June), pp. 1407–1411. doi: 10.1016/j.matpr.2020.05.048.

Larrañaga, A. and Lizundia, E. (2019) 'A review on the thermomechanical properties and biodegradation behaviour of polyesters', *European Polymer Journal*, 121(October), p. 109296. doi: 10.1016/j.eurpolymj.2019.109296.

Lascano, D. *et al.* (2019) 'Kinetic analysis of the curing of a partially biobased epoxy resin using dynamic differential scanning calorimetry', *Polymers*, 11(3). doi: 10.3390/polym11030391.

Lascano, D. *et al.* (2021) 'Kinetic analysis of the curing process of biobased epoxy resin from epoxidized linseed oil by dynamic differential scanning calorimetry', *Polymers*, 13(8). doi: 10.3390/polym13081279.

Li, S. *et al.* (1997) 'Studies on relaxation and thermal expansion behavior of polysiloxane-modified epoxy resin', *Journal of Macromolecular Science - Physics*, 36(3), pp. 357–366. doi: 10.1080/00222349708212389.

Li, Y., Li, Q. and Ma, H. (2015) 'The voids formation mechanisms and their effects on the mechanical properties of flax fiber reinforced epoxy composites', *Composites Part A: Applied Science and Manufacturing*, 72, pp. 40–48. doi: 10.1016/j.compositesa.2015.01.029.

Liang, Q. *et al.* (2022) 'Reaction model and cure kinetics of fiber-reinforced phenolic system', *Acta Mechanica Sinica/Lixue Xuebao*, 38(6). doi: 10.1007/s10409-022-22081-2.

Limpricht, H. and Schwanert, H. (1870) *Ueber das Toluylenoxyd oder Desoxybenzoïn, C14H12O*. doi: https ://doi.org/10.1002/jlac.18701 55010 6.

Little, J. E., Yuan, X. and Jones, M. I. (2012) 'Characterisation of voids in fibre reinforced composite materials', *NDT and E International*, 46(1), pp. 122–127. doi: 10.1016/j.ndteint.2011.11.011.

Liu, J. *et al.* (2021) 'Recent development on bio-based thermosetting resins', *Journal of Polymer Science*, 59(14), pp. 1474–1490. doi: 10.1002/pol.20210328.

Lopez De Vergara, U. *et al.* (2014) 'Polymerization and curing kinetics of furan resins under conventional and microwave heating', *Thermochimica Acta*, 581, pp. 92–99. doi: 10.1016/j.tca.2014.02.017.

López De Vergara, U. *et al.* (2014) 'Impact behaviour of basalt fibre reinforced furan composites cured under microwave and thermal conditions', *Composites Part B: Engineering*, 66, pp. 156–161. doi: 10.1016/j.compositesb.2014.05.009.

Luckeneder, P. *et al.* (2016) 'Sustainable phenolic fractions as basis for furfuryl alcohol-based co-polymers and their use as wood adhesives', *Polymers*, 8(11). doi: 10.3390/polym8110396.

Lutton, R. E. M., Taylor, S. E. and Sonebi, M. (2017) 'Commercial potential of bioresins and their success in thermosetting composites: an overview', *2nd International Conference on Bio-based Building Materials & 1st Conference on Ecological valorisation of Granular and*

FIbrous materials, (June), pp. 1–10.

Lyu, J. *et al.* (2018) 'Non-isothermal kinetics of epoxy resin curing reaction under compressed CO2', *Journal of Thermal Analysis and Calorimetry*, 131(2), pp. 1499–1507. doi: 10.1007/s10973-017-6574-z.

Ma, C. C. M. *et al.* (1995) 'Pultruded fibre-reinforced furfuryl alcohol resin composites: 1. Process feasibility study', *Composites Manufacturing*, 6(1), pp. 45–52.

Ma, H. *et al.* (2018) 'A Study on Curing Kinetics of Nano-Phase Modified Epoxy Resin', *Scientific Reports*, 8(1), pp. 1–15. doi: 10.1038/s41598-018-21208-0.

Ma, Y. *et al.* (2020) 'Preparation and characterization of furan-matrix composites blended with modified hollow glass microsphere', *Polymers*, 12(7), pp. 1–12. doi: 10.3390/polym12071480.

Machado, G. *et al.* (2016) 'Literature Review on Furfural Production from Lignocellulosic Biomass', *Natural Resources*, 07(03), pp. 115–129. doi: 10.4236/nr.2016.73012.

Mahmood, H. *et al.* (2021) 'A comparative study on suitability of model-free and model-fitting kinetic methods to non-isothermal degradation of lignocellulosic materials', *Polymers*, 13(15). doi: 10.3390/polym13152504.

Malathi, B. and Kumar, P. P. (2018) 'Experimental Investigation for Evaluation of Mechanical Properties of Rice Husk and Saw Dust Composites', 5(6), pp. 6–10.

Marefat Seyedlar, R., Imani, M. and Mirabedini, S. M. (2016) 'Curing of poly(furfuryl alcohol) resin catalyzed by a homologous series of dicarboxylic acid catalysts: Kinetics and pot life', *Journal of Applied Polymer Science*, 133(43). doi: 10.1002/app.44009.

Marefat Seyedlar, R., Imani, M. and Mirabedini, S. M. (2017) 'Rheokinetics in curing process of polyfurfuryl alcohol: effect of homologous acid catalysts', *Iranian Polymer Journal (English Edition)*, 26(4), pp. 281–293. doi: 10.1007/s13726-017-0518-0.

Marefat Seyedlar, R., Imani, M. and Mirabedini, S. M. (2018) 'Curing of polyfurfuryl alcohol resin catalyzed by a homologous series of dicarboxylic acid catalysts. II. Swelling behavior and thermal properties', *Journal of Applied Polymer Science*, 135(5), pp. 1–11. doi: 10.1002/app.45770.

Marefat Seyedlar, R., Imani, M. and Mirabedini, S. M. (2020) 'Bio-based furan coatings:

adhesion, mechanical and thermal properties', *Polymer Bulletin*, (0123456789). doi: 10.1007/s00289-020-03124-4.

Marefat Seyedlar, R., Imani, M. and Mirabedini, S. M. (2021) 'Bio-based furan coatings: adhesion, mechanical and thermal properties', *Polymer Bulletin*, 78(2), pp. 577–599. doi: 10.1007/s00289-020-03124-4.

Mariscal, R. *et al.* (2016) 'Furfural: A renewable and versatile platform molecule for the synthesis of chemicals and fuels', *Energy and Environmental Science*, 9(4), pp. 1144–1189. doi: 10.1039/c5ee02666k.

Mashouf Roudsari, G., Misra, M. and Mohanty, A. K. (2017) 'A study of mechanical properties of biobased epoxy network: Effect of addition of epoxidized soybean oil and poly(furfuryl alcohol)', *Journal of Applied Polymer Science*, 134(1), pp. 1–9. doi: 10.1002/app.44352.

Mashouf Roudsari, G., Mohanty, A. K. and Misra, M. (2014) 'Study of the curing kinetics of epoxy resins with biobased hardener and epoxidized soybean oil', *ACS Sustainable Chemistry and Engineering*, 2(9), pp. 2111–2116. doi: 10.1021/sc500176z.

Masuelli, M. A. (2013) 'Introduction of Fibre-Reinforced Polymers − Polymers and Composites: Concepts, Properties and Processes', in *Fiber Reinforced Polymers - The Technology Applied for Concrete Repair*. IntechOpen. doi: http://dx.doi.org/10.5772/54629.

Medina, L., Schledjewski, R. and Schlarb, A. K. (2009) 'Process related mechanical properties of press molded natural fiber reinforced polymers', *Special Issue on the 12th European Conference on Composite Materials, ECCM 2006*, 69(9), pp. 1404–1411. doi: 10.1016/j.compscitech.2008.09.017.

Mehdikhani, M. *et al.* (2019) 'Voids in fiber-reinforced polymer composites: A review on their formation, characteristics, and effects on mechanical performance', *Journal of Composite Materials*, 53(12), pp. 1579–1669. doi: 10.1177/0021998318772152.

Menager, C. *et al.* (2019) '"Green" composites prepared from polyfurfuryl alcohol and cork residues: Thermal and mechanical properties', *Composites Part A: Applied Science and Manufacturing*, 124(February), p. 105473. doi: 10.1016/j.compositesa.2019.105473.

Menard, K. P. and Menard, N. R. (2015) *Dynamic Mechanical Analysis in the Analysis of Polymers and Rubbers*, *Encyclopedia of Polymer Science and Technology*. doi:

10.1002/0471440264.pst102.pub2.

Meng, J. *et al.* (2020) 'Flame Retardancy and Mechanical Properties of Bio-Based Furan Epoxy Resins with High Crosslink Density', *Macromolecular Materials and Engineering*, 305(1), pp. 1–8. doi: 10.1002/mame.201900587.

Michael, S. and Carbon Composites e.V. (2019) *Composites Market Report The global CF- und CC-Market Market developments, Trends, outlook and challenges*.

Moazzen, K. *et al.* (2018) 'Toward poly(furfuryl alcohol) applications diversification: Novel self-healing network and toughening epoxy–novolac resin', *Journal of Applied Polymer Science*, 135(12), pp. 1–11. doi: 10.1002/app.45921.

Modica, P. Di *et al.* (2015) 'Bio-resin for new bio-composite passive fire protection for off-shore application', *ICCM International Conferences on Composite Materials*, 2015-July(July).

Mofidi, A., Abila, J. and Ng, J. T. M. (2020) 'Novel advanced composite bamboo structural members with bio-based and synthetic matrices for sustainable construction', *Sustainability (Switzerland)*, 12(6). doi: 10.3390/su12062485.

Mohajeri, S. *et al.* (2017) 'Advanced isoconversional cure kinetic analysis of epoxy/poly(furfuryl alcohol) bio-resin system', *Journal of Applied Polymer Science*, 134(42), pp. 1–10. doi: 10.1002/app.45432.

Mohajeri, S. and Pazokifard, S. (2015) 'Toughening of Epoxy Resin through Blending with Furan Resin The 6th International Color & Coating Congress', (November), pp. 2–3.

Mohanty, A. K., Misra, M. and Drzal, L. T. (2002) 'Sustainable Bio-Composites from renewable resources: Opportunities and challenges in the green materials world', *Journal of Polymers and the Environment*, 10(1–2), pp. 19–26. doi: 10.1023/A:1021013921916.

Mokhothu, T. H. and John, M. J. (2017) 'Bio-based coatings for reducing water sorption in natural fibre reinforced composites', *Scientific Reports*, 7(1), pp. 1–8. doi: 10.1038/s41598-017-13859-2.

Monti, M. *et al.* (2015) 'Thermal and combustion behavior of furan resin/silica nanocomposites', *European Polymer Journal*, 67(November), pp. 561–569. doi: 10.1016/j.eurpolymj.2015.02.005.

Moukhina, E. (2012) 'Determination of kinetic mechanisms for reactions measured with thermoanalytical instruments', *Journal of Thermal Analysis and Calorimetry*, 109(3), pp. 1203–1214. doi: 10.1007/s10973-012-2406-3.

Murias, P. *et al.* (2015) 'A quantitative approach to dynamic and isothermal curing of an epoxy resin modified with oligomeric siloxanes', *Journal of Thermal Analysis and Calorimetry*, 122(1), pp. 215–226. doi: 10.1007/s10973-015-4703-0.

Muthukumar, M. and Mohan, D. (2005) 'Studies on furan polymer concrete', *Journal of Polymer Research*, 12(3), pp. 231–241. doi: 10.1007/s10965-004-3206-7.

Nagashree, K. (2015) 'Research and Reviews : Journal of Pharmaceutical Analysis Solid dosage forms : Tablets', 4(2), pp. 60–71.

Nanni, G. *et al.* (2019) 'Poly(furfuryl alcohol)-polycaprolactone blends', *Polymers*, 11(6), pp. 1–14. doi: 10.3390/POLYM11061069.

Newcomb, B. A. (2019) 'Time-Temperature-Transformation (TTT) diagram of a carbon fiber epoxy prepreg', *Polymer Testing*, 77(April), p. 105859. doi: 10.1016/j.polymertesting.2019.04.006.

Ogunsona, E. O., Misra, M. and Mohanty, A. K. (2017) 'Sustainable biocomposites from biobased polyamide 6,10 and biocarbon from pyrolyzed miscanthus fibers', *Journal of Applied Polymer Science*, 134(4), pp. 1–11. doi: 10.1002/app.44221.

Oishi, S. S. *et al.* (2013) 'Viscosity, pH, and moisture effect in the porosity of poly(furfuryl alcohol)', *Journal of Applied Polymer Science*, 128(3), pp. 1680–1686. doi: 10.1002/app.38332.

Oishi, S. S. *et al.* (2017) 'Structural and surface functionality changes in reticulated vitreous carbon produced from poly(furfuryl alcohol) with sodium hydroxide additions', *Applied Surface Science*, 394, pp. 87–97. doi: 10.1016/j.apsusc.2016.10.112.

Origo, F. D. *et al.* (2016) 'Acid catalyst influence on the polymerization time of polyfurfuryl alcohol and on the porosity of monolithic vitreous carbon', *Journal of Applied Polymer Science*, 133(20), pp. 1–10. doi: 10.1002/app.43272.

Ozawa, T. (1965) 'A New Method of Analyzing Thermogravimetric Data', *Bulletin of the Chemical Society of Japan*, 38(11), pp. 1881–1886. doi: 10.1246/bcsj.38.1881.

Palumbo, R. *et al.* (2019) 'A multi-scale reinforced sandwich panel for vibroacoustic applications: Shear transition effects', *9th ECCOMAS Thematic Conference on Smart Structures and Materials, SMART 2019*, pp. 1058–1065.

Pemberton, R., Edser, D. and Gower, M. (2020) *Optimisation of Acid Digestion Conditions for Volume Fraction Measurements of Hard to Digest Fibre-Reinforced Polymer Composites*. doi: https://doi.org/10.47120/npl.MN12.

Peters, F. N. (1936) 'The Furans Fifteen Years of Progress', *Industrial and Engineering Chemistry*, 28(7), pp. 755–759. doi: 10.1021/ie50319a002.

Pin, J. M., Misra, M. and Mohanty, A. (2017) 'Green design of nanoporous materials and carbonaceous foams from polyfurfuryl alcohol and epoxidized linseed oil', *Materials Letters*, 196, pp. 238–241. doi: 10.1016/j.matlet.2017.03.058.

Pizzi, A., Papadopoulos, A. N. and Policardi, F. (2020) 'Wood composites and their polymer binders', *Polymers*, 12(5). doi: 10.3390/POLYM12051115.

Pophali, A. *et al.* (2019) 'First synthesis of poly(furfuryl) alcohol precursor-based porous carbon beads as an efficient adsorbent for volatile organic compounds', *Chemical Engineering Journal*, 373(January), pp. 365–374. doi: 10.1016/j.cej.2019.05.029.

Porc, O. *et al.* (2020) *European Bioeconomy in Figures*, *Industrial Biotechnology*. doi: 10.1089/ind.2016.29030.spi.

Prasanth, S. M. *et al.* (2021) 'Application of biomass derived products in mid-size automotive industries: A review', *Chemosphere*, 280(March). doi: 10.1016/j.chemosphere.2021.130723.

Principe, M. *et al.* (2000) 'Furfuryl Alcohol Polymerization, Principe, J Pol Ciên e Tecnol, 2000', *Polímeros: Ciência e Tecnologia*, 10(1), pp. 8–14.

Purnal L. McWhorter, J. (1949) 'Process of Making Furfuryl Alcohol Resin'. United State of America. Available at: https://patents.google.com/patent/US2471438A/en?q.

Ramon, E., Sguazzo, C. and Moreira, P. M. G. P. (2018) 'A review of recent research on bio-based epoxy systems for engineering applications and potentialities in the aviation sector', *Aerospace*, 5(4). doi: 10.3390/aerospace5040110.

Ren, R. *et al.* (2016) 'Isothermal curing kinetics and mechanism of DGEBA epoxy resin with

phthalide-containing aromatic diamine', *Thermochimica Acta*, 623, pp. 15–21. doi: 10.1016/j.tca.2015.11.011.

Resch-fauster, K. *et al.* (2018) 'High Performance Composites Produced From Polyfurfuryl Alcohol : Enhancing the Process Ability At Short Cycle Times By Applying Hydrophilic', (June), pp. 24–28.

Resch-Fauster, K. *et al.* (2018) 'Effect of the water absorptive capacity of reinforcing fibers on the process ability, morphology, and performance characteristics of composites produced from polyfurfuryl alcohol', *Advanced Manufacturing: Polymer and Composites Science*, 4(1), pp. 13–23. doi: 10.1080/20550340.2018.1436234.

Rivero, G. *et al.* (2011) 'Curing kinetics of a furan resin and its nanocomposites', *Thermochimica Acta*, 516(1–2), pp. 79–87. doi: 10.1016/j.tca.2011.01.022.

Rivero, G. *et al.* (2014) 'Furan resins as replacement of phenolic protective coatings: Structural, mechanical and functional characterization', *Progress in Organic Coatings*, 77(1), pp. 247–256. doi: 10.1016/j.porgcoat.2013.09.015.

Rivero, G., Villanueva, S. and Manfredi, L. B. (2013) 'Furan resin as a replacement of phenolics: influence of the clay addition on its thermal degradation and fire behaviour', *Fire and Materials*, (September 2013). doi: 10.1002/fam.2209.

Rivero, G., Villanueva, S. and Manfredi, L. B. (2014) 'Furan resin as a replacement of phenolics: influence of the clay addition on its thermal degradation and fire behaviour', *Fire and Materials*, 38(6), pp. 683–694. doi: 10.1002/fam.2209 Furan.

Ruiz, V. and Pandolfo, A. G. (2011) 'High-frequency carbon supercapacitors from polyfurfuryl alcohol', *Journal of Power Sources*, 196(18), pp. 7816–7822. doi: 10.1016/j.jpowsour.2010.12.111.

S. Giannis *et al.* (2008) 'Development of High performance Bio-Composite based on Furan Bio Resin for Vehicle Panel', in *13th European Conference on Composite Material*. Stockholm, pp. 1–10.

Sadler, J. M. *et al.* (2018) 'Kinetics studies and characterization of poly(furfuryl alcohol) for use as bio-based furan novolacs', *Journal of Applied Polymer Science*, 135(34), pp. 1–14. doi: 10.1002/app.46608.

Safranski, D. L. and Gall, K. (2008) 'Effect of chemical structure and crosslinking density on

the thermo-mechanical properties and toughness of (meth)acrylate shape memory polymer networks', *Polymer*, 49(20), pp. 4446–4455. doi: 10.1016/j.polymer.2008.07.060.

Sangregorio, A. *et al.* (2021) 'Natural fibre composites with furanic thermoset resins. Comparison between polyfurfuryl alcohol and humins from sugar conversion', *Composites Part C: Open Access*, 4(September 2020), p. 100109. doi: 10.1016/j.jcomc.2021.100109.

Sarika, P. R. *et al.* (2020) 'Bio-based alternatives to phenol and formaldehyde for the production of resins', *Polymers*, 12(10), pp. 1–24. doi: 10.3390/polym12102237.

Savabieh, H. *et al.* (2019) 'Kinetics of crystallization in 13.2Li 2 O-67.6SiO 2 -14.49Al 2 O 3 -3.3TiO 2 -0.4BaO-0.97ZnO glass ceramic powder: Part I: A model-free vs. model-fitting approach', *Ceramics International*, 45(7), pp. 8856–8865. doi: 10.1016/j.ceramint.2019.01.214.

Sbirrazzuoli, N. (2019) 'Advanced isoconversional kinetic analysis for the elucidation of complex reaction mechanisms: A new method for the identification of rate-limiting steps', *Molecules*, 24(9). doi: 10.3390/molecules24091683.

Sbirrazzuoli, N. (2020) 'Interpretation and physical meaning of kinetic parameters obtained from isoconversional kinetic analysis of polymers', *Polymers*, 12(6). doi: 10.3390/POLYM12061280.

Sbirrazzuoli, N. (2021) 'Model-free isothermal and nonisothermal predictions using advanced isoconversional methods', *Thermochimica Acta*, 697(December 2020), p. 178855. doi: 10.1016/j.tca.2020.178855.

Shah, D. B. *et al.* (2019) 'Thermo-mechanical characterization of carbon fiber composites with different epoxy resin systems', *Thermochimica Acta*, 676(April), pp. 39–46. doi: 10.1016/j.tca.2019.03.041.

Shanmugam, D. and Thiruchitrambalam, M. (2013) 'Static and dynamic mechanical properties of alkali treated unidirectional continuous Palmyra Palm Leaf Stalk Fiber/jute fiber reinforced hybrid polyester composites', *Materials and Design*, 50, pp. 533–542. doi: 10.1016/j.matdes.2013.03.048.

Sharib, M., Kumar, R. and Kumar, K. D. (2018) 'Polylactic acid incorporated polyfurfuryl alcohol bioplastics: thermal, mechanical and curing studies', *Journal of Thermal Analysis and Calorimetry*, 132(3), pp. 1593–1600. doi: 10.1007/s10973-018-7087-0.

Sharma, M. and Chopra, E. A. (2019) 'Comparative Analysis of Furan Resin Modified Asphalt Mix and Conventional Asphalt Mix', *International Journal of Civil Engineering and Technology (IJCIET)*, 10(3), pp. 1574–1582. Available at: http://www.iaeme.com/IJCIET/index.asp1574http://www.iaeme.com/ijciet/issues.asp?JType=IJCIET&VType=10&IType=03http://www.iaeme.com/IJCIET/issues.asp?JType=IJCIET&VType=10&IType=03.

Singh, N. *et al.* (2022) 'Global status of lignocellulosic biorefinery: Challenges and perspectives', *Bioresource Technology*, 344(November 2021). doi: 10.1016/j.biortech.2021.126415.

Sommerauer, L. *et al.* (2019) 'Furfuryl alcohol and lactic acid blends: Homo-or co-polymerization?', *Polymers*, 11(10). doi: 10.3390/polym11101533.

Stanko, M. and Stommel, M. (2018) 'Kinetic prediction of fast curing polyurethane resins by model-free isoconversional methods', *Polymers*, 10(7). doi: 10.3390/polym10070698.

Stark, W. (2013) 'Investigation of the curing behaviour of carbon fibre epoxy prepreg by Dynamic Mechanical Analysis DMA', *Polymer Testing*, 32(2), pp. 231–239. doi: 10.1016/j.polymertesting.2012.11.004.

Suárez-García, F. *et al.* (2002) 'Characterization of porous texture in composite adsorbents based on exfoliated graphite and polyfurfuryl alcohol', *Fuel Processing Technology*, 77–78, pp. 401–407. doi: 10.1016/S0378-3820(02)00088-7.

Sun, B. G. *et al.* (2019) 'Enhanced mechanical properties at 400 °C of carbon fabric reinforced phthalonitrile composites by high temperature postcure', *Composites Part B: Engineering*, 166(October 2018), pp. 681–687. doi: 10.1016/j.compositesb.2019.02.066.

Talent, M. and Wang, J. (2015) 'Unidirectional Cordenka Fibre-Reinforced Furan Resin Full Biocomposite: Properties and Influence of High Fibre Mass Fraction', *Journal of Composites*, 2015(2015), p. 8. doi: http://dx.doi.org/10.1155/2015/707151.

Tarani, E. *et al.* (2019) 'Kinetics of crystallization and thermal degradation of an isotactic polypropylene matrix reinforced with graphene/glass-fiber filler', *Molecules*, 24(10). doi: 10.3390/molecules24101984.

Tharazi, I. *et al.* (2017) 'Optimization of Hot Press Parameters on Tensile Strength for Unidirectional Long Kenaf Fiber Reinforced Polylactic-Acid Composite', *Procedia*

Engineering, 184, pp. 478–485. doi: 10.1016/j.proeng.2017.04.150.

Tondi, G. *et al.* (2015) 'A simple approach to distinguish classic and formaldehyde-free tannin based rigid foams by ATR FT-IR', *Journal of Spectroscopy*, 2015(February). doi: 10.1155/2015/902340.

Tondi, G. *et al.* (2019) 'Understanding the polymerization of polyfurfuryl alcohol: Ring opening and diels-alder reactions', *Polymers*, 11(12), pp. 1–15. doi: 10.3390/polym11122126.

Tumolva, T. *et al.* (2011) 'Evaluating the carbon storage potential of furan resin-based green composites', *ICCM International Conferences on Composite Materials*, (January).

Ugryumov, S. A., Varankina, G. S. and Katsadze, V. A. (2019) 'A Method for Manufacturing Glued Plywood Based on Furan Resins', *Polymer Science - Series D*, 12(4), pp. 398–400. doi: 10.1134/S1995421219040191.

Ünal, H. Y., Öner, G. and Pekbey, Y. (2017) 'Comparison of the Experimental Mechanical Properties and DMA Measurement of Nanoclay Hybrid Composites', *European Mechanical Science*, 2(1), pp. 31–36. doi: 10.26701/ems.356823.

Vafayan, M. *et al.* (2013) 'Advanced integral isoconversional analysis for evaluating and predicting the kinetic parameters of the curing reaction of epoxy prepreg', *Thermochimica Acta*, 557, pp. 37–43. doi: 10.1016/j.tca.2013.01.035.

Vargas-Hernández, M. Á., Sulbarán-Rangel, B. and Vázquez-Torres, H. (2020) 'Non-isothermal curing kinetics of biocomposite from poly(furfuryl alcohol) and graphene oxide or reduced graphene oxide with different contents of oxygen-groups by DSC', *Thermochimica Acta*, 684(September 2019), p. 178485. doi: 10.1016/j.tca.2019.178485.

Vargas, M. A., Scheubner, M. and Guthausen, G. (2018) 'Reaction kinetics of polyfurfuryl alcohol bioresin and nanoparticles by 1H-NMR transverse relaxation measurements', *Polymer Composites*, 39(9), pp. 3280–3288. doi: 10.1002/pc.24342.

Varodi, A. M., Beldean, E. and Timar, M. C. (2019) 'Furan Resin as potential substitute for phenol-formaldehyde resin in Plywood Manufacturing', *BioResources*, 14(2), pp. 2727–2739. doi: 10.15376/biores.14.2.2727-2739.

Vasilopoulos, Y., Skořepová, E. and Šoóš, M. (2020) 'Comf: Comprehensive model-fitting method for simulating isothermal and single-step solid-state reactions', *Crystals*, 10(2). doi:

10.3390/cryst10020139.

Vyazovkin, S. *et al.* (2011) 'ICTAC Kinetics Committee recommendations for performing kinetic computations on thermal analysis data', *Thermochimica Acta*, 520(1–2), pp. 1–19. doi: 10.1016/j.tca.2011.03.034.

Vyazovkin, S. *et al.* (2014) 'ICTAC Kinetics Committee recommendations for collecting experimental thermal analysis data for kinetic computations', *Thermochimica Acta*, 590, pp. 1–23. doi: 10.1016/j.tca.2014.05.036.

Vyazovkin, S. (2019) '"Nothing Can Hide Itself from Thy Heat": Understanding Polymers via Unconventional Applications of Thermal Analysis', *Macromolecular Rapid Communications*. doi: 10.1002/marc.201800334.

Vyazovkin, S. *et al.* (2020) 'ICTAC Kinetics Committee recommendations for analysis of multi-step kinetics', *Thermochimica Acta*, 689(March), p. 178597. doi: 10.1016/j.tca.2020.178597.

Vyazovkin, S. *et al.* (2022) 'ICTAC Kinetics Committee recommendations for analysis of thermal polymerization kinetics', *Thermochimica Acta*, 714(July), p. 179243. doi: 10.1016/j.tca.2022.179243.

Vyazovkin, S. and Sbirrazzuoli, N. (2006) 'Isoconversional kinetic analysis of thermally stimulated processes in polymers', *Macromolecular Rapid Communications*, 27(18), pp. 1515–1532. doi: 10.1002/marc.200600404.

Vyazovkin, S. and Wight, C. A. (1998) 'Isothermal and non-isothermal kinetics of thermally stimulated reactions of solids', *International Reviews in Physical Chemistry*, 17(3), pp. 407–433. doi: 10.1080/014423598230108.

Wang, F. *et al.* (2016) 'Size effect of graphene nanoplatelets on the morphology and mechanical behavior of glass fiber/epoxy composites', *Journal of Materials Science*, 51(7), pp. 3337–3348. doi: 10.1007/s10853-015-9649-x.

Wang, H. and Yao, J. (2006) 'Use of Poly(furfuryl alcohol) in the fabrication of nanostructured carbons and nanocomposites', *Industrial and Engineering Chemistry Research*. doi: 10.1021/ie0602660.

Wang, J., Laborie, M. P. G. and Wolcott, M. P. (2005) 'Comparison of model-free kinetic methods for modeling the cure kinetics of commercial phenol-formaldehyde resins',

Thermochimica Acta, 439(1–2), pp. 68–73. doi: 10.1016/j.tca.2005.09.001.

Wang, Z. *et al.* (2017) 'Mechanical and anticorrosion properties of furan/epoxy-based basalt fiber-reinforced composites', *Journal of Applied Polymer Science*, 134(19), pp. 1–6. doi: 10.1002/app.44799.

Wang, Z. *et al.* (2018) 'Cure behaviors of furfuryl alcohol/epoxy/methyltetrahydrophthalic anhydride and their enhanced mechanical and anti-acid properties of basalt fiber reinforced composites', *Composites Part B: Engineering*, 154(August), pp. 263–271. doi: 10.1016/j.compositesb.2018.08.011.

Win, D. T. (2005) 'Furfural – Gold from Garbage', *AU Journal of Technology*, 8(4), pp. 185–190.

Witold, B., Joshua, W. and Goodman, S. H. (2014) 'Epoxies', in Hanna, D. and Goodman, S. H. (eds) *Handbook of Thermoset Plastics*. 3rd Editio, pp. 191–252. doi: https://doi.org/10.1016/C2011-0-09694-1.

Witten, E. and Mathes, V. (2019) *The Market for Glass Fibre Reinforced Plastics (GRP) in 2019*.

Wu, F., Zhou, X. and Yu, X. (2018) 'Reaction mechanism, cure behavior and properties of a multifunctional epoxy resin, TGDDM, with latent curing agent dicyandiamide', *RSC Advances*, 8(15), pp. 8248–8258. doi: 10.1039/c7ra13233f.

Yan, J. *et al.* (2020) 'Investigation of kinetic and thermodynamic parameters of coal pyrolysis with model-free fitting methods', *Carbon Resources Conversion*, 3(December), pp. 173–181. doi: 10.1016/j.crcon.2020.11.002.

Yasnó, J. P. *et al.* (2021) 'Non-isothermal reaction mechanism and kinetic analysis for the synthesis of monoclinic lithium zirconate (m-Li2ZrO3) during solid-state reaction', *Journal of Analytical Science and Technology*, 12(1). doi: 10.1186/s40543-021-00267-5.

Zaharopoulou, A., Yannopoulos, S. N. and Ioannides, T. (2020) 'Carbon Membranes Prepared from Poly (Furfuryl Alcohol–Furfural) Precursors: Effect of FeCl3 Additive', *C — Journal of Carbon Research*, 6(3), p. 53. doi: 10.3390/c6030053.

Zarbin, A. J. G., Bertholdo, R. and Oliveira, M. A. F. C. (2002) 'Preparation, characterization and pyrolysis of poly(furfuryl alcohol)/porous silica glass nanocomposites: Novel route to carbon template', *Carbon*, 40(13), pp. 2413–2422. doi: 10.1016/S0008-6223(02)00130-6.

Zhang, C. *et al.* (2011) 'Kinetic study of the novolac resin curing process using model fitting and model-free methods', *Thermochimica Acta*, 523(1–2), pp. 63–69. doi: 10.1016/j.tca.2011.04.033.

Zhang, X. F. *et al.* (2017) 'Curing kinetics and mechanical properties of bio-based composite using rosin-sourced anhydrides as curing agent for hot-melt prepreg', *Science China Technological Sciences*, 60(9), pp. 1318–1331. doi: 10.1007/s11431-016-9029-y.

Zheng, T. *et al.* (2019) 'Studies on curing kinetics and tensile properties of silica-filled phenolic amine/epoxy resin nanocomposite', *Polymers*, 11(4). doi: 10.3390/polym11040680.

Zheng, T. *et al.* (2020) 'The curing kinetics and mechanical properties of epoxy resin composites reinforced by PEEK microparticles', *Polymer Testing*, 91(May), p. 106781. doi: 10.1016/j.polymertesting.2020.106781.

Zhijun, Y. *et al.* (2019) 'Multiobjective optimization method for polymer injection molding based on a genetic algorithm', *Advances in Polymer Technology*, 2019. doi: 10.1155/2019/9012085.

Zolghadr, M. *et al.* (2019) 'Epoxy resin modification by reactive bio-based furan derivatives: Curing kinetics and mechanical properties', *Thermochimica Acta*, 673(January), pp. 147–157. doi: 10.1016/j.tca.2019.01.025.

Appendix A: Experimental

Optical Microscopy

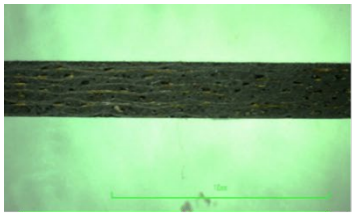

OVC

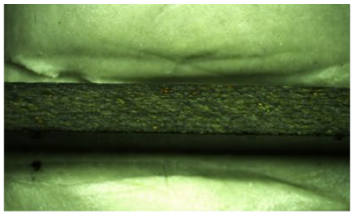

CM5

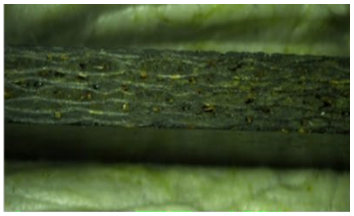

CM10

Representative evaluation fibre fraction using image J software.

Representative fibre fraction evaluation of the OVC sample images

Representative fibre fraction evaluation of the CM5 sample images

Representative fibre fraction evaluation of the CM10 sample images

Tensile Stress - strain curves for the individual laminates

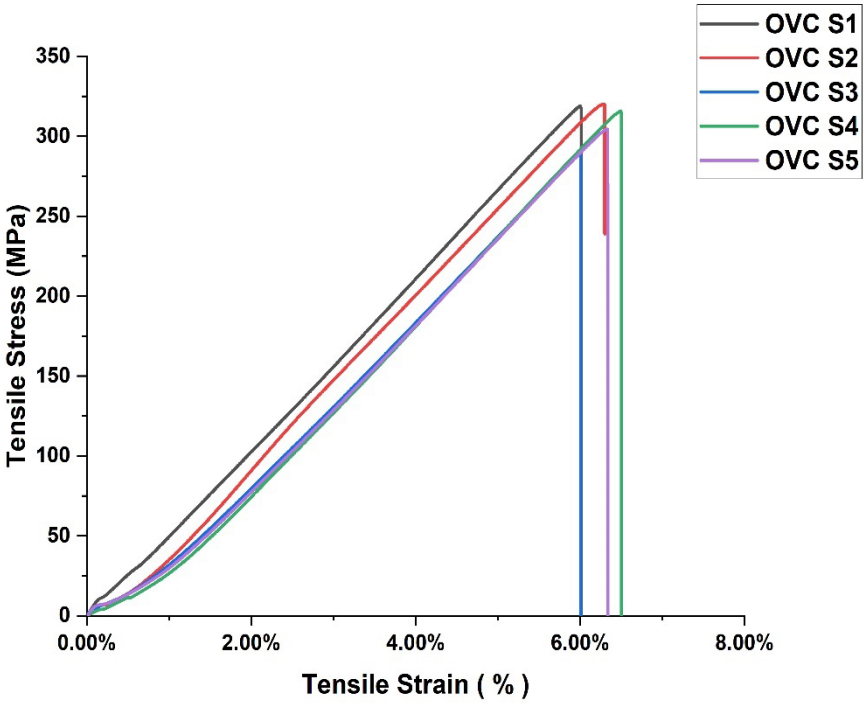

Oven cured sample (OVC)

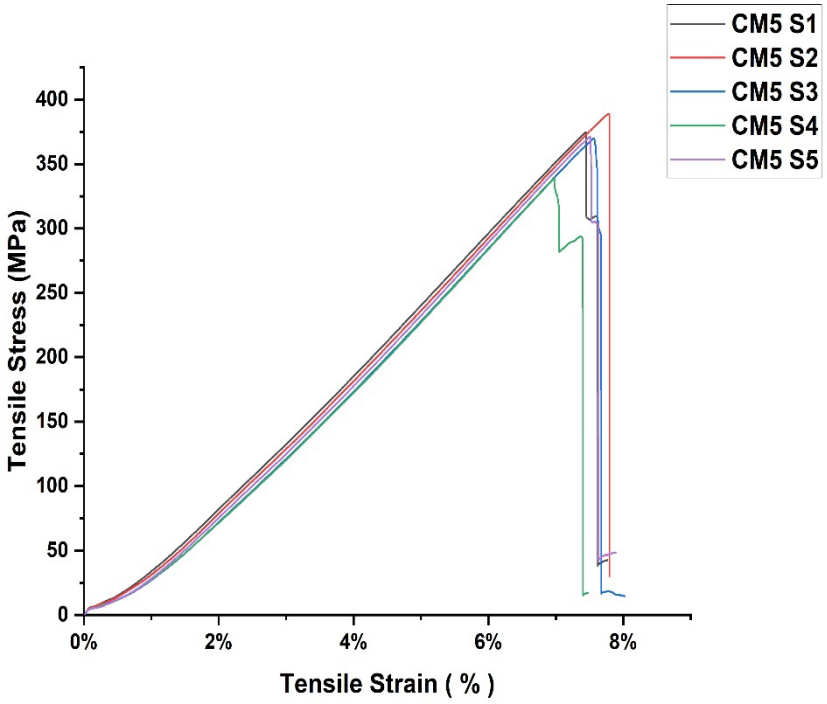

Hot press manufactured sample (CM5)

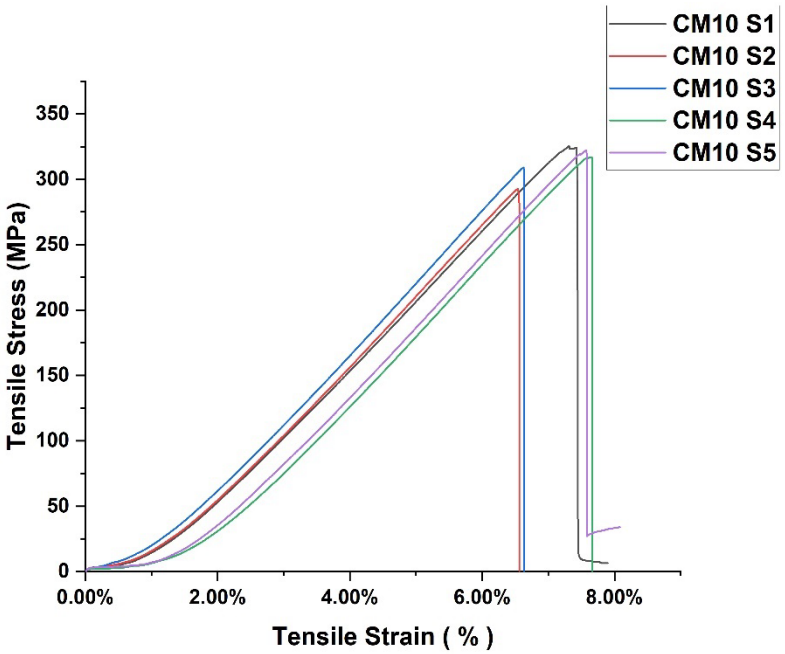

Hot press manufactured sample (CM10)

Flexural stress - strain curves for the individual laminates

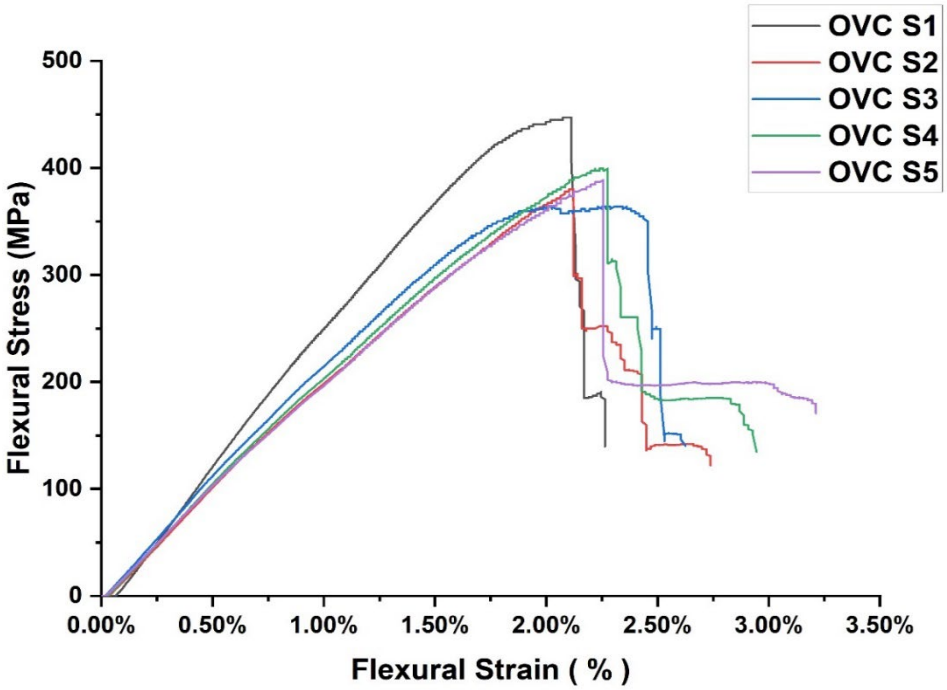

Oven cured sample (OVC)

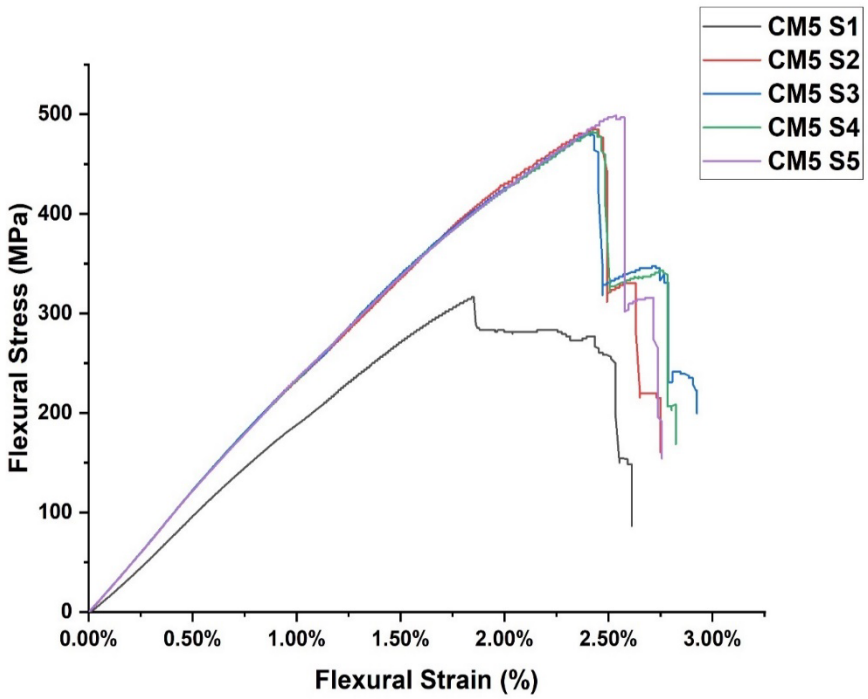

Hot press manufactured sample (CM5)

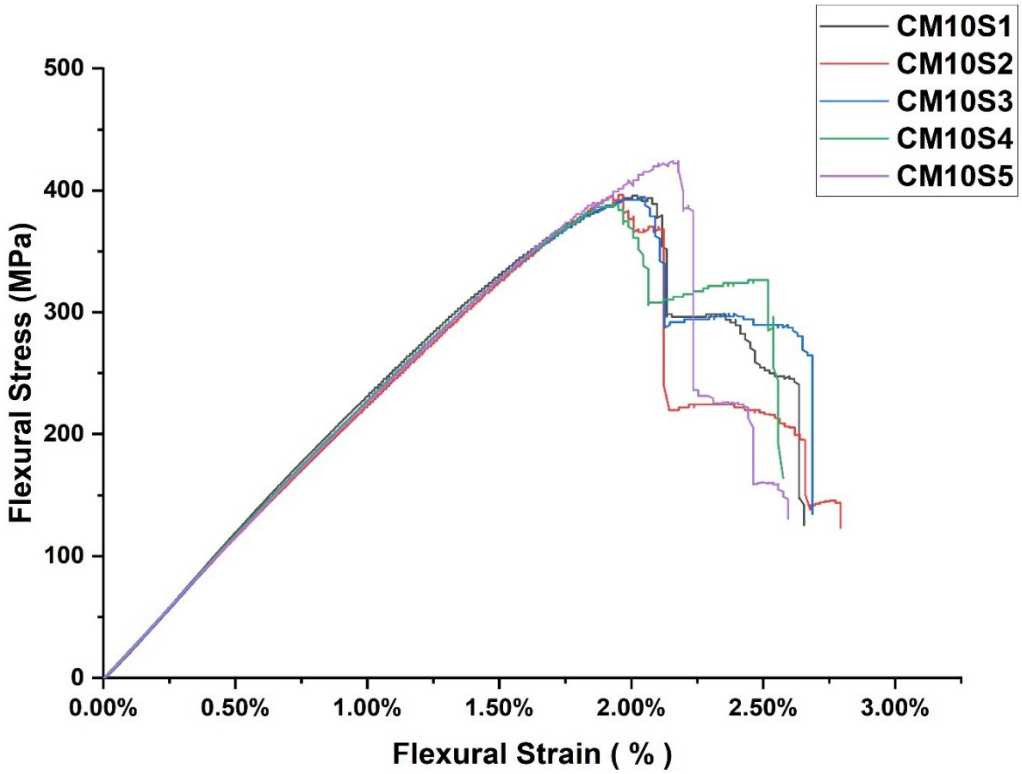

Hot press manufactured sample (CM10)

Interlaminar shear strength test Force – displacement plot

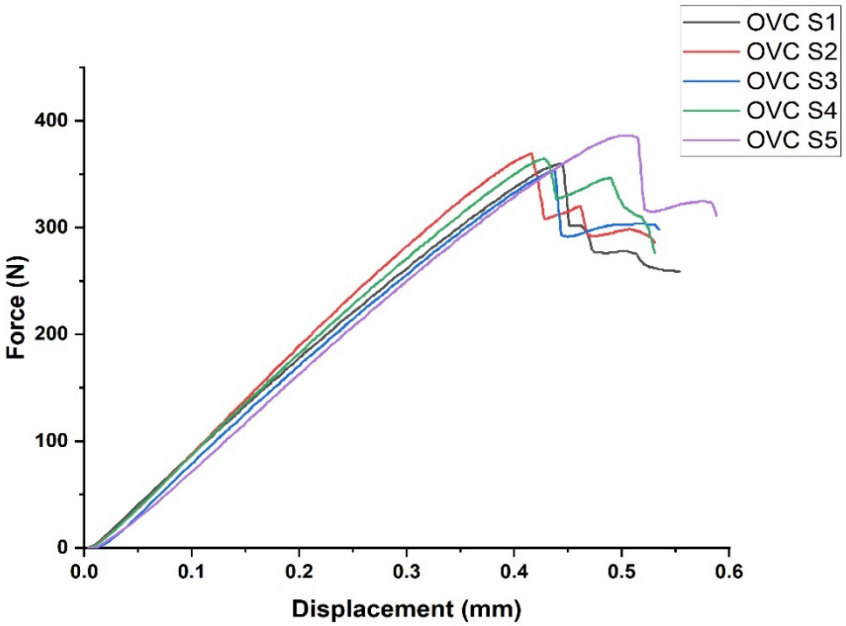

Oven cured sample (OVC)

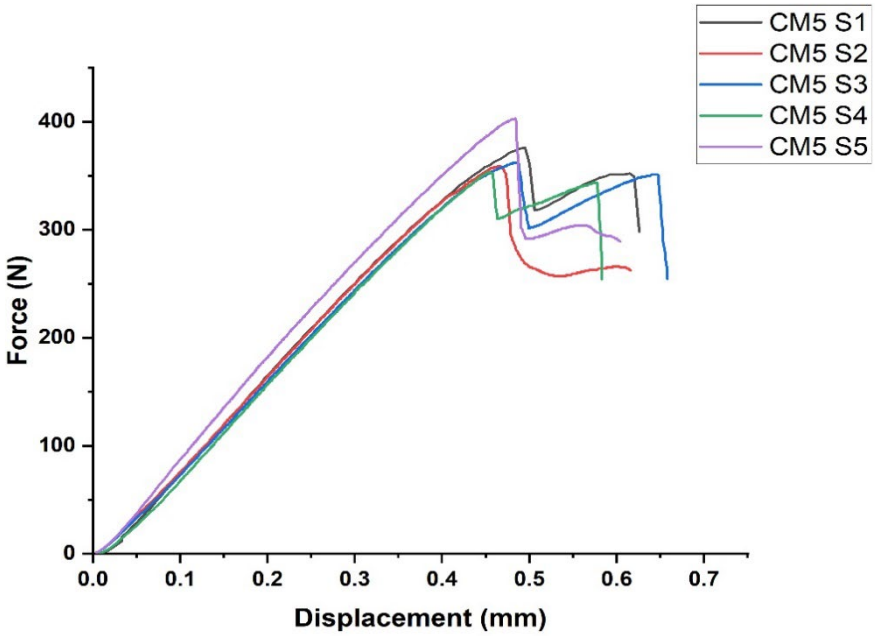

Hot press manufactured sample (CM5)

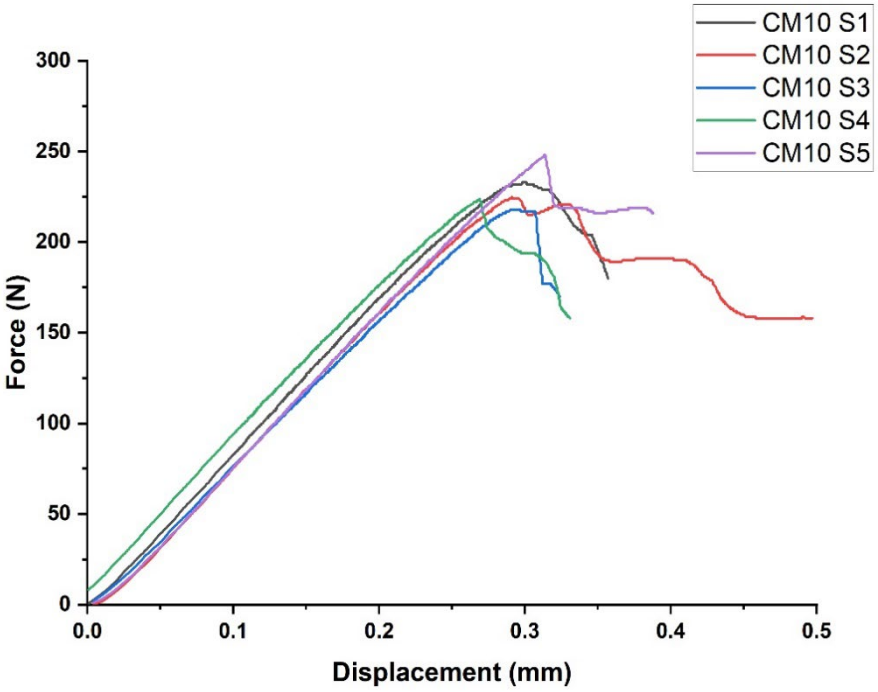

Hot press manufactured sample (CM10)

Appendix B: Published work and conferences

1. D. C. Odiyi, T. Sharif, R. S. Choudhry, S. Maalik, Cure Mechanisms and Kinetic prediction of biobased Glass/Polyfurfuryl Alcohol (PFA) prepreg by Model-free Kinetics, Thermochimica Acta, Volume 708, February 2022, 179133, https://doi.org/10.1016/j.tca.2021.179133
2. D. Odiyi, T. Sharif, R. S. Choudhry, Polyfurfuryl Alcohol Resin composites: Synthesis, Properties, Manufacturing and Challenges in Biomaterials: Playing a Key Role in the Composites Industry's Net Zero Future | Composites UK, 17 Nov 2021, Warwick, UK.
3. D. Odiyi, T. Sharif, R. S. Choudhry, C.Rao Gudur, Sustainable high-performance green composite for emerging applications 2nd International Conference on Polymers and Composite ICPC 2022, 6-7 December 2022, Pakistan.
4. D. Odiyi, T. Sharif, R. S. Choudhry, A review of advancements in synthesis, manufacturing and properties of environment friendly biobased Polyfurfuryl Alcohol Resin and its Composites (Under review)

Requisition for ethical approval

Request for ethical approval for students on taught programmes

Please complete this form and return it to your supervisor as advised in your module handbook. Feedback on your application will be via your supervisor or co-ordinator.

Your Name:	**Odiyi Daniel**
Student ID:	
Unimail address:	
Other contact information	
Programme name and code	**Postgraduate Research / PHDTDOCL**
Name of supervisor	**Dr Tahir Sharif**

Title of proposed research study	
Optimization of Composite Material for Interior Applications in Aerospace	
Supervisor Comments	
Are the ethical implications of the proposed research adequately described in this application?	Yes ❑ No ❑
Does the overall study have low, moderate or high risk in terms of ethical implications?	Low ❑ Moderate ❑ High ❑
Does the study method describe a process of research that is ethically sound?	Yes ❑ No ❑
Signatures	
The information supplied is, to the best of my knowledge and belief, accurate. I clearly understand my obligations and the rights of the participants. I agree to act at all times in accordance with University of Derby Policy and Code of Practice on Research Ethics: http://www.derby.ac.uk/research/ethics-and-governance/research-ethics-and-governance	
Signature of applicant	
Date of submission by applicant	02/07/2018

Signature of supervisor	
Date of signature by supervisor	

For Committee Use Reference Number (Subject area initials/year/ID number) …….

Date received…… Date approved ……. Signed……

Comments

What is the aim of your study?

To develop and optimize the Polyfurfuryl Alcohol (PFA) based resin composite materials for interior application in aerospace.

What are the objectives for your study?

Critical review of the suitability of a PFA based resin system for interior application and investigate the impact of their advantages and disadvantages in terms of processing on quality of the product, processing time, process reliability.

Undertake mechanical characterization of the optimized PFA based resin for interior application.

Investigation and development of suitable fibre reinforcement for optimized PFA matrix for interior application.

Investigate and analyses the optimum manufacturing methods manufacturing of the optimized PFA based resin.

Comparative technical and performance analysis between the optimized or developed matrix and fully bio-based matrix as well as conventional matrices.

Explain the rationale for this study (refer to relevant research literature in your response).

Generally, for fire sensitive application such as interior applications in aircrafts, phenolic based fibre reinforced composite is commonly used in the manufacture of parts and products. This is because aside other mechanical properties, it possesses excellent flame retardancy property which is required to meet very stringent fire, smoke and toxicity standard required by the regulatory authority. Despite its suitability, a major drawback to the continued use of this matrix for application is its potential health hazard during manufacture. Conventionally, it uses formaldehyde as a hardener, a chemical known for its potential adverse effects on humans and often targeted by REACH regulations. As a result, there have been ongoing research and development to mitigate this challenge. A lot of work extensive work has been done to mitigate this challenge while maintain the required properties. Consideration has been given to different resin formulations. For instance, (Rimdusit and Dueramae, 2014) proposed the alloying of modified Polybenzoxazine and epoxy resin. This achieved the purpose but had the drawback of reduced thermal stability and fire resistance. (Benelli et al., 2017) researched further to suggest improving flame retardancy in epoxy resin by the inclusion of flame-retardant Nano-additives made from organically modified clay a

better alternative. This however had the limitation of being very expensive at a commercial scale. Therefore, in recent times, attention has been focused on a bio-based alternative. With focus on the (Polyfurfuryl Alcohol) PFA based resin, studies have shown it to be better environmentally friendly in comparison to the petrochemical based resins. A comparative study by (E. Hoydonckx et al., 2015) has shown that this type of resin favorably competes with the conventional phenolic resin. Results from a study by (Crossley, Schubel and Stevenson, 2013) in which they characterized the mechanical properties of laminates of polyester, epoxy, phenolic and PFA indicates comparability between the phenolic and (Polyfurfuryl Alcohol) PFA laminate. The positives from the previous studies have inform the need to further improve upon this resin with a view to making it viable at a commercial scale. Against this background this research works intends to focus more on investigation and optimization of bio based PFA resin for sensitive applications.

References

Benelli, T., Loris Giorgini, L., Franchini, M. and Laura Mazzocchetti, L. (2017). Improving flame retardancy of epoxy resins. *Society of Plastics Engineers journal*, pp.1-2.

Choudhry, R., Khan, K., Khan, S., Khan, M. and Hassan, A. (2016). Micromechanical modeling of 8-harness satin weave glass fiber-reinforced composites. *Journal of Composite Materials*, 51(5), pp.705-720.

Crossley, R., Schubel, P. and Stevenson, A. (2013). Furan matrix and flax fibre as a sustainable renewable composite: Mechanical and fire-resistant properties in comparison to phenol, epoxy and polyester. *Journal of Reinforced Plastics and Composites*, 33(1), pp.58-68.

E. Hoydonckx, H., Monti, M., Camino, G., Pietro Di Monica, P. and O'Neill, C. (2015). Polyfurfuryl Alcohol Thermosets Resins in Fire Resistant Composite Applications. In: *20th International Conference on Composite Materials*.

Rimdusit, S. and Dueramae, D. (2014). Modified resin for high-performance composite. *Society of Plastics Engineers journal*, pp.1-2

4. **Provide an outline of study design and methods**.

The methodology of the proposed research includes an effective framework which will involve.

1.Theoretical Analysis.

This involves firstly applying theoretical composite micromechanics to generate various analytical models with which different mechanical properties of the laminates of the different resins can be predicted. Data generated from these models will then be compared to results of actual experimental results as well as data obtained from previous extensive work by (Choudhry et al., 2016) for validation.

2.Experimentation and Analysis

With the aid of the composite facilities at the University a very detailed and robust comparative experimentation will be carried out. It will involve setting up and curing composite laminate samples of the different matrices (Epoxy, PFA,) using two methods (Hot-press and Oven Cure). The resultant cure samples will then undergo mechanical, thermal and visco-elastic characterization using appropriate equipment (Tensile test, DSC, DMA). Resultant samples from the different cure methods will also be subjected to flame test. Results data from the experiment will be compared to the initial result from the model prediction for validation. A further comparative analysis will be carried out between the validated results of the samples of different manufacturing methods and a benchmarked industry standard(phenolic). The PFA based resin performance evaluation from these

analyses will inform the optimization technique based on the initial analytical micromodel followed consequently by another round experimentation to validate optimized results.

4. **Research Ethics**

Does the proposed study entail ethical considerations? No

If 'No' provide a statement below to support this position.

The proposed study aims to contribute to knowledge and in so doing, does not violate any ethical concern related to data confidentiality, effect on human, animal and environment. Through period of this work, the researcher intends to strictly ensure compliance with the university's research ethics and integrity guidelines.

If 'Yes' move on to Question 5.

Please note: PROPOSALS INVOLVING HUMAN PARTICIPANTS MUST ADDRESS QUESTIONS 5 - 11.

5. Please provide a detailed description of the study sample, covering selection, sample profile, recruitment and if appropriate, inclusion and exclusion criteria.

N/A

6**. Are payments or rewards/incentives going to be made to the participants? Yes ☐ No ☐ N/A**

If so, please give details below.

7. Please indicate how you intend to address each of the following ethical considerations in your study. If you consider that they do not relate to your study, please say so.

Guidance to completing this section of the form is provided at the end of the document.

Consent N/A

Deception N/A

Debriefing

Withdrawal from the investigation N/A

Confidentiality N/A

Protection of participants N/A

Observation research N/A

Giving advice N/A

Research undertaken in public places N/A

Data protection N/A

Animal Rights N/A

Environmental protection N/A

8. Are there any further ethical implications arising from your proposed research? Yes ☐ No ☐

If your answer was no, please explain why.

N/A

9. Have / do you intend to request ethical approval from any other body/organisation? Yes ☐ No ☐

If 'Yes' – please give details

10. What resources will you require? (e.g., psychometric scales, IT equipment, specialised software, access to specialist facilities, such as microbiological containment laboratories).

N/A

11. What study materials will you use? (Please give full details here of validated scales, bespoke questionnaires, interview schedules, focus group schedules etc and attach all materials to the application)

N/A

Which of the following have you appended to this application?

- ❑ **Focus group questions**
- ❑ **Psychometric scales**
- ❑ **Self-completion questionnaire**
- ❑ **Interview questions**
- ❑ **Other debriefing material**
- ❑ **Covering letter for participants**

❑ **Information sheet about your research study** ❑ **Informed consent forms for participants**

❑ **Other (please describe)**

PLEASE SUBMIT THIS APPLICATION WITH ALL APPROPRIATE DOCUMENTATION

Advice on completing the ethical considerations aspects of a programme of research.

Consent

Informed consent must be obtained for all participants before they take part in your project. The form should clearly state what they will be doing, drawing attention to anything they could conceivably object to subsequently. It should be in language that the person signing it will understand. It should also state that they can withdraw from the study at any time and the measures you are taking to ensure the confidentiality of data. If children are recruited from schools, you will require the permission, depending on the school, of the head teacher, and of parents. Children over 14 years should also sign an individual consent form themselves. If conducting research on children, you will normally also require Criminal Records Bureau clearance. You will need to check with the school if they require you to obtain one of these. It is usually necessary if working alone with children, however, some schools may request you have CRB clearance for any type of research you want to conduct within the school. Research to be carried out in any institution (prison, hospital, etc.) will require permission from the appropriate authority.

Covert or Deceptive Research

Research involving any form of deception can be particularly problematical, and you should provide a full explanation of why a covert or deceptive approach is necessary, why there are no acceptable alternative approaches not involving deception, and the scientific justification for deception.

Debriefing

Debriefing is a process of reflection once the research intervention is complete, for example at the end of an interview session. How will participants be debriefed (written or spoken feedback)? If they will not be debriefed, give reasons. Please attach the written debrief or transcript for the oral debrief. This can be particularly important if covert or deceptive research methods are used.

Withdrawal from investigation

Participants should be told explicitly that they are free to leave the study at any time without jeopardy. It is important that you clarify exactly how and when this will be explained to participants. Participants also have the right to withdraw their data in retrospect, after you have received it. You will need to clarify how they will do this and at what point they will not be able to withdraw (i.e., after the data has been analysed and disseminated).

Protection of participants

Are the participants at risk of physical, psychological or emotional harm greater than encountered ordinary life? If yes, describe the nature of the risk and steps taken to minimise it.

Observational research

If observational research is to be conducted without prior consent, please describe the situations in which observations will take place and say how local cultural values and privacy of individuals and/or institutions will be taken into account.

Giving advice

Students should not put themselves in a position of authority from which to provide advice and should in all cases refer participants to suitably qualified and appropriate professionals.

Research in public places

You should pay particular attention to the implications of research undertaken in public places. The impact on the social environment will be a key issue. You must observe the laws of obscenity and public decency. You should also have due regard to religious and cultural sensitivities.

Confidentiality/Data Protection

You must comply with the Data Protection Act and the University's Good Scientific Practice http://www.derby.ac.uk/research/policy-and-strategy This means:

- It is very important that the Participant Information Sheet includes information on what the research is for, who will conduct the research, how the personal information will be used, who will have access to the information and how long the information will be kept for. This is known as a 'fair processing statement.'
- You must not do anything with the personal information you collect over and above that for which you have consent.
- You can only make audio or visual recordings of participants with their consent (this should be stated on the Participant Information sheet)
- Identifiable personal information should only be conveyed to others within the framework of the act and with the participant's permission.
- You must store data securely. Consent forms and data should be stored separately and securely.
- You should only collect data that is relevant to the study being undertaken.
- Data may be kept indefinitely providing its sole use is for research purposes and meets the following conditions:
- The data is not being used to take decisions in respect of any living individual.
- The data is not being used in any which is, or is likely to, cause damage and/or distress to any living individual.

- You should always protect a participant's anonymity unless they have given their permission to be identified (if they do so, this should be stated on the Informed Consent Form).
- All data should be returned to participants or destroyed if consent is not given after the fact, or if a participant withdraws.

Animal rights.

Research which might involve the study of animals at the University is not likely to involve intrusive or invasive procedures. However, you should avoid animal suffering of any kind and should ensure that proper animal husbandry practices are followed. You should show respect for animals as fellow sentient beings.

Environmental protection

The negative impacts of your research on the natural environment and animal welfare, must be minimised and must be compliant to current legislation. Your research should appropriately weigh longer-term research benefit against short-term environmental harm needed to achieve research goals.

Ethics Approval

UNIVERSITY of DERBY

Approval Letter: College of Engineering and Technology Research Ethics Committee (Chair's action)

University of Derby

Date : 5 July 2018
Chair : Prof Stamatis Zoras

Dear , Odiyi Daniel

Re: your request for ethical approval of your Research Project

Thank you for submitting your application to the College of Engineering and Technology Research Ethics Committee. The application has now been reviewed on a chair's action basis. I have reviewed the documents and consulted colleagues.

I am happy to approve the application on a chair's action basis. If any changes to the procedures etc. described in the application or supporting documentation is necessary, you must notify the committee and may be required to make a resubmission of the application.

We will look forward to receiving an application for the full study in due course.

Good luck with your research,

Yours Sincerely,

Prof Stamatis Zoras
Deputy Chair, CREC for Engineering and Technology